Recent Science Highlights at Beamline 10.0.1 of the Advanced Light Source

Wednesday 24 Nov 2010 at 11:00 (01h00')

Beamline 10.0.1 of the ALS has typically a dozen or so of groups per year. These produce an average of 25 refereed papers and 4 articles of high impact (PRL, Nature or Science) per year. The beamtime is equally divided for groups doing condense matter physics and groups from the atomic and molecular community. A selected group of recent science highlights from the research done at this beamline will be presented.

Primary authors : Dr. AGUILAR, Alejandro (LBNL-ALS)

Co-authors :

Presenter : Dr. AGUILAR, Alejandro (LBNL-ALS)

Recent Science Highlights from Beamline 10.0.1 of the Advanced Light Source

Alex Aguilar
Scientist
Beamline 10.0.1

Outline

- **Beamline 10.0.1**
- **Condense Matter Physics**
  - Angle Resolved Photoemission Spectroscopy (ARPES)
- **Atomic and Molecular Physics**
  - Velocity Map Imaging Spectroscopy
  - Photoelectron Spectroscopy (Scienta 2000) gas phase
  - Double Ionization Chamber
  - COLTRIMS
  - **Photon-Ion Merged Beams Apparatus**

Photon-ion merged beams apparatus

- Photoionization of Se ions;

  Determination of elemental abundances in PNe

  Sterling *et al.*, accepted JPB (2010)

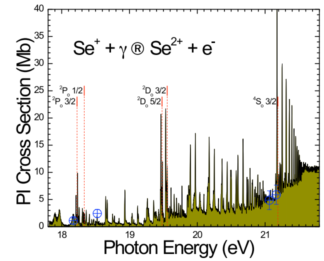

N.C. Sterling, D. Esteves, A.L. Kilcoyne, E. Red, R.A. Phaneu R.C. Bilodeau,and A. Aguilar

Photon-ion merged beams apparatus

- Photoionization of Se ions;
  Determination of elemental abundances in PNe

  Sterling *et al.*, accepted JPB (2010)

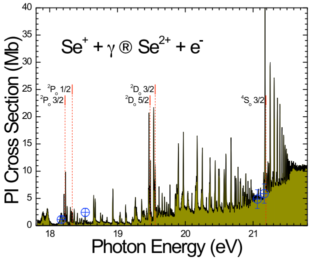

N.C. Sterling, D. Esteves, A.L. Kilcoyne, E. Red, R.A. Phaneuf, R.C. Bilodeau,and A. Aguilar

- Photoionization of $Ce@C_{82}^{+}$ $Xe@C_{60}^{+}$;
  Confinement resonances,
  Quantum computing,
  Cancer therapy

  Müller *et al.*, PRL 101, 133001 (2008)
  Kilcoyne *et al.* PRL 105, 213001 (2010)

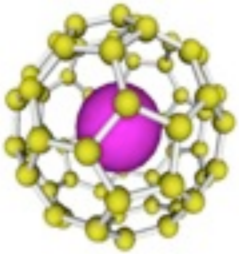

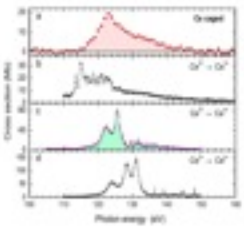

A. Müller, S. Schippers, M.Habibi, D. Esteves, J.C. Wang, R.A. Phaneuf, A.L.D. Kilcoyne, A. Aguilar and L. Dunsch

Photon-ion merged beams apparatus

- Photoionization of Se ions;

  Determination of elemental abundances in PNe

  Sterling *et al.*, accepted JPB (2010)

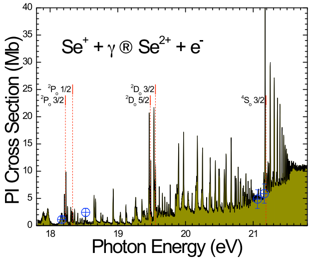

N.C. Sterling, D. Esteves, A.L. Kilcoyne, E. Red, R.A. Phaneu R.C. Bilodeau,and A. Aguilar

- Photoionization of $Ce@C_{82}{}^{+}$ $Xe@C_{60}{}^{+}$;

  Confinement resonances,

  Quantum computing, Cancer therapy

  Müller *et al.*, PRL 101, 133001 (2008)

  Kilcoyne *et al.* PRL 105, 213001 (2010)

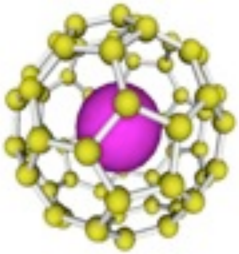

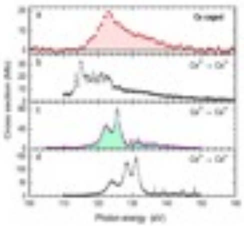

A. Müller, S. Schippers, M.Habibi, D. Esteves, J.C. Wang, R.A. Phaneuf, A.L.D. Kilcoyne, A. Aguilar and L. Dunsch

These experiments were only possible due to the high resolution and high photon flux of this beamline.

U10 Undulator

U10 Undulator
- 10.0 cm period, 43 periods
- 12 – 1500 eV energy range (@ 1.9 GeV)

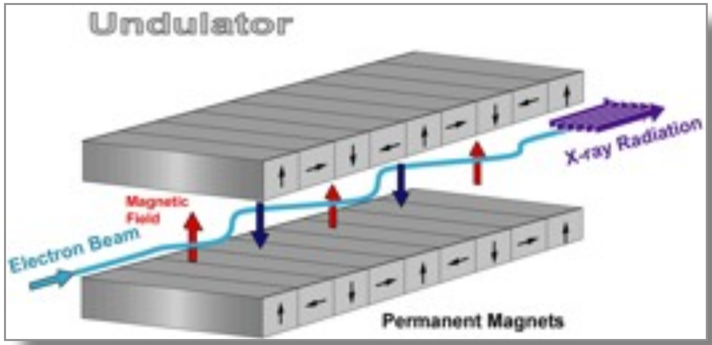

www-xfel.spring8.or.jp/cband/j/Undulator.htm

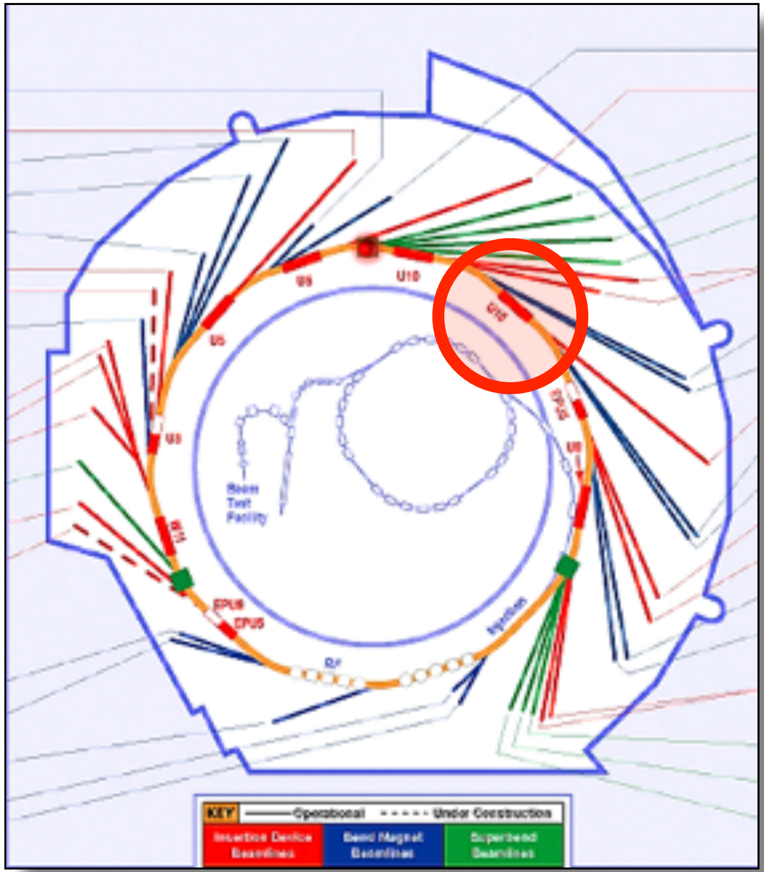

Schematic Drawing of Beamline 10.0.1

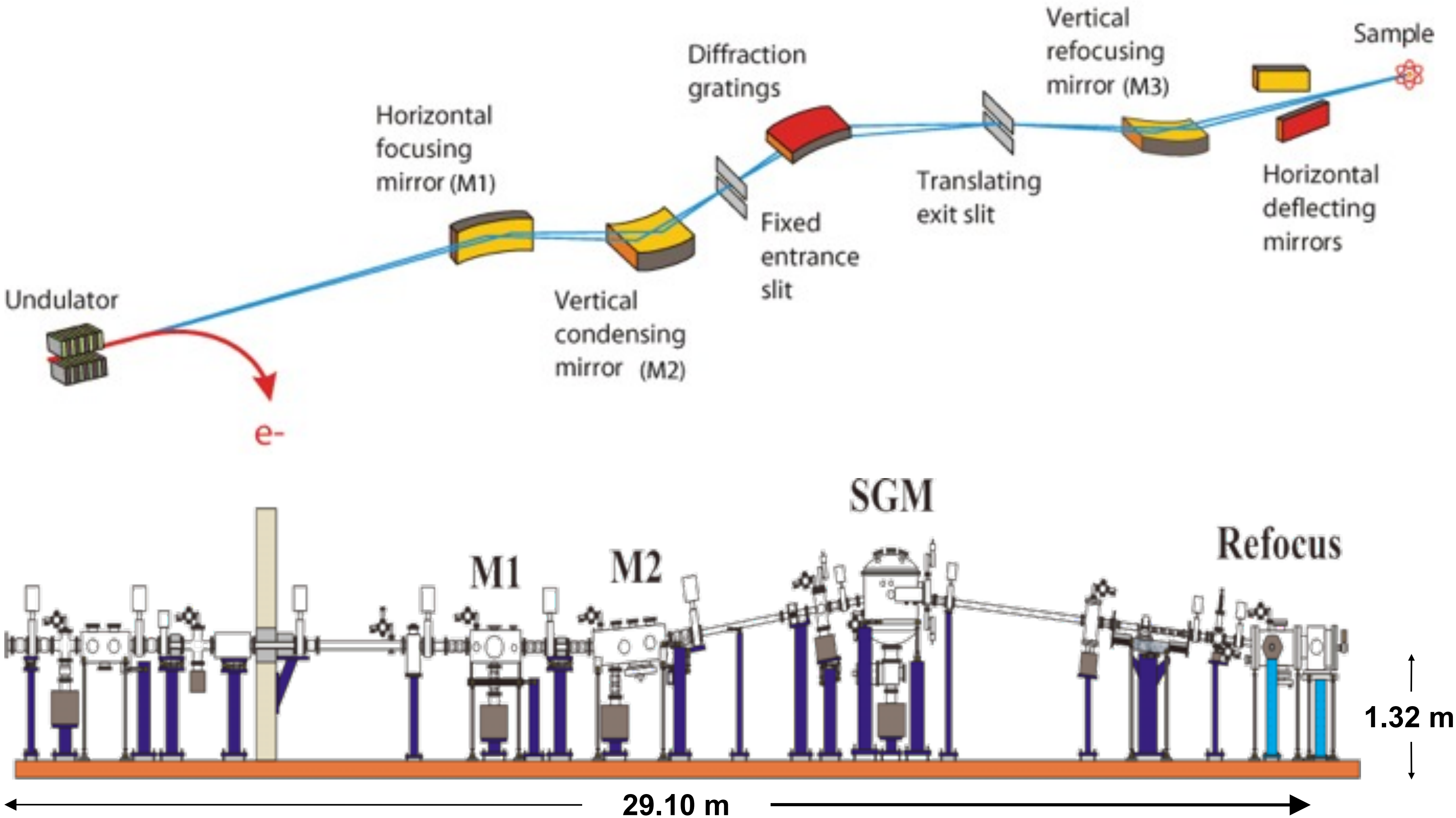

Beamline 10.0.1 Monochromator

Spherical Grating Monochromator

- 3 gratings: 380, 925, and 2100 lines/mm
- 17 – 340 eV energy range

Grating	Ruling (lines/	Energy Range
Low	380	17 – 75
Medium	925	40 – 170
High	2100	100 – 340

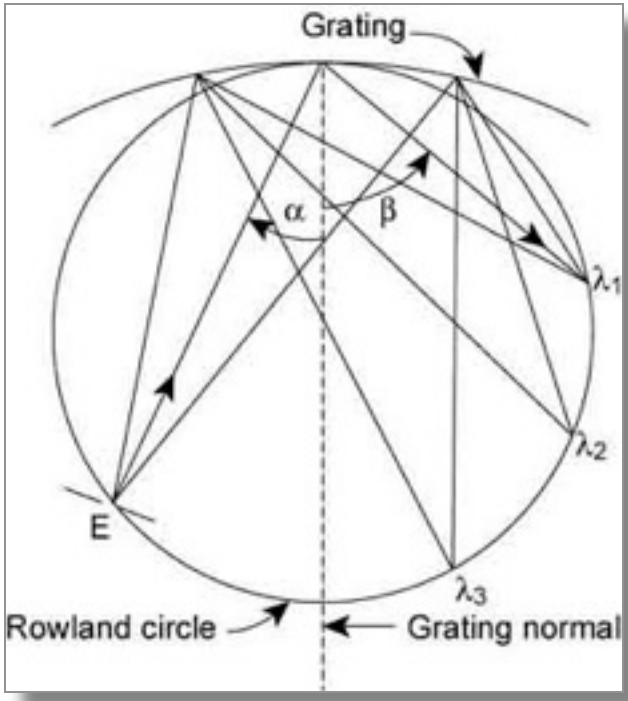

Three Branch Lines (2 for AMO)

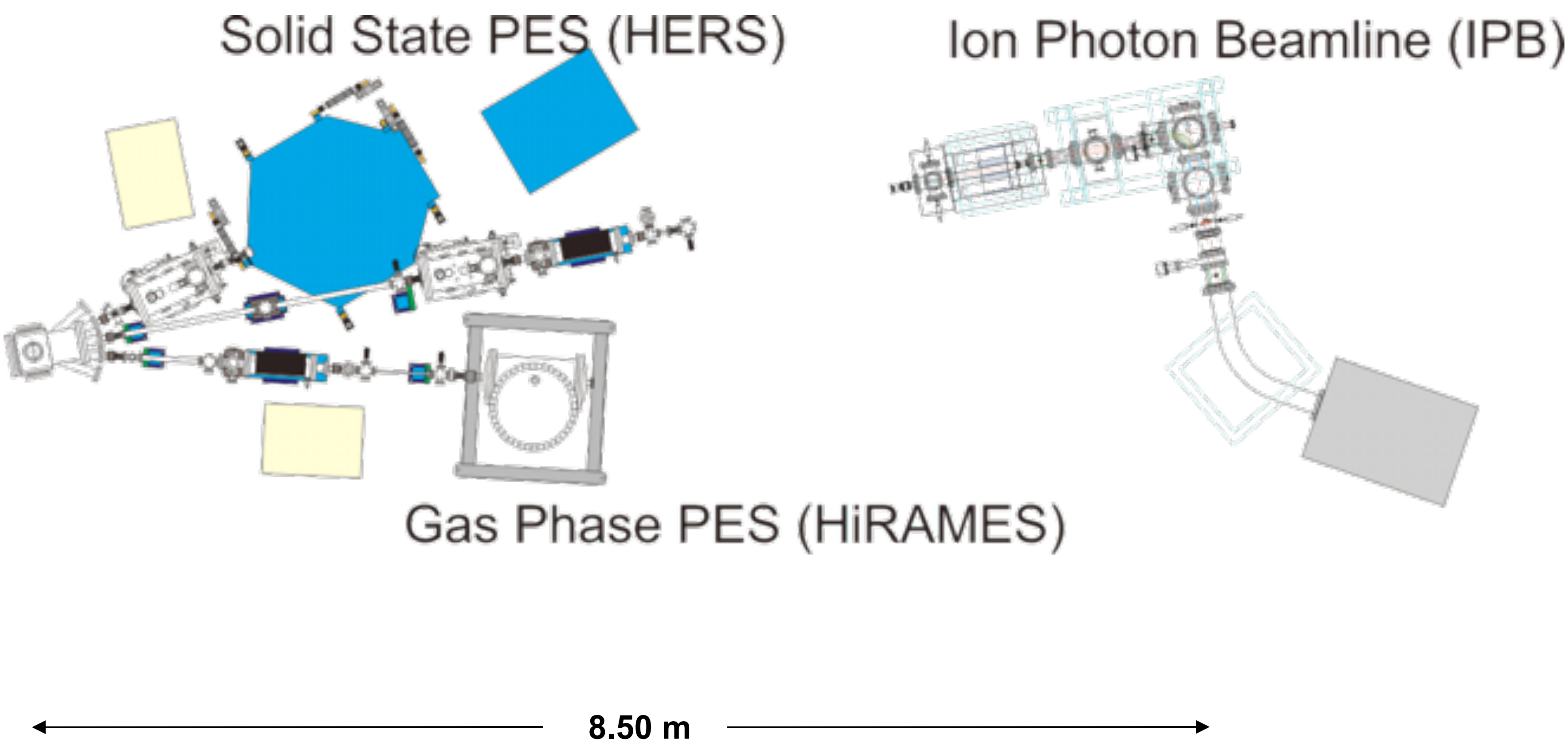

Angle Resolved Photoemission

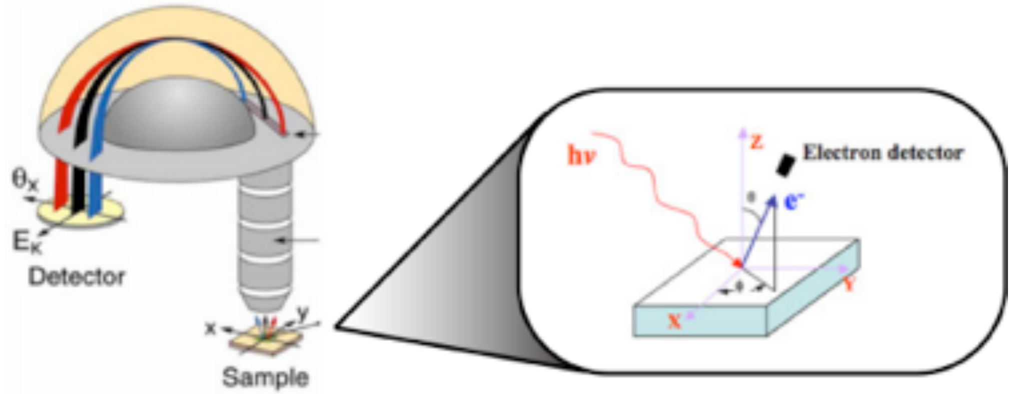

NaMo$_6$O$_{17}$

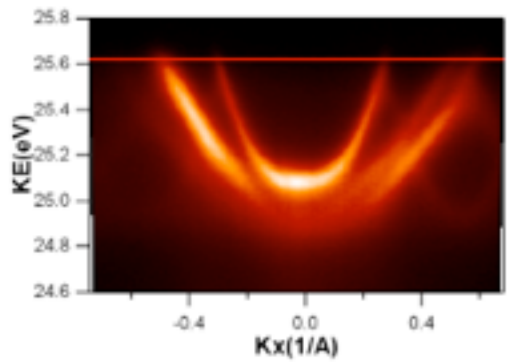

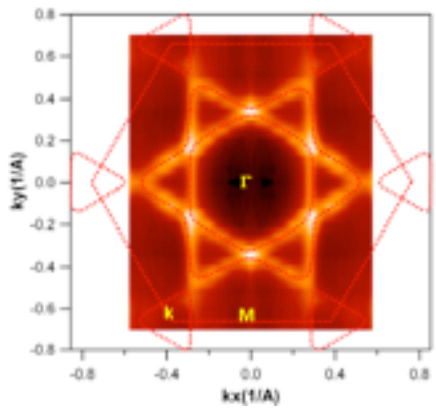

Experimentally obtain E(**k**) dispersion & Fermi surface topology

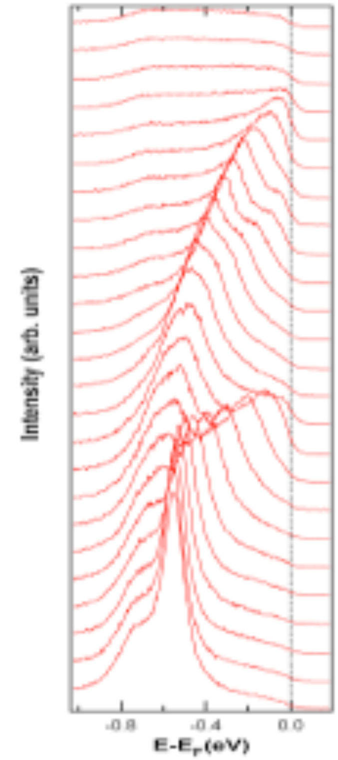

Extract information on the many-body interaction from spectral lineshapes

Two gaps in the cuprate superconductors

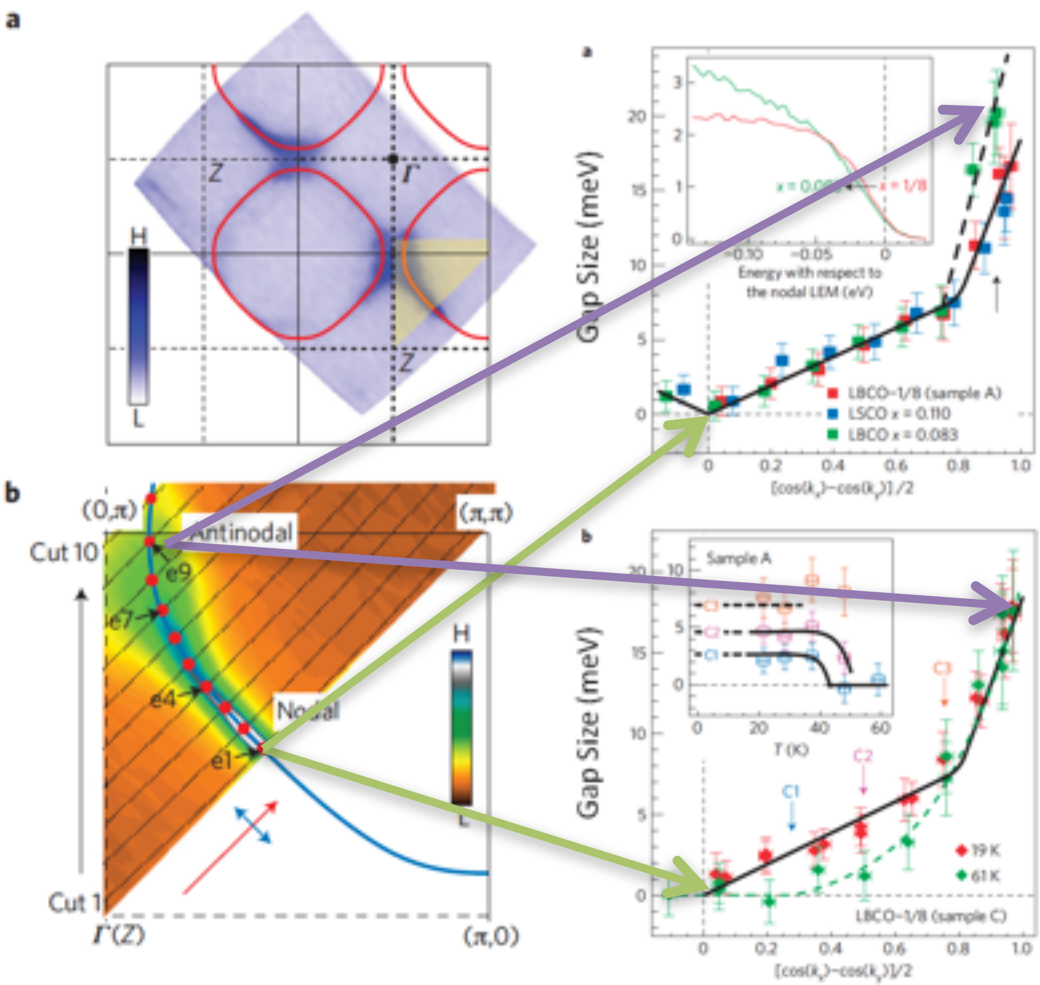

The pseudogap profile along the Fermi arc of $La_{1.875}Ba_{0.125}CuO_4$ reveals two distinct components.

This debunks a simple precursor scenario of pseudogap, and makes us rethink on the nature of pseudogap state.

Ruihua He et al. Nat. Phys. 5, 119 (2009)

Iron pnictide superconductors

New type of high Tc superconductors other than cuprates

Wide range of photon energy, polarization control essential to study electronic structure

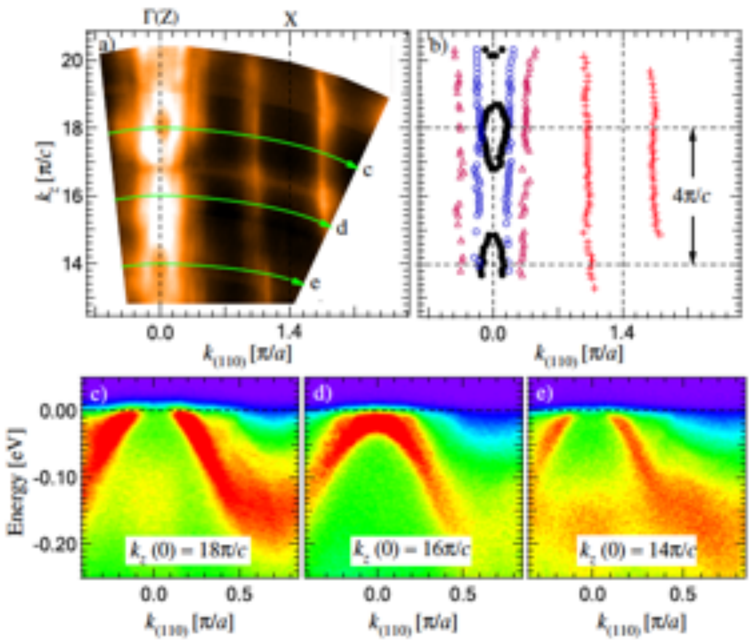

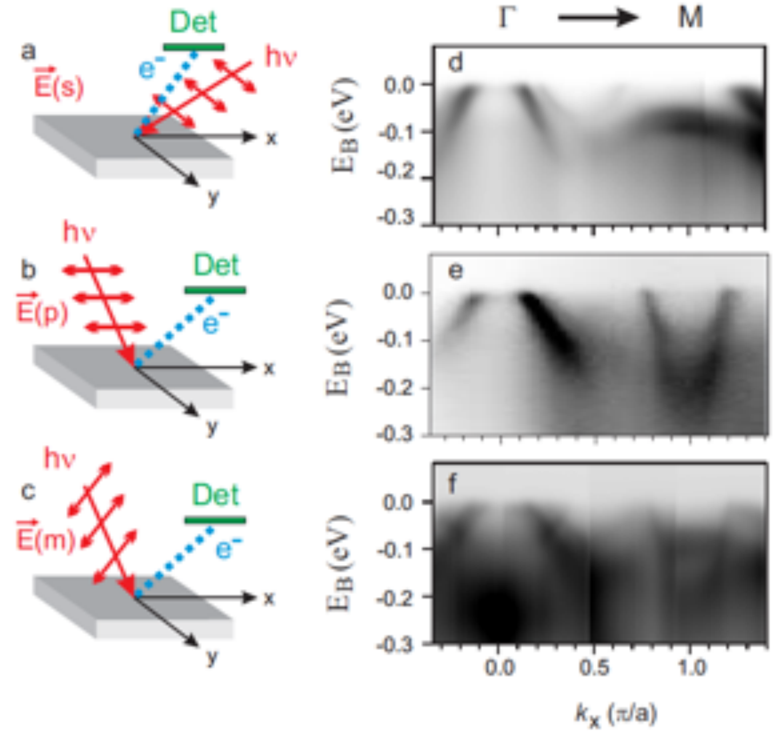

hν

Y. Xia et al. PRL 103, 037002 (2009)
C. Liu et al. PRL 102, 167004 (2009)
P. Vilmercati et al. PRB 79, 220503(R) (2009)

Topological Insulators

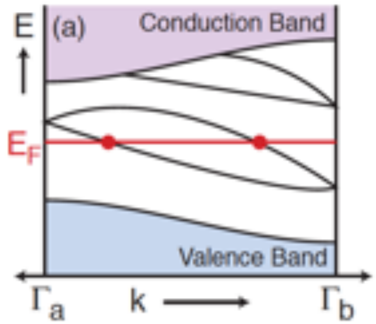

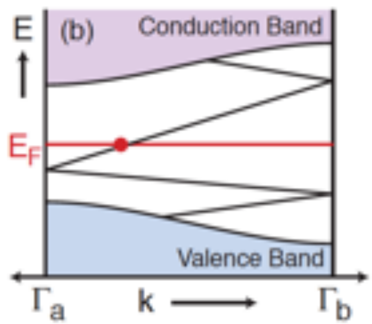

Topology of electronic structure defines non-trivial metallic surface state

"Locking" of current & spin

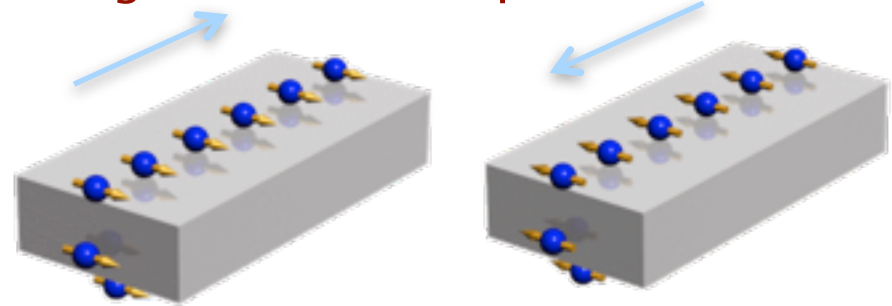

No back-scattering (by non-magnetic impurities)

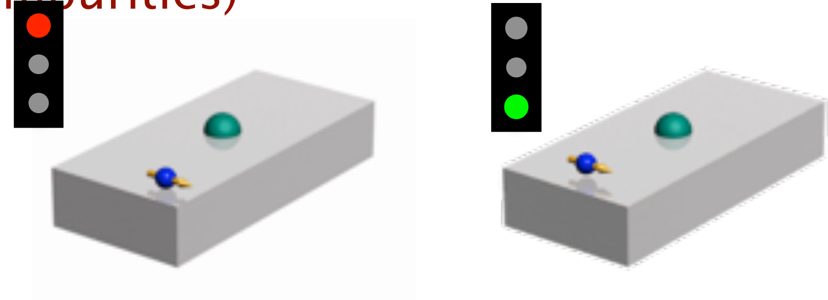

Spin can flow on the surface without backscattering

⇨ Essential for Spintronics

Topological Insulators

First experimental realization of 3D topological insulator in Sn-doped Bi_2Te_3

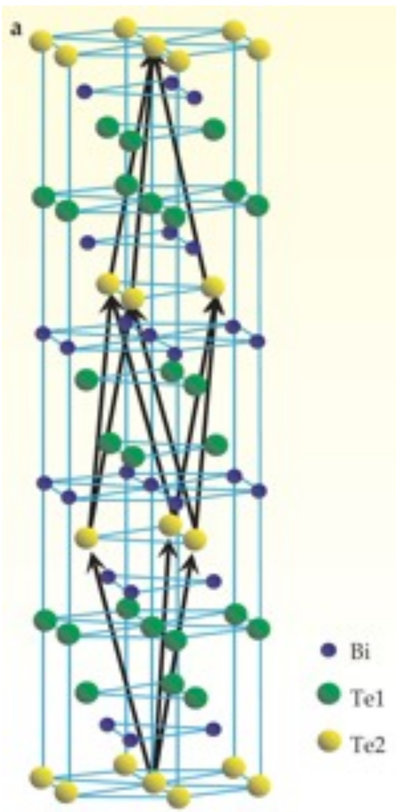

Doping

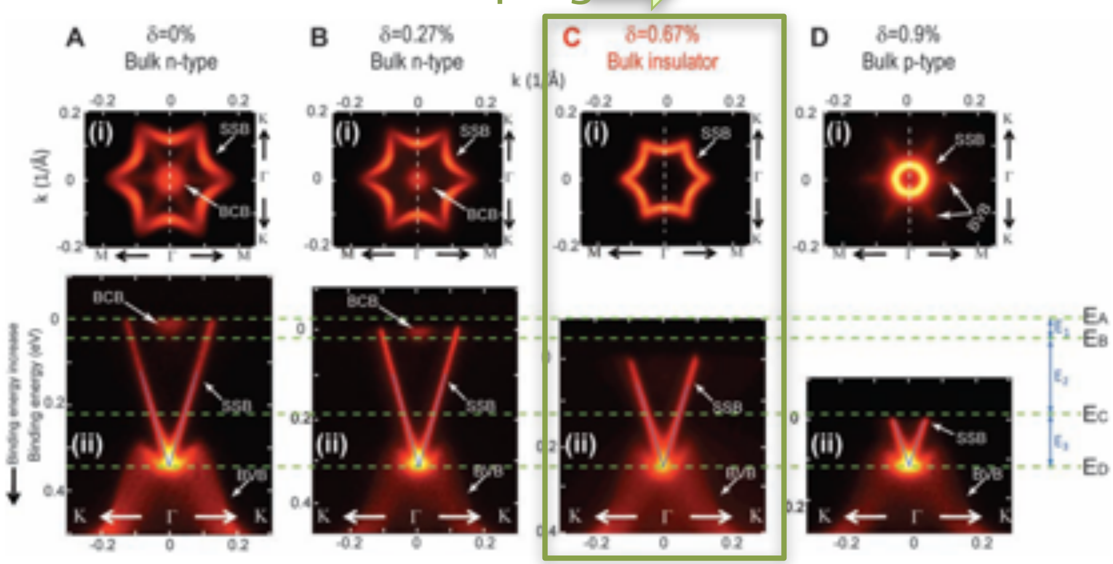

Just right topology of electronic structure

Yulin Chen et al. Science 325, 178 (2009)

Mechanics of Photoionization

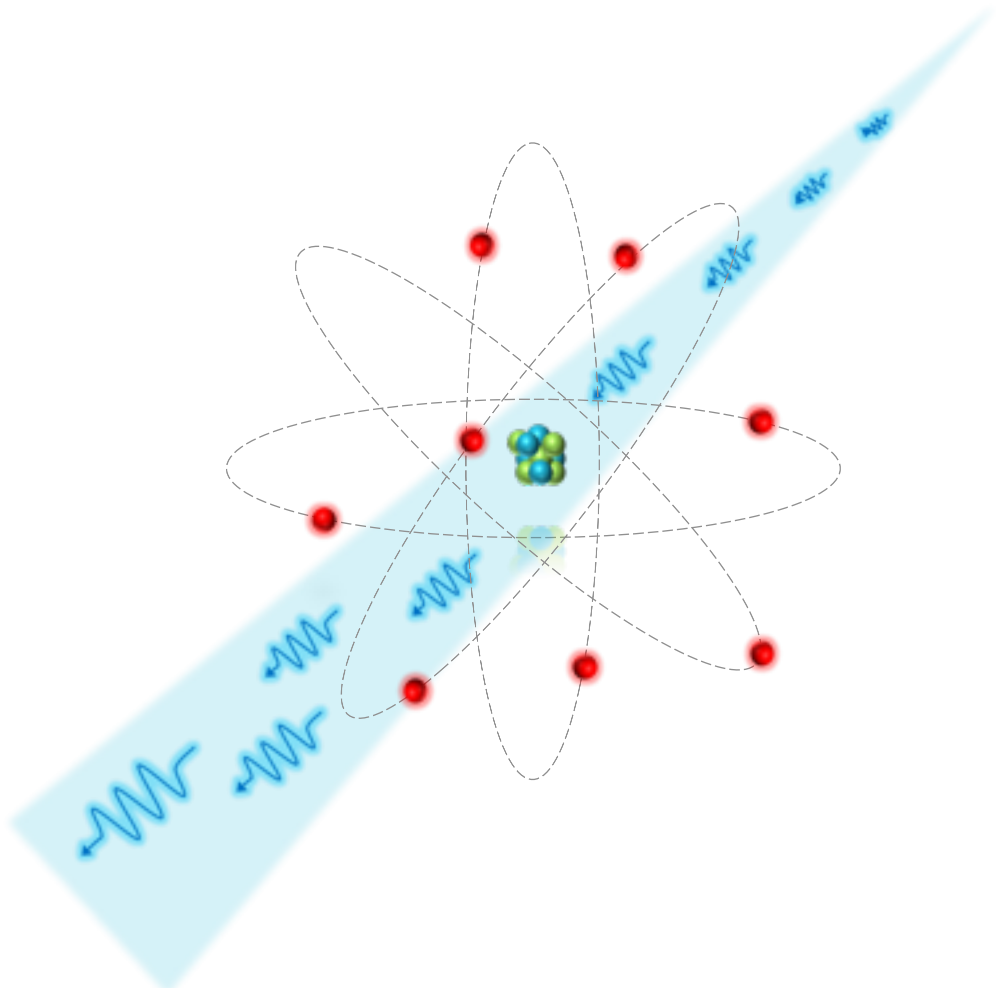

Direct Photoionization

- Incident photon energy ≥ ionization threshold
- A single electron is ejected without excitation

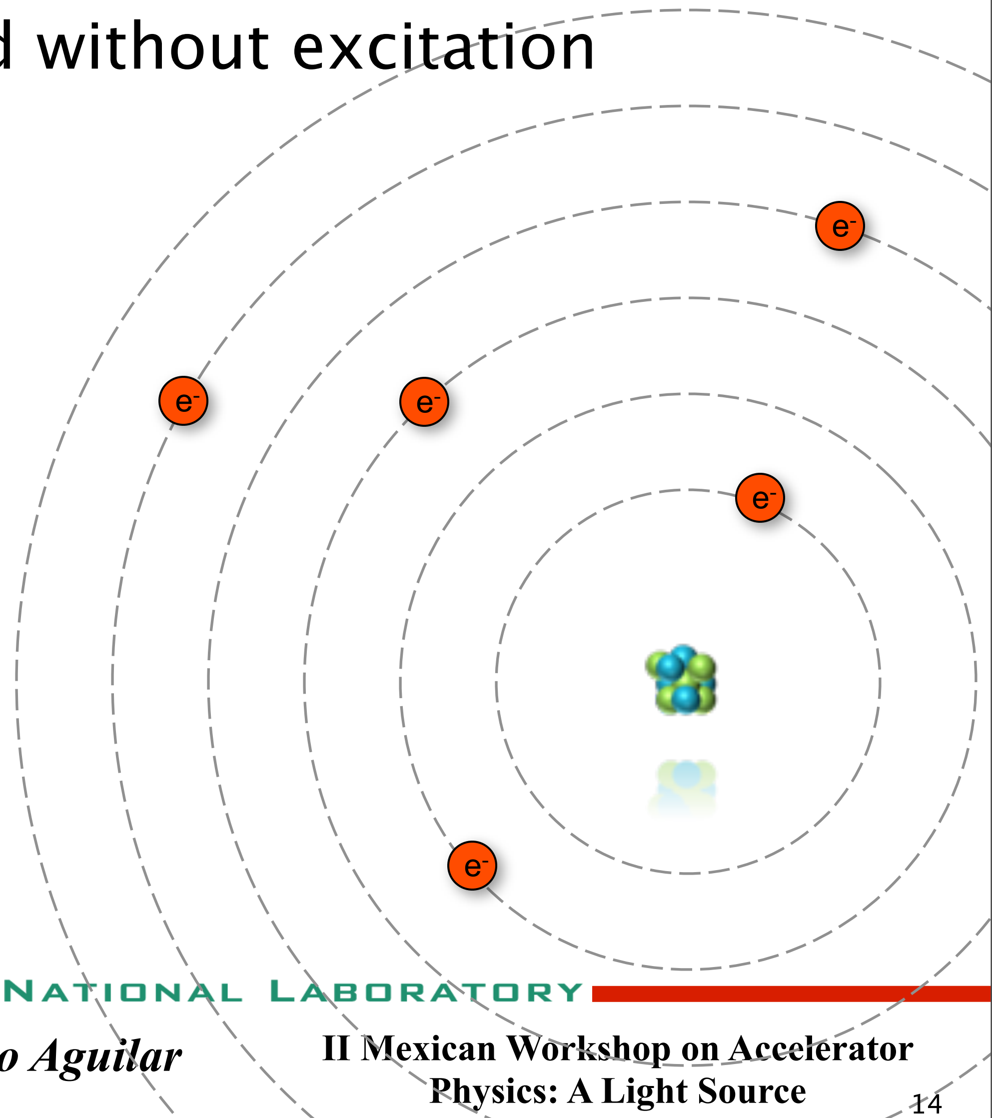

Direct Photoionization

- Incident photon energy ≥ ionization threshold
- A single electron is ejected without excitation

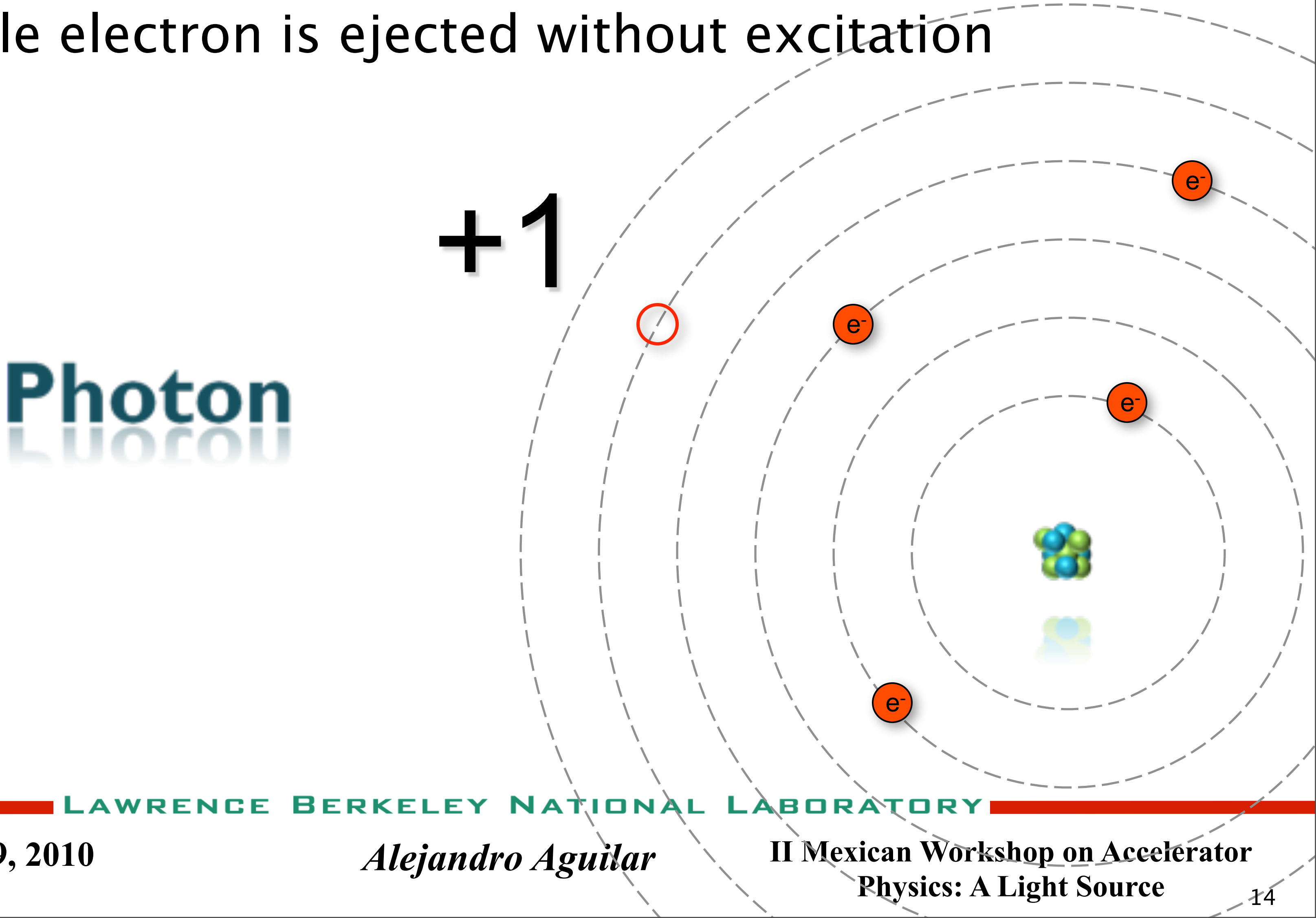

Indirect Photoionization

- Excitation of an inner shell electron, followed by <u>autoionization</u>

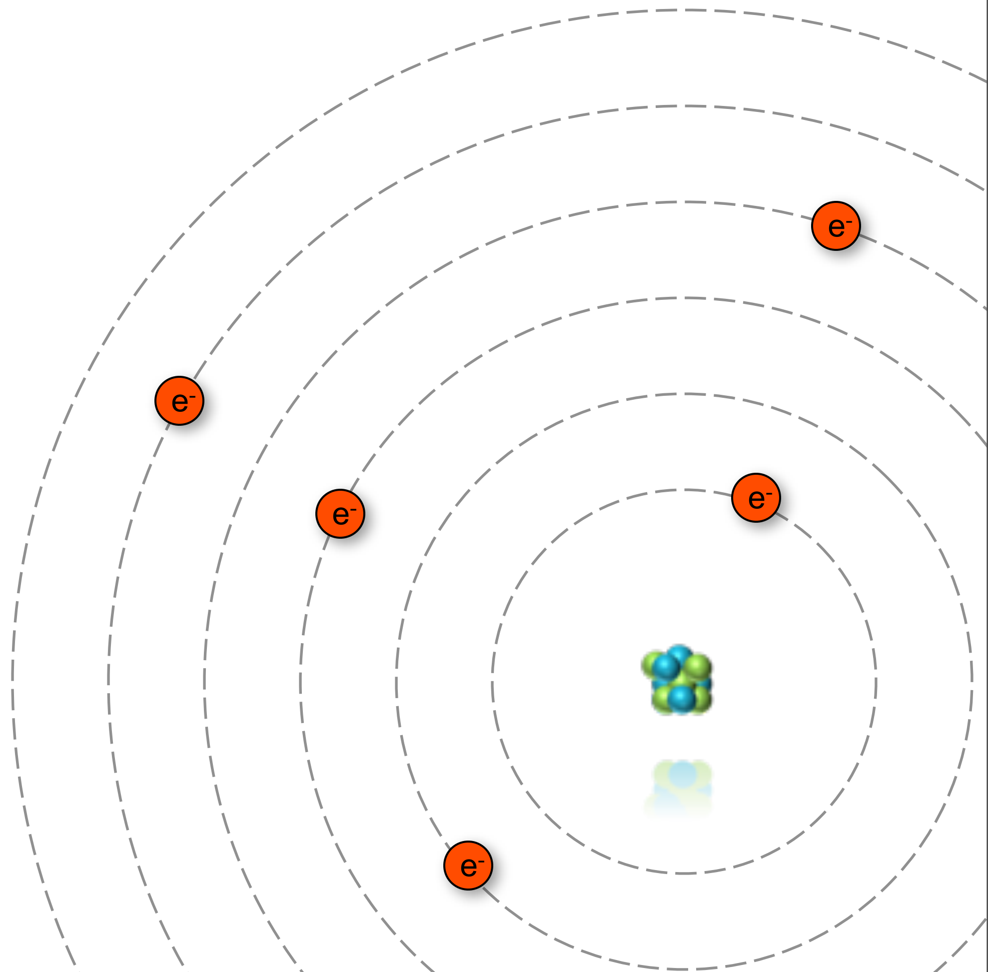

Indirect Photoionization

- Excitation of an inner shell electron, followed by <u>autoionization</u>

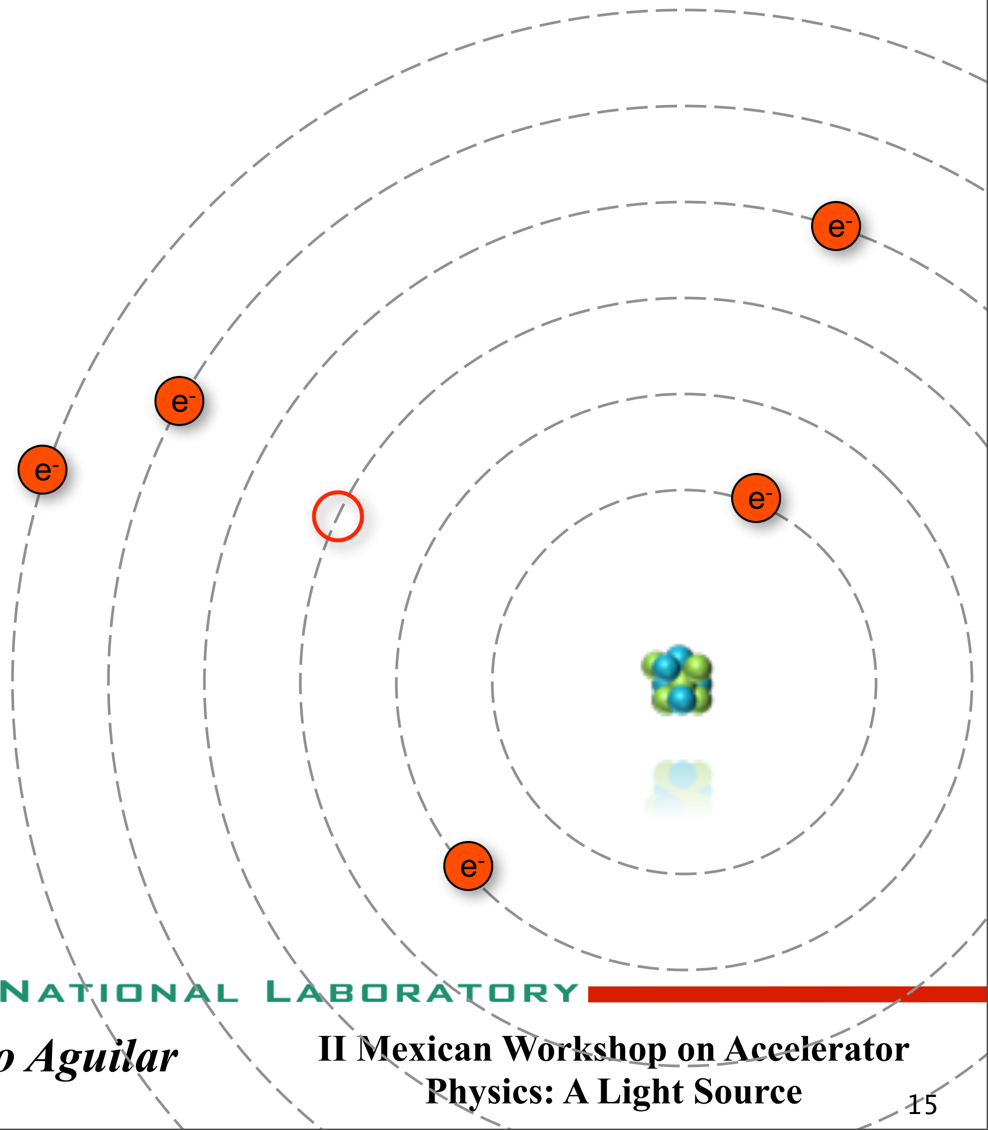

Indirect Photoionization

- Excitation of an inner shell electron, followed by <u>autoionization</u>

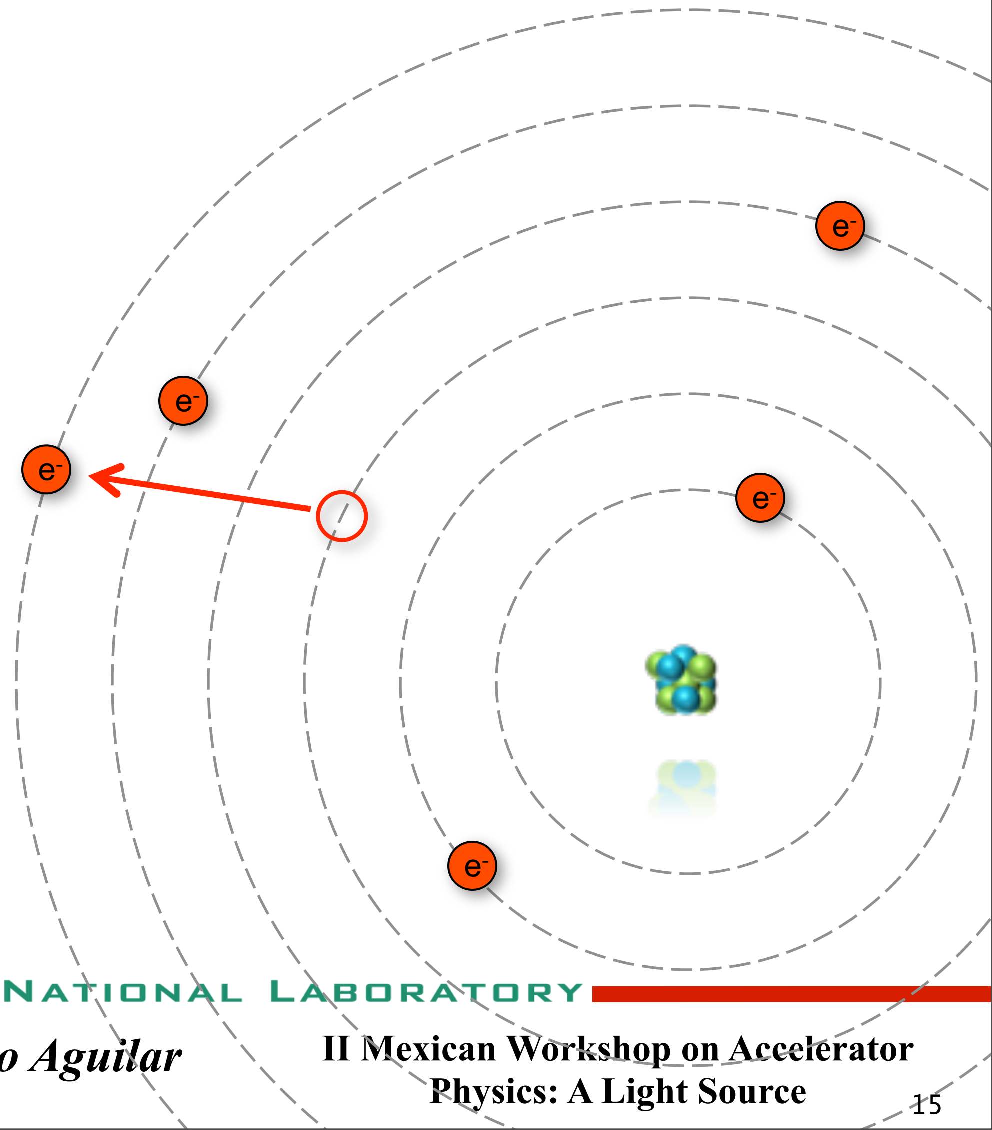

Indirect Photoionization

- Excitation of an inner shell electron, followed by <u>autoionization</u>
  - Lifetimes ≈ nanoseconds – picoseconds

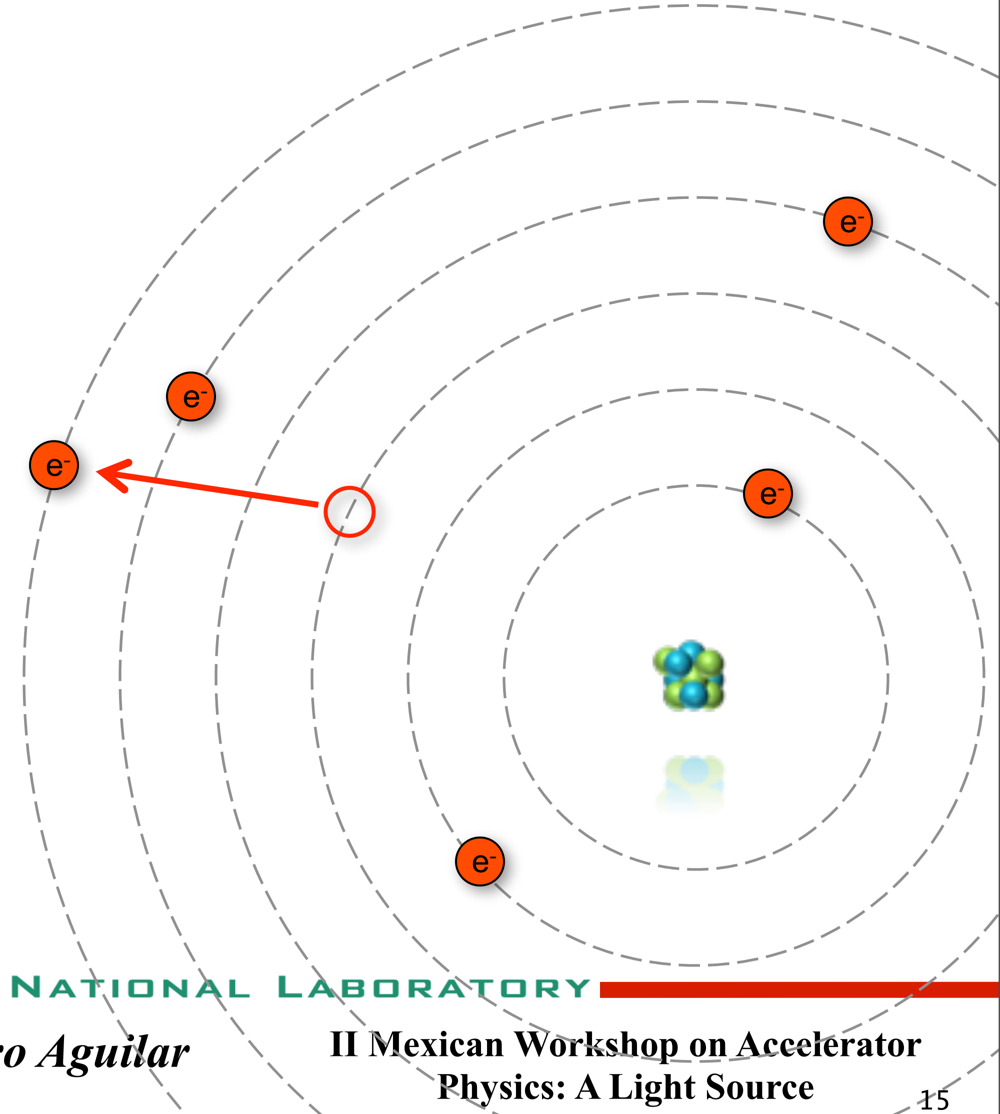

Indirect Photoionization

- Excitation of an inner shell electron, followed by <u>autoionization</u>
  - Lifetimes ≈ nanoseconds – picoseconds

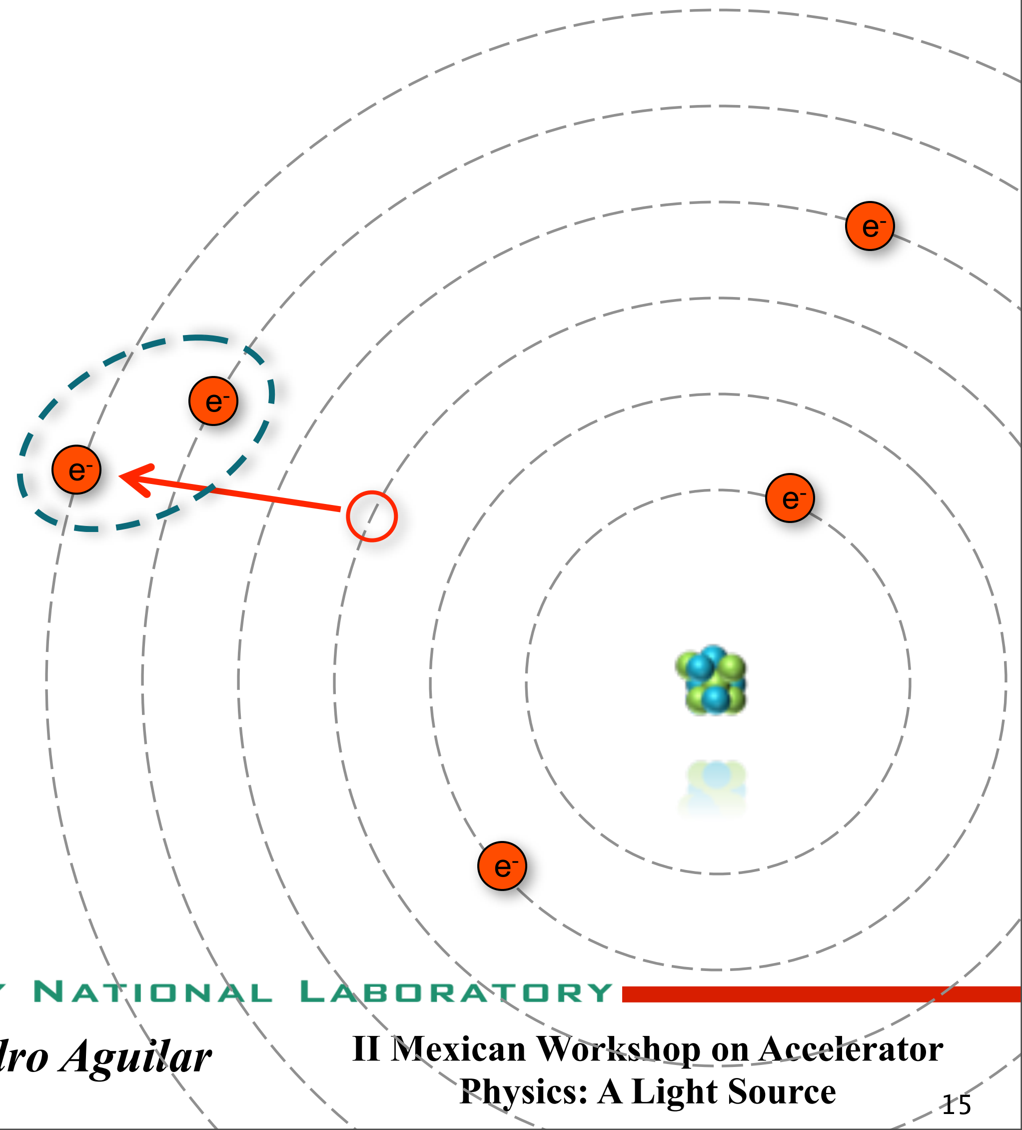

Indirect Photoionization

- Excitation of an inner shell electron, followed by <u>autoionization</u>
  - Lifetimes ≈ nanoseconds – picoseconds

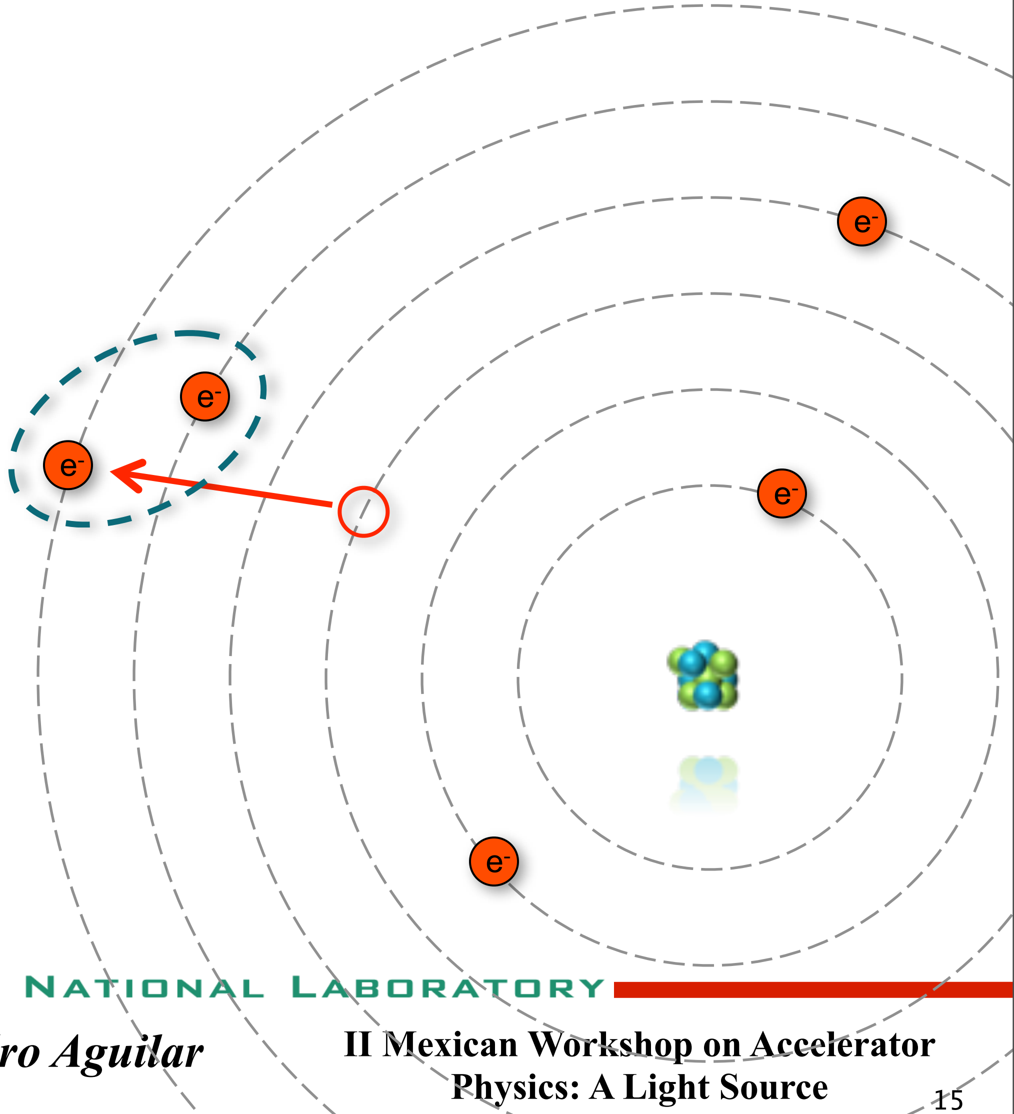

Indirect Photoionization

- Excitation of an inner shell electron, followed by <u>autoionization</u>
  - Lifetimes ≈ nanoseconds – picoseconds

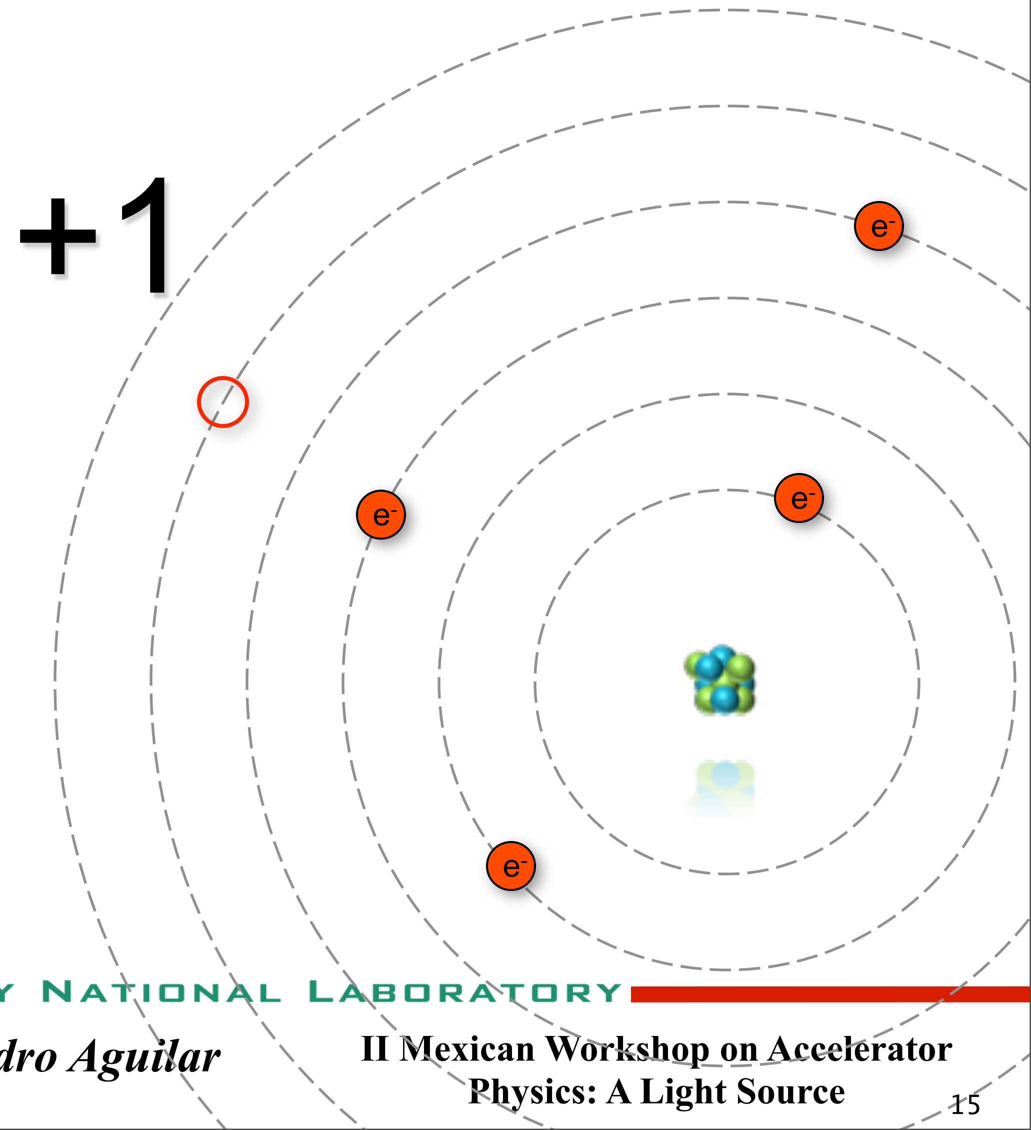

Indirect Photoionization

- Excitation of an inner shell electron, followed by <u>autoionization</u>
  - Lifetimes ≈ nanoseconds – picoseconds
  - Resonances occur at

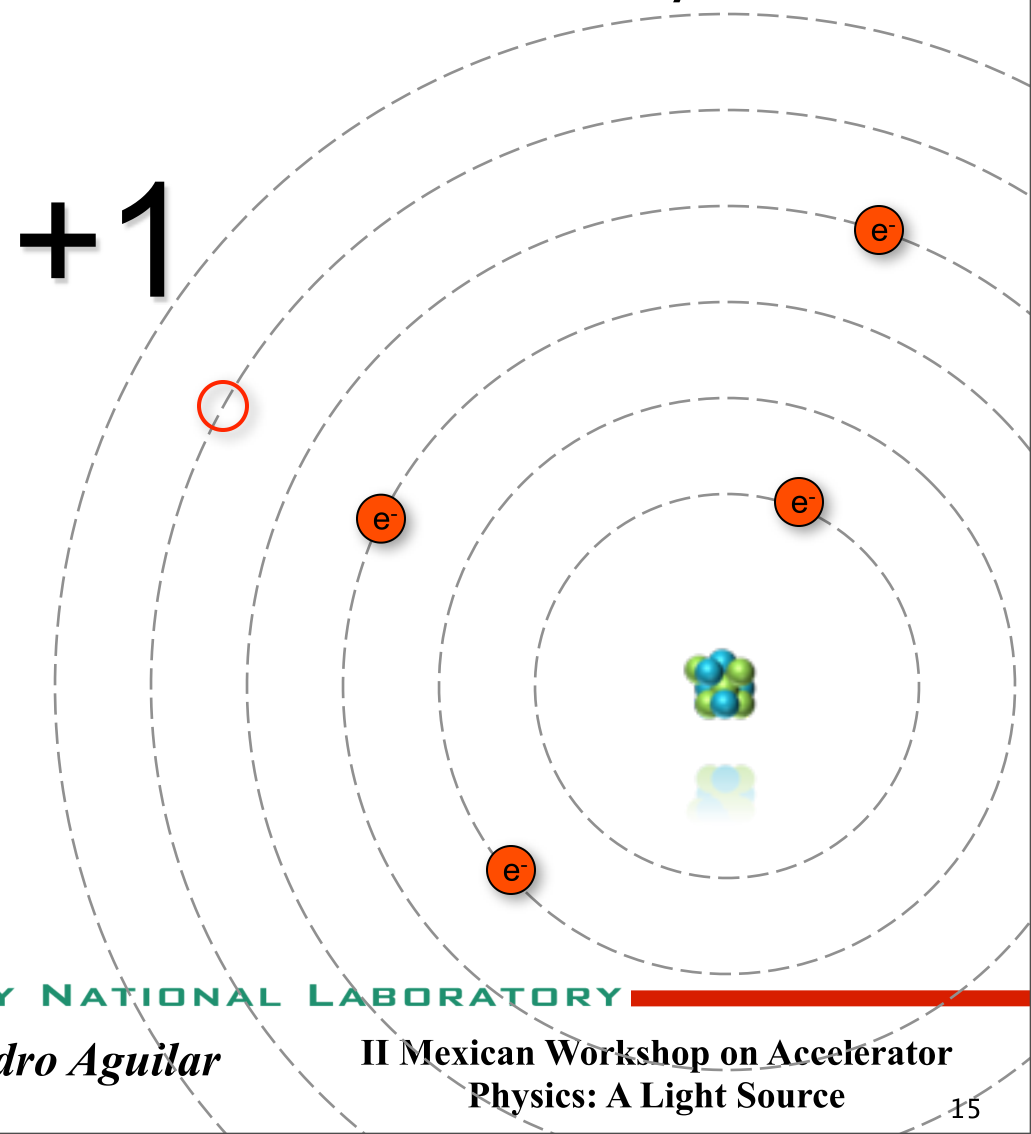

Indirect Photoionization

- Excitation of an inner shell electron, followed by <u>autoionization</u>
  - Lifetimes ≈ nanoseconds – picoseconds
  - Resonances occur at discrete energies

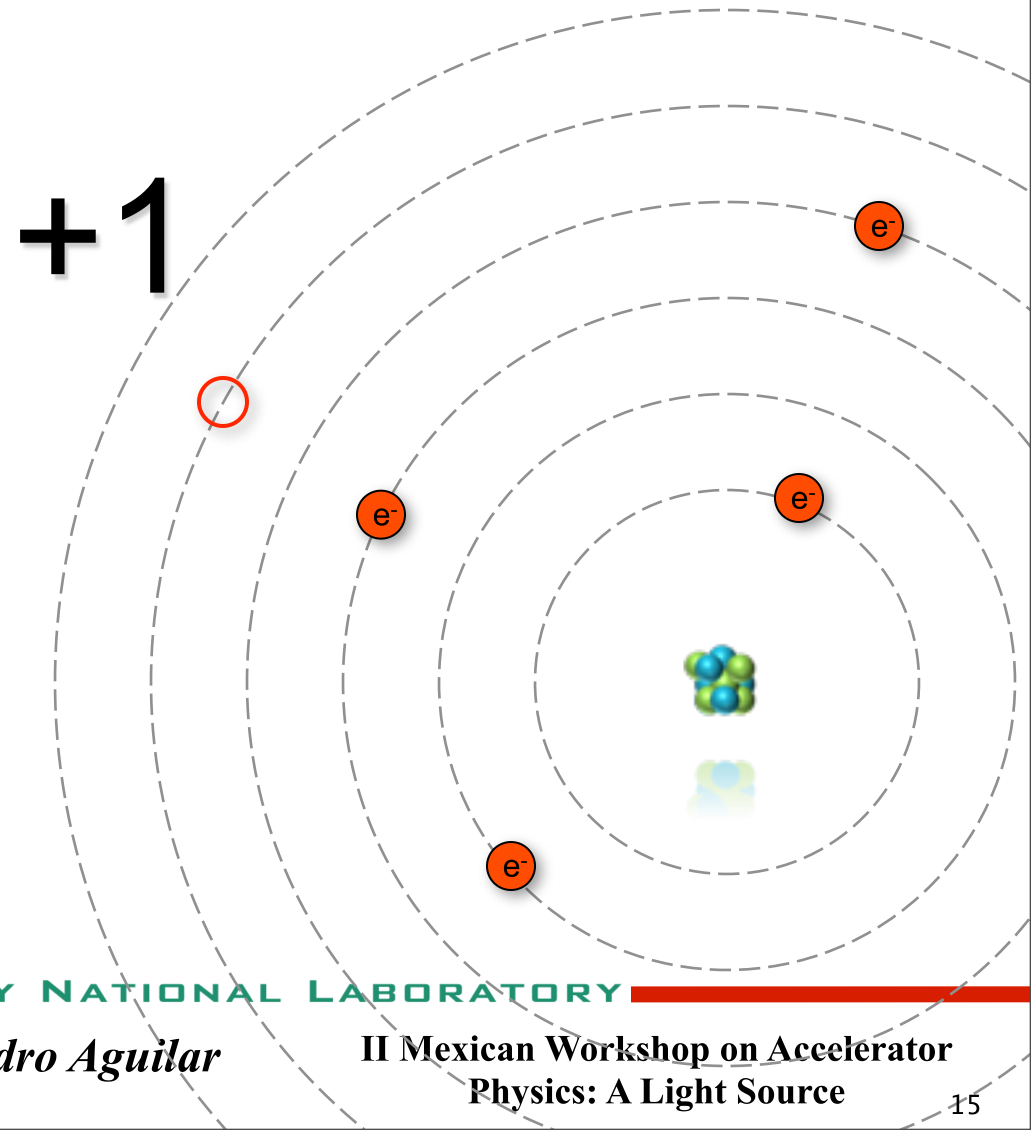

Direct vs. Indirect Photoionization

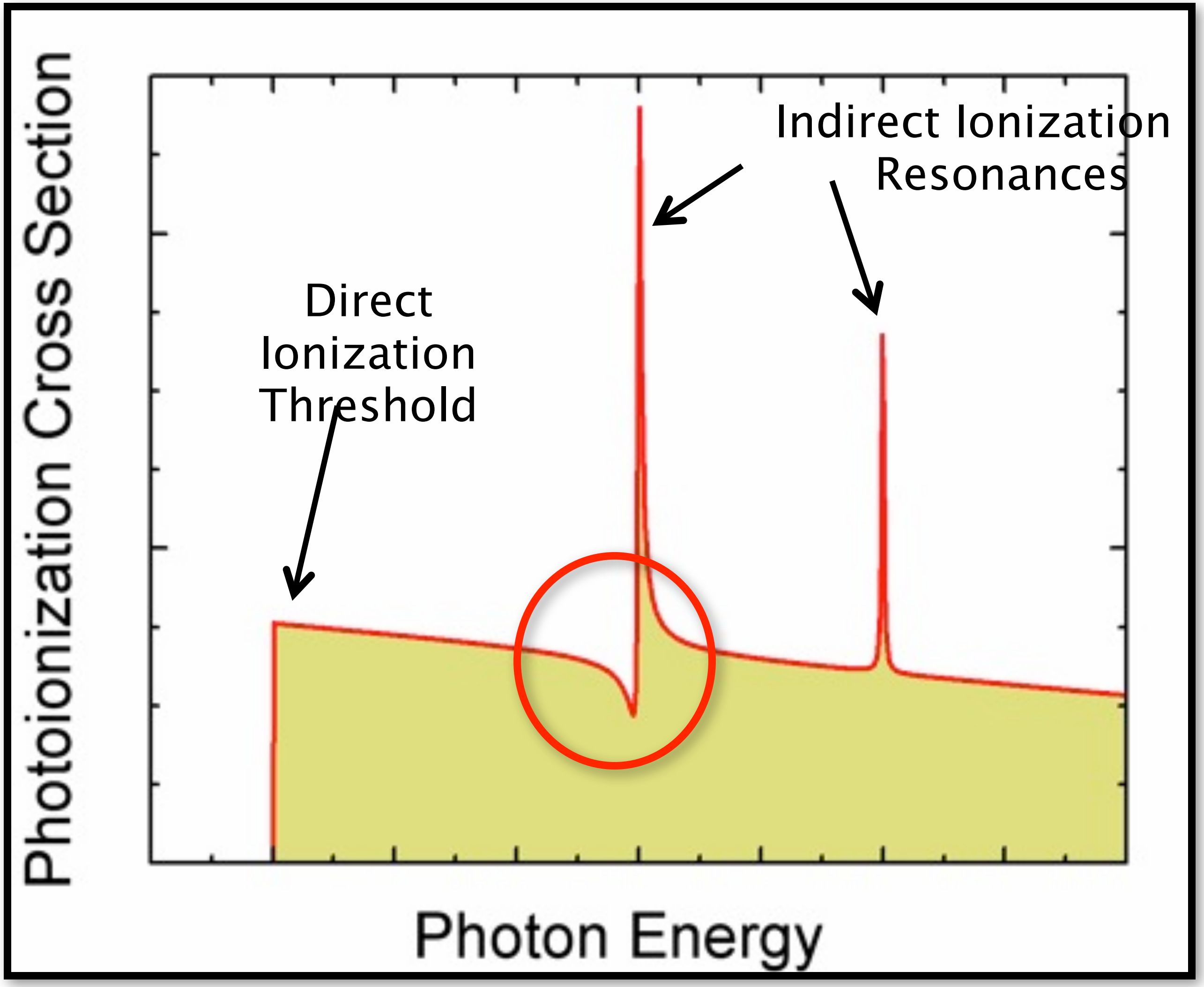

Indirect Photoionization

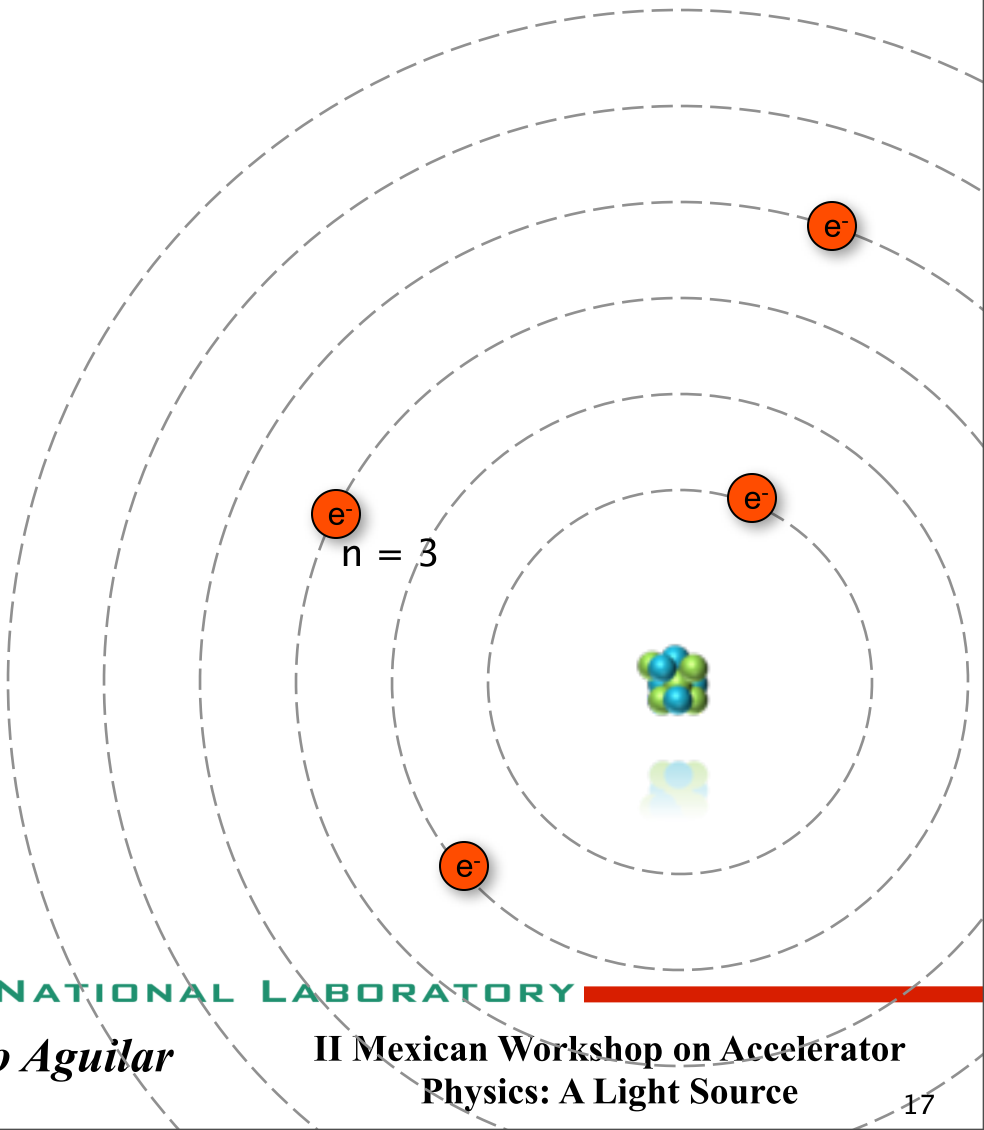

Indirect Photoionization

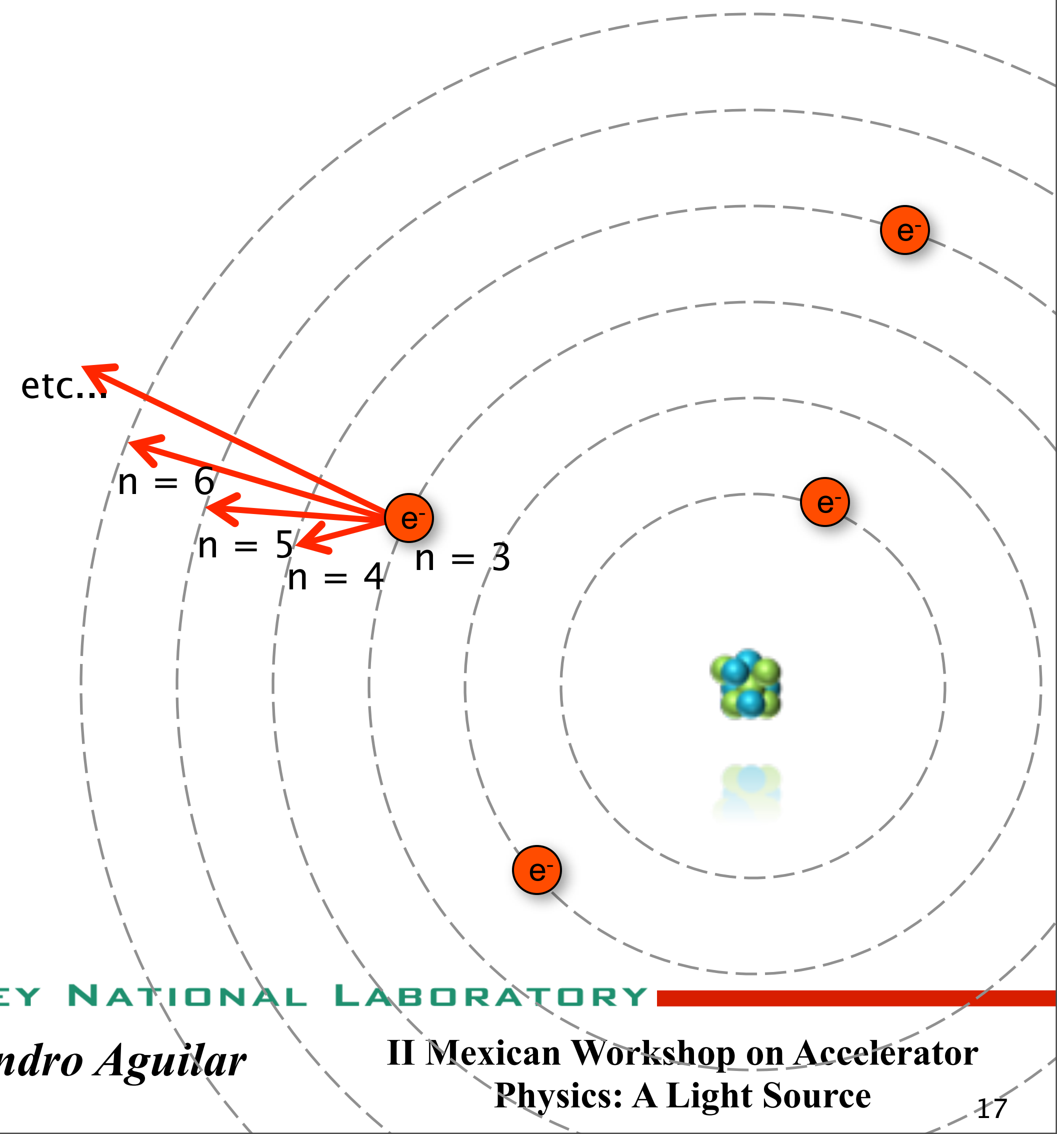

Indirect Photoionization

- As photon energy is increased, core electrons are excited to higher discrete energy levels

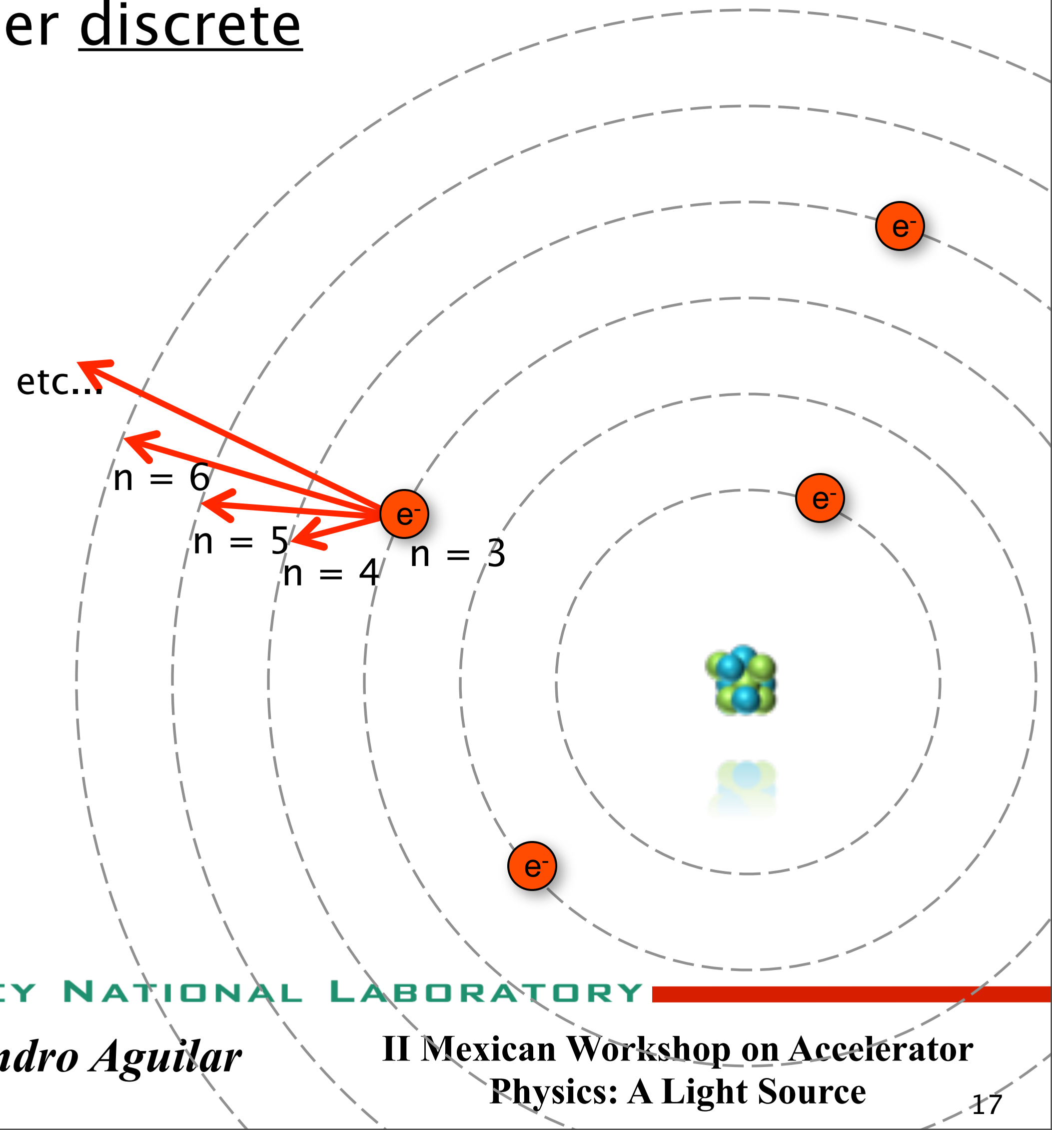

Indirect Photoionization

- As photon energy is increased, core electrons are excited to higher discrete energy levels

- Higher principal quantum number, n

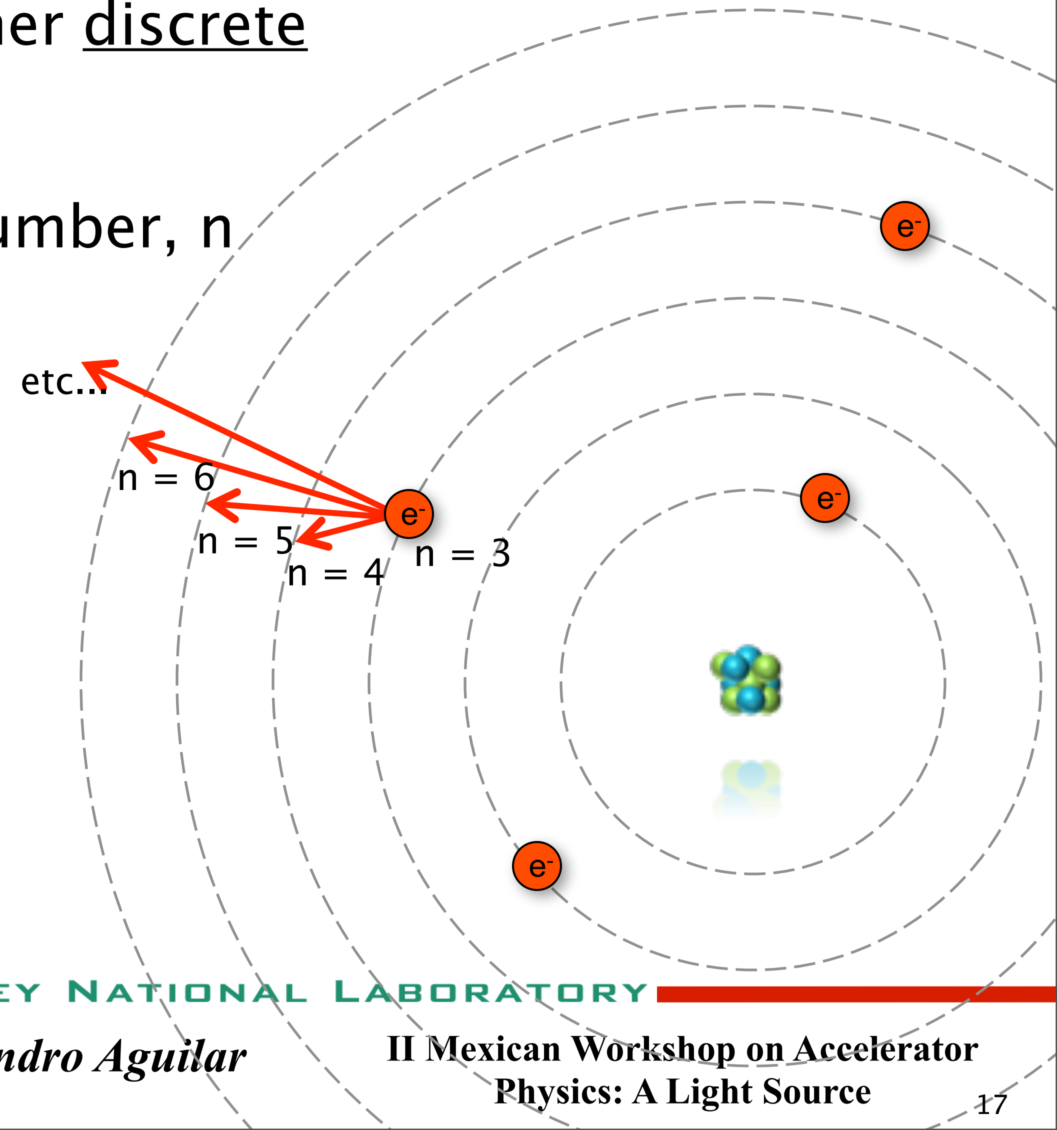

Indirect Photoionization

- As photon energy is increased, core electrons are excited to higher discrete energy levels
- Higher principal quantum number, n
- Resonances follow selection rule criteria

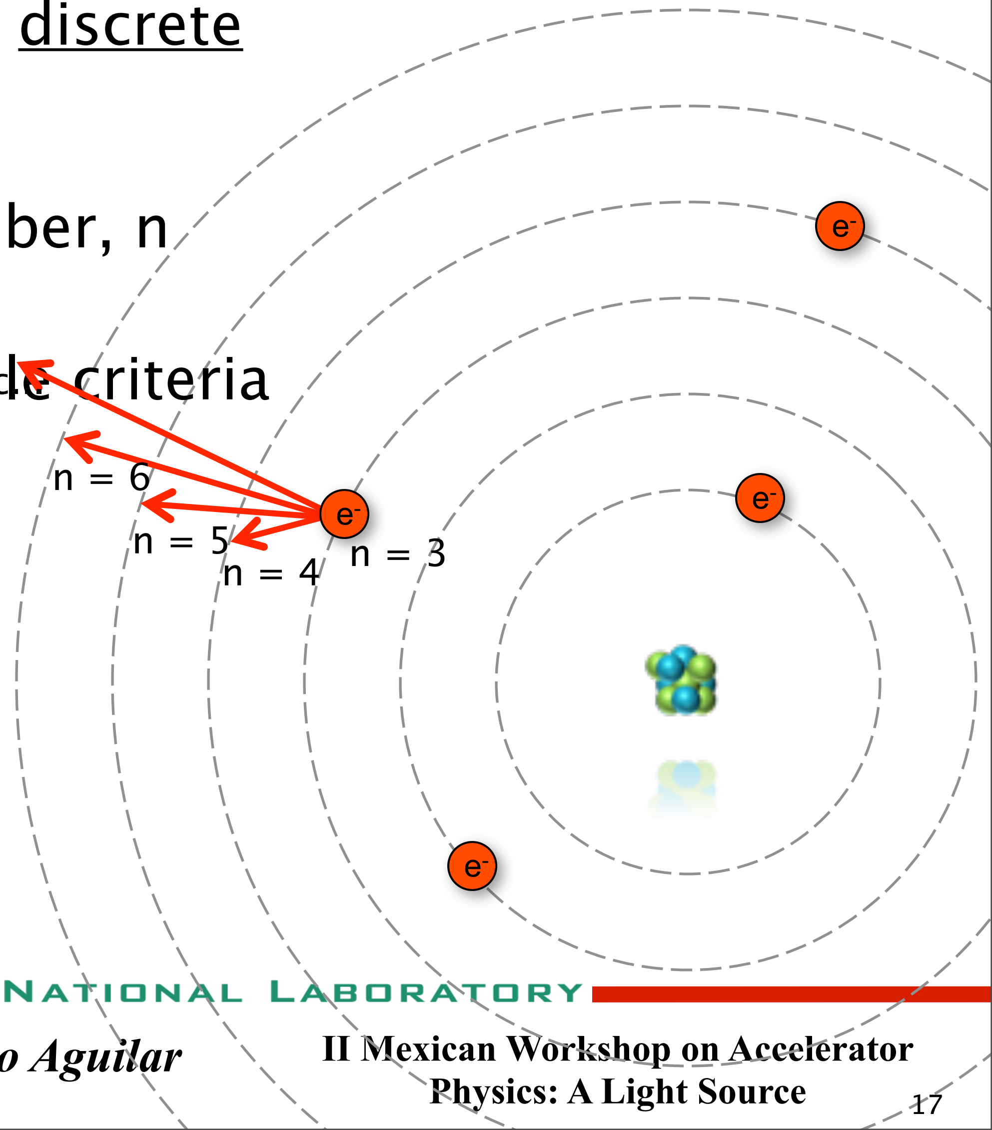

Indirect Ionization & Rydberg Series

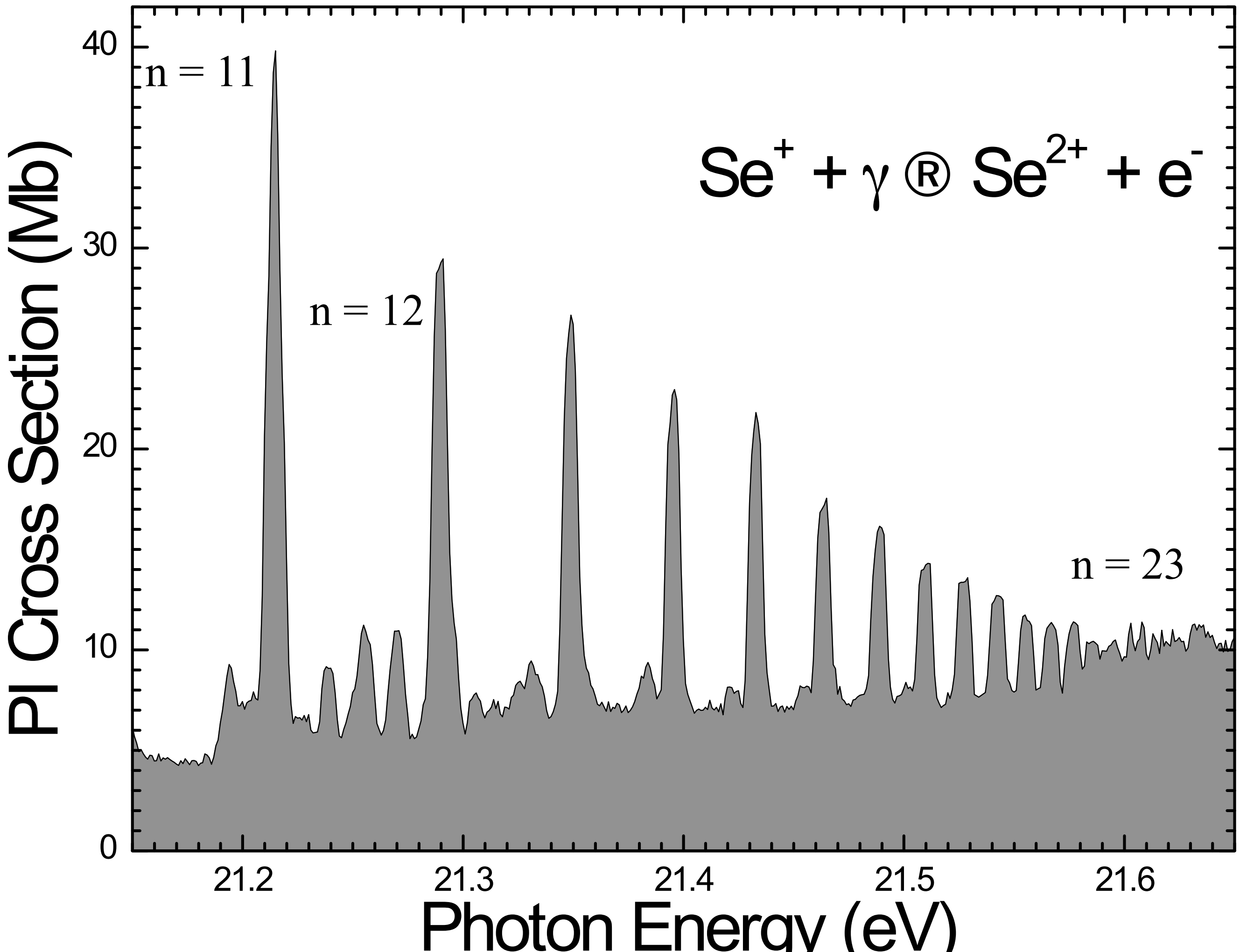

Indirect Ionization & Rydberg Series

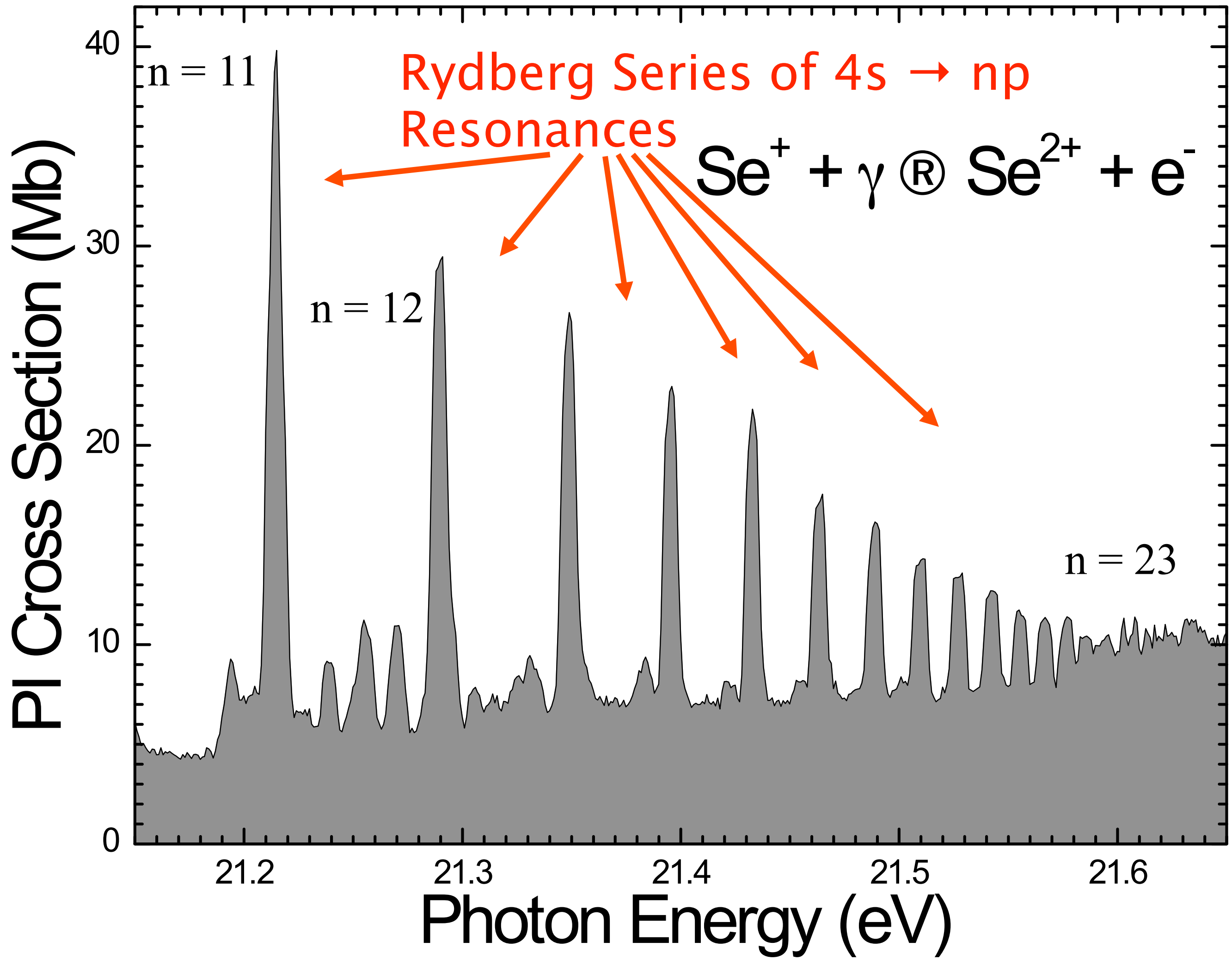

Experimental Technique

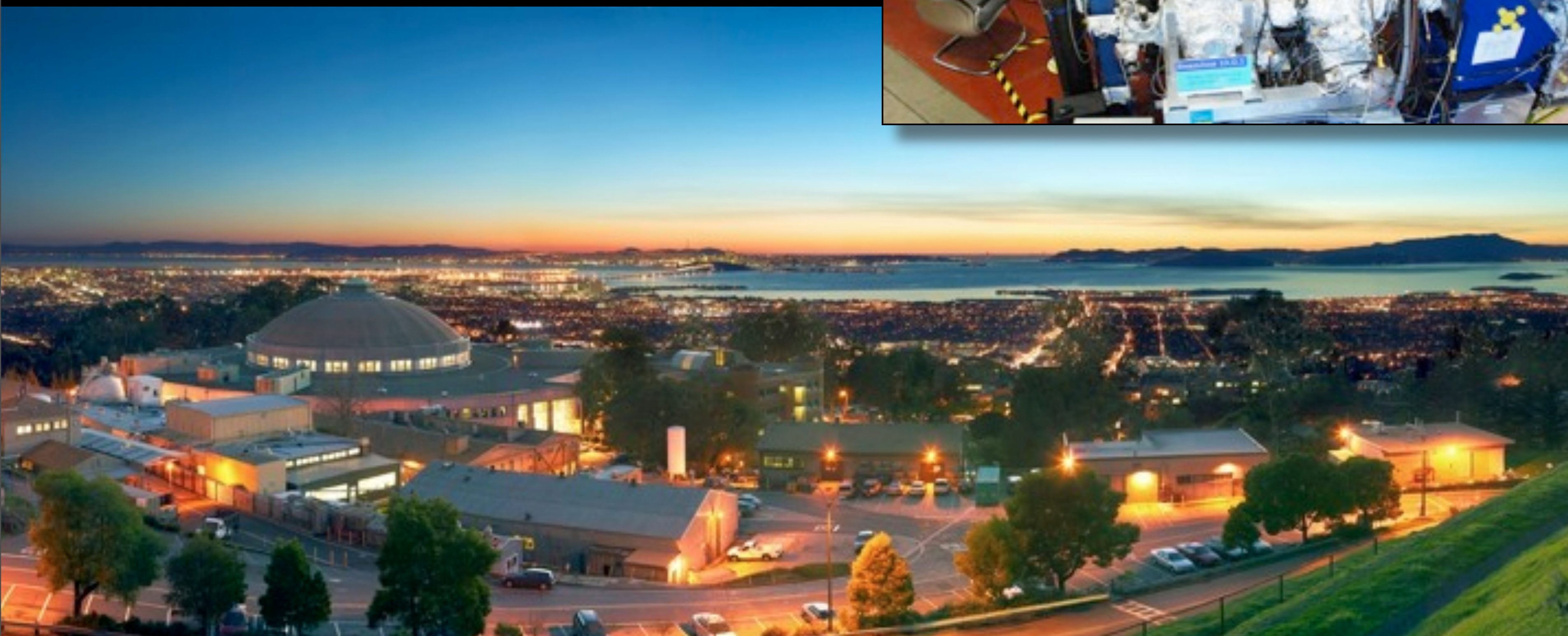

Ion-Photon-Beam (IPB) Endstation

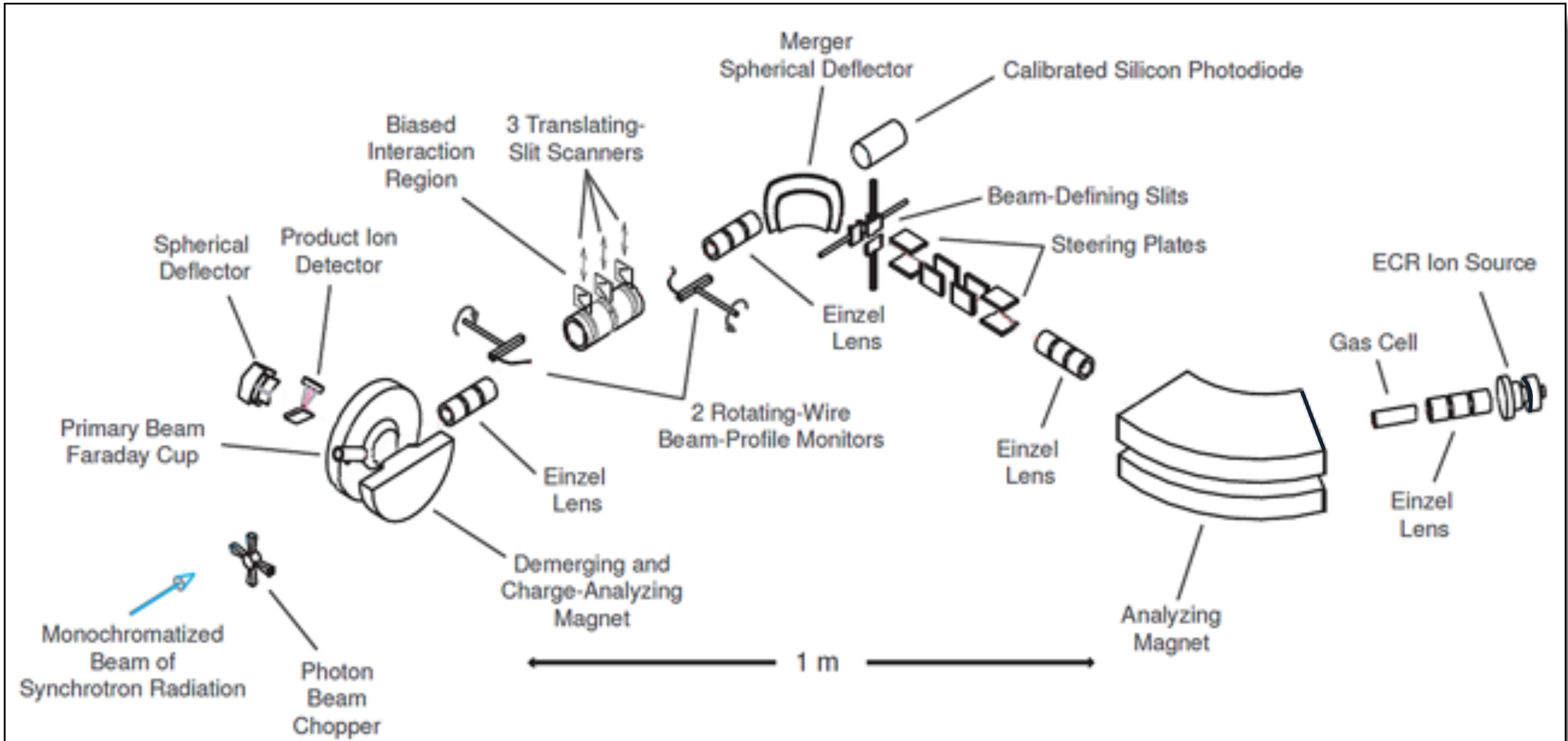

Start with neutral sample

Ion-Photon-Beam (IPB) Endstation

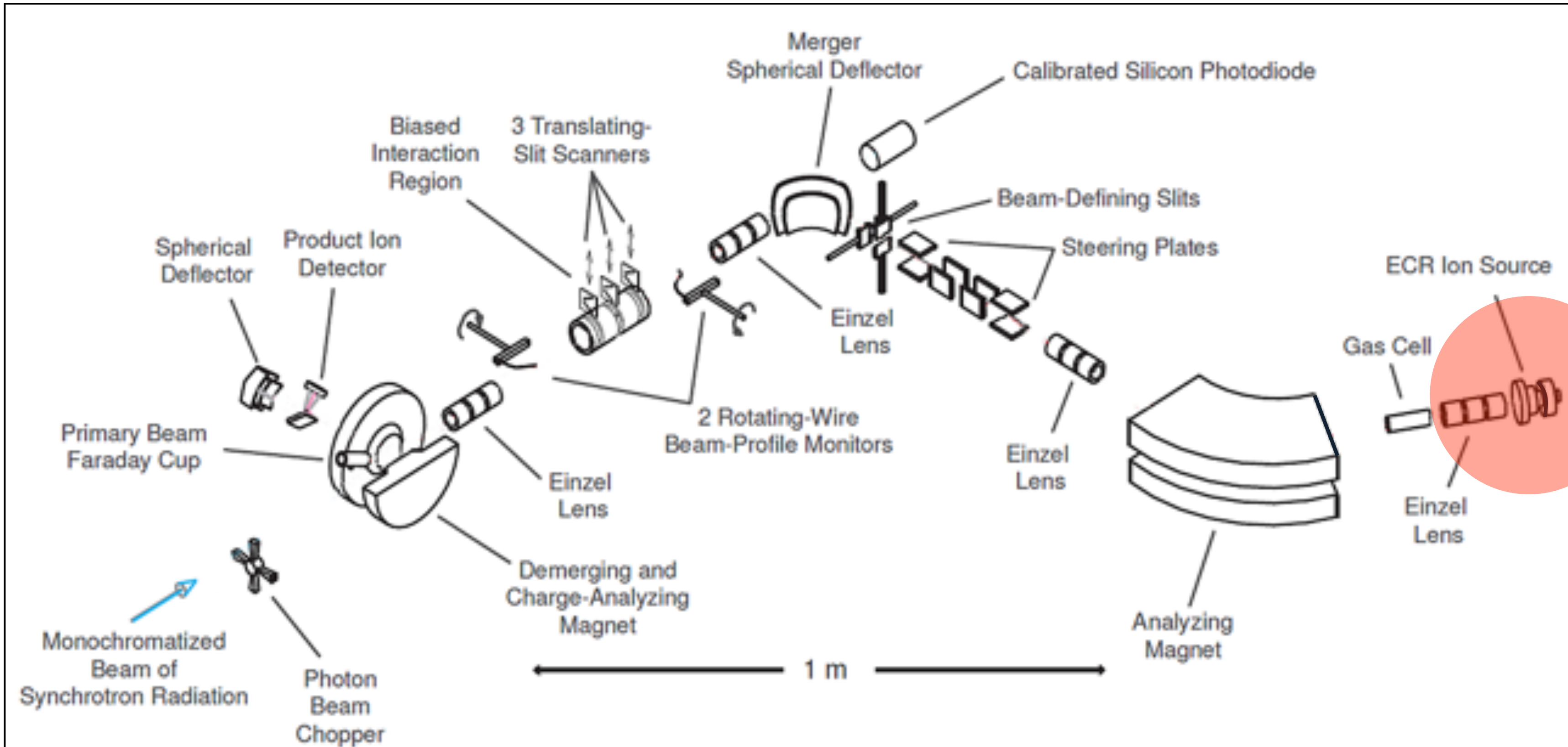

Ionize the sample via electron/atom collisions in an Electron-Cyclotron-Resonance (ECR) Ion Source.

Ion-Photon-Beam (IPB) Endstation

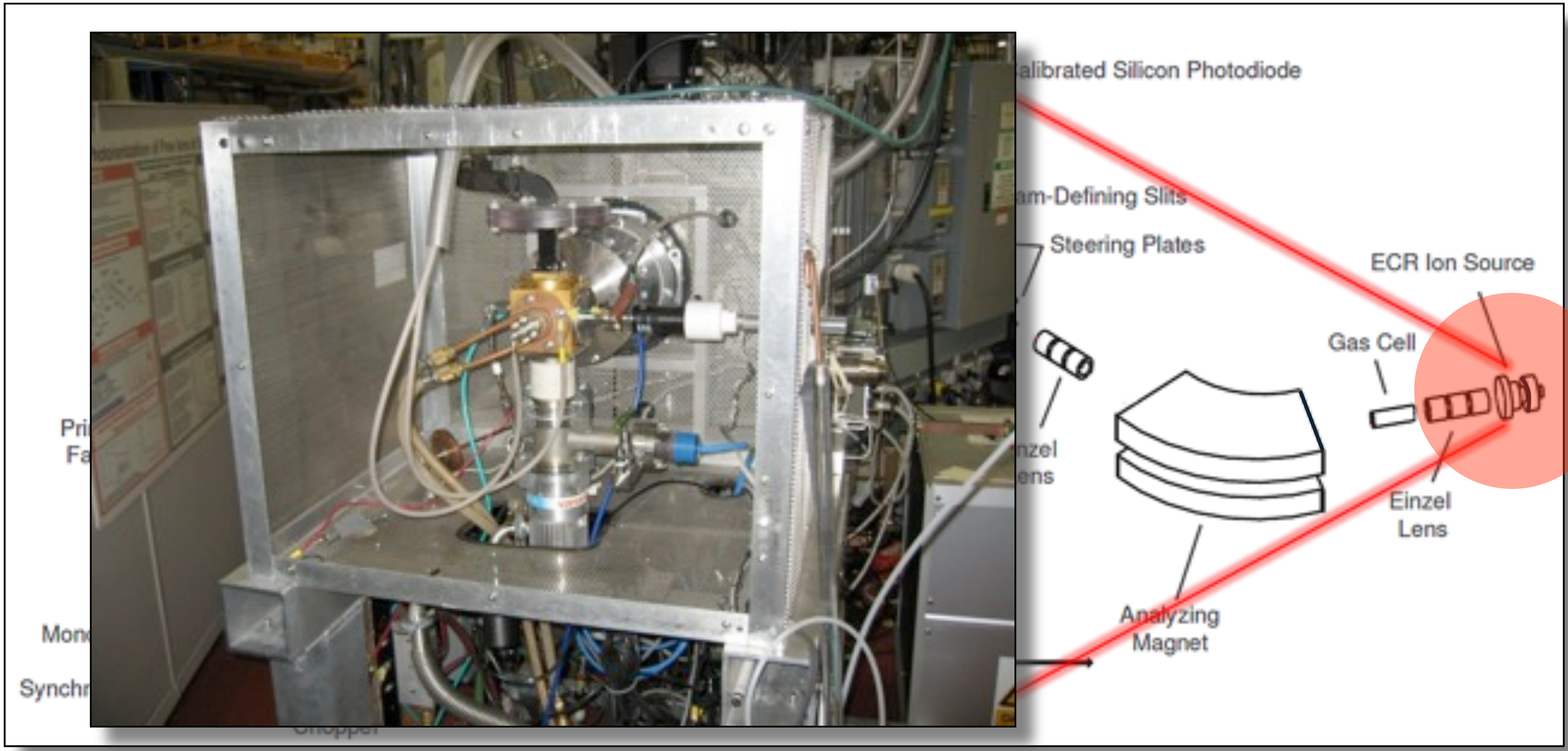

Ionize the sample via electron/atom collisions in an Electron-Cyclotron-Resonance (ECR) Ion Source.

Ion-Photon-Beam (IPB) Endstation

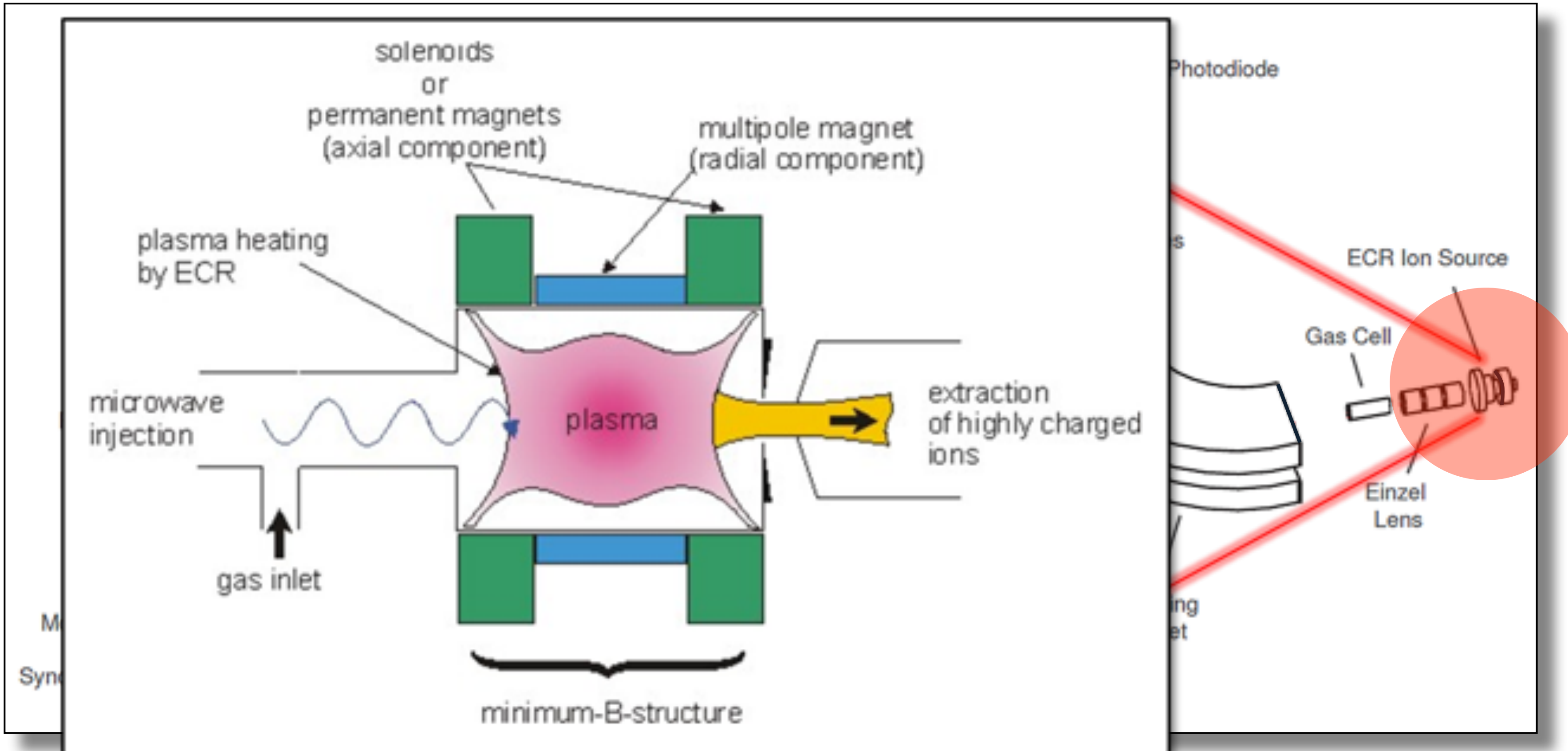

Ionize the sample via electron/atom collisions in an Electron-Cyclotron-Resonance (ECR) Ion Source.

Ion-Photon-Beam (IPB) Endstation

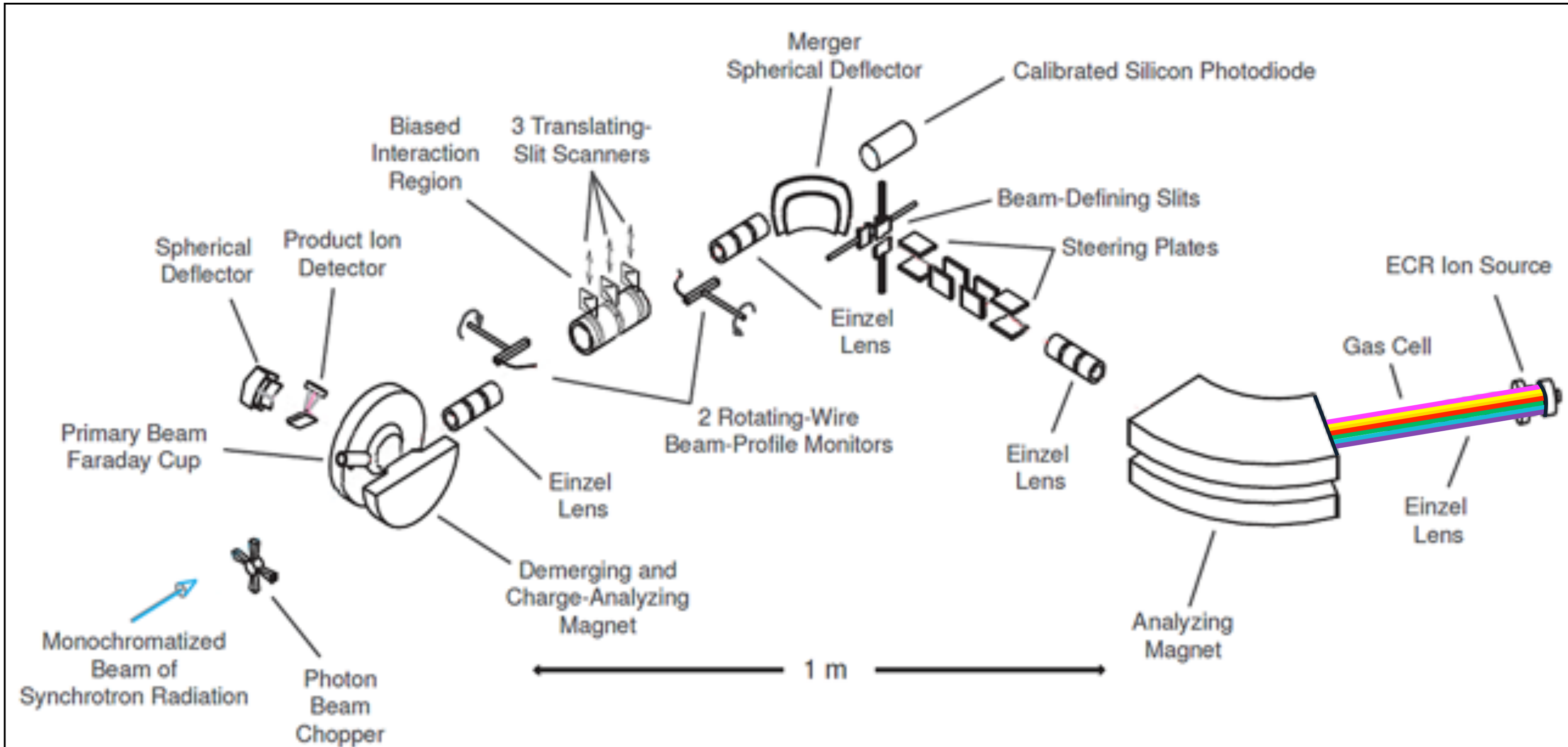

Accelerate the Mixed Ions using a high voltage potential difference.

Ion-Photon-Beam (IPB) Endstation

$$\sigma = \frac{R\, q\, e^2\, v_i\, \varepsilon\, F_{av}}{I_+\, I_\gamma\, L\, \Omega\, \delta\, \Delta}$$

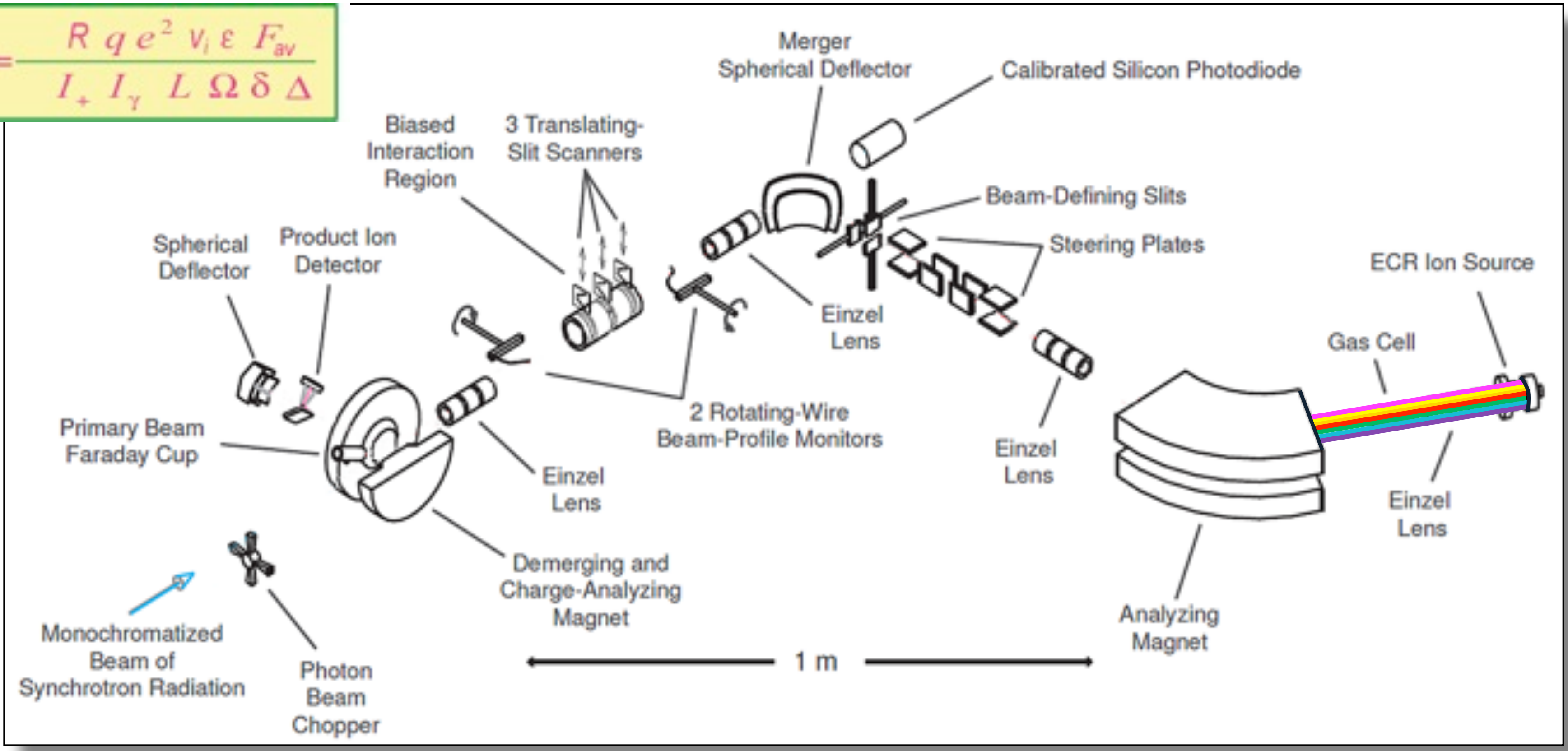

Ion–Photon–Beam (IPB) Endstation

$$\sigma = \frac{R\, q\, e^2\, v_i\, \varepsilon\, F_{av}}{I_+\, I_\gamma\, L\, \Omega\, \delta\, \Delta}$$

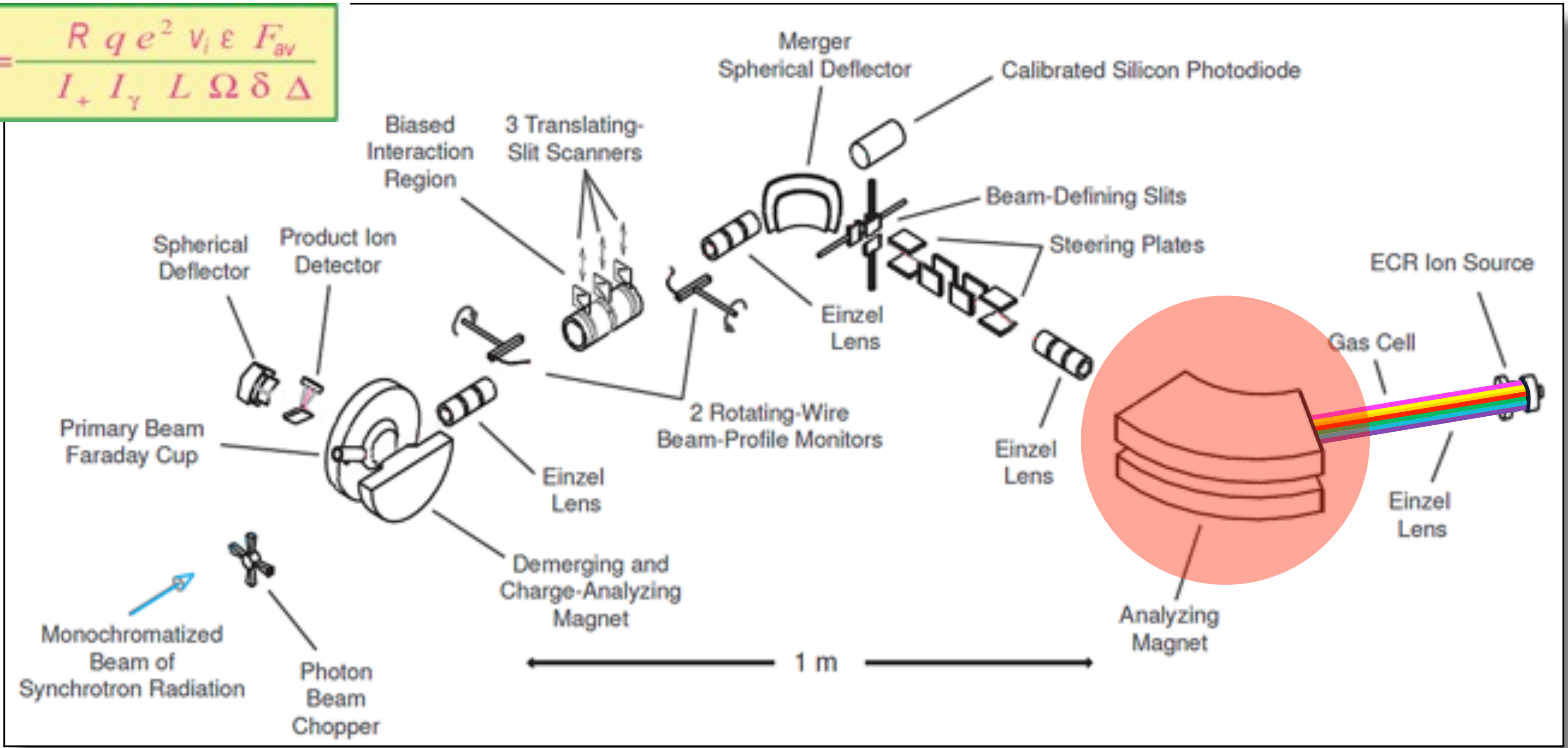

Select the ion to be studied. The analyzing magnet selects based on the mass-to-charge ratio, m/q.

Ion-Photon-Beam (IPB) Endstation

$$\sigma = \frac{R\, q\, e^2\, v_i\, \varepsilon\, F_{av}}{I_+\, I_\gamma\, L\, \Omega\, \delta\, \Delta}$$

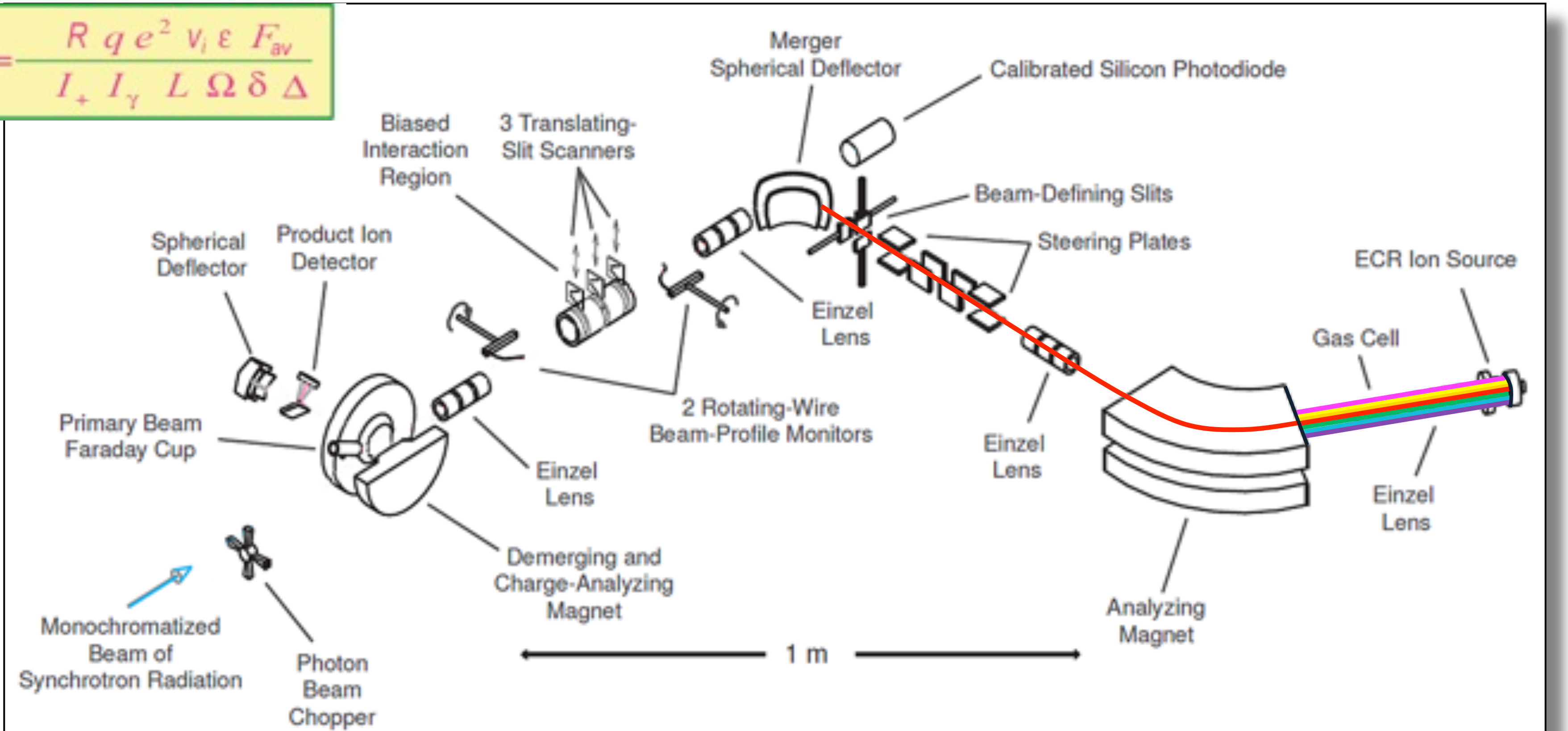

Select the ion to be studied. The analyzing magnet selects based on the mass-to-charge ratio, m/q.

Ion-Photon-Beam (IPB) Endstation

$$\sigma = \frac{R\, q\, e^2\, v_i\, \varepsilon\, F_{av}}{I_+\, I_\gamma\, L\, \Omega\, \delta\, \Delta}$$

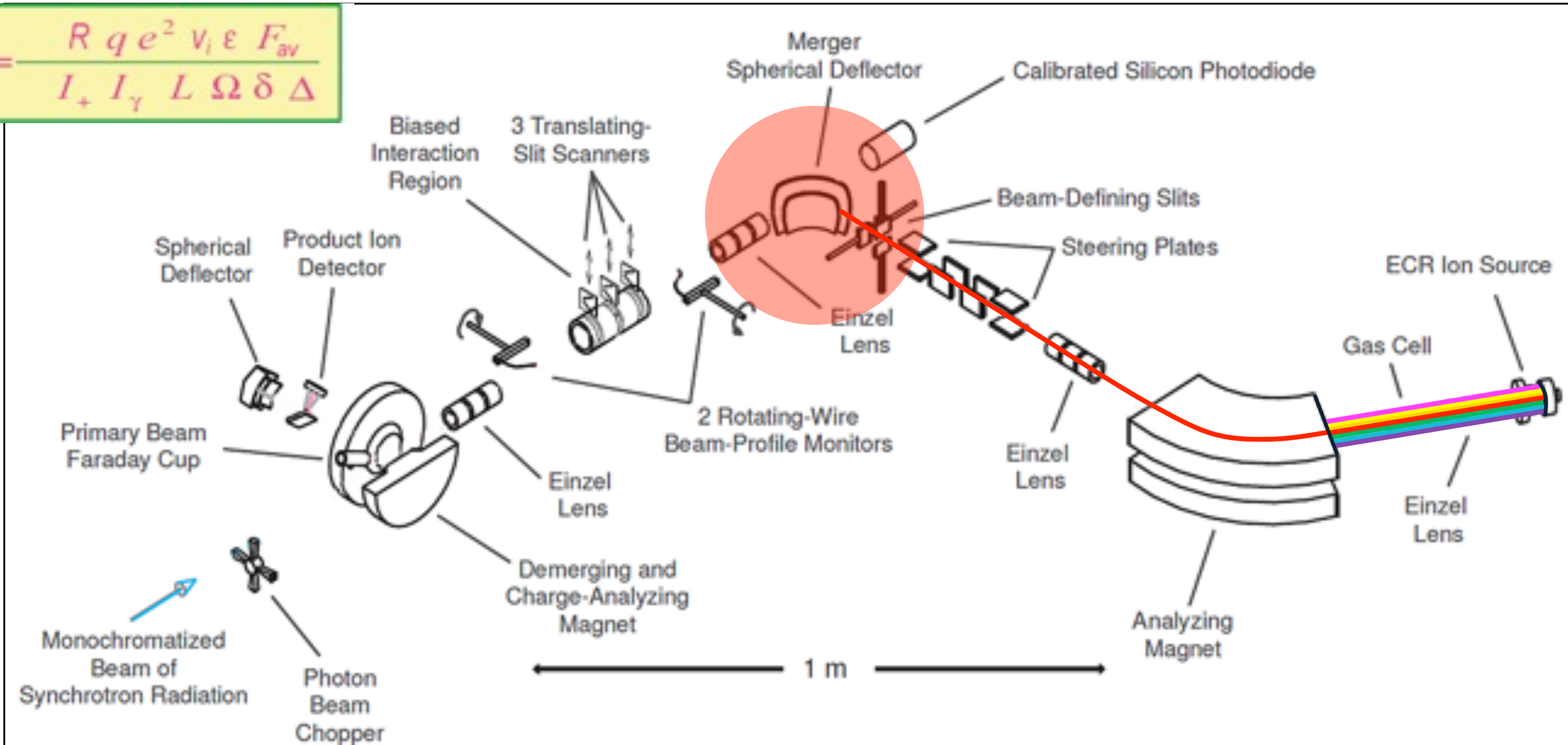

Merge the primary beam with a counter-propagating beam of photons using the merger spherical deflector.

Ion-Photon-Beam (IPB) Endstation

$$\sigma = \frac{R\, q\, e^2\, v_i\, \varepsilon\, F_{av}}{I_+\, I_\gamma\, L\, \Omega\, \delta\, \Delta}$$

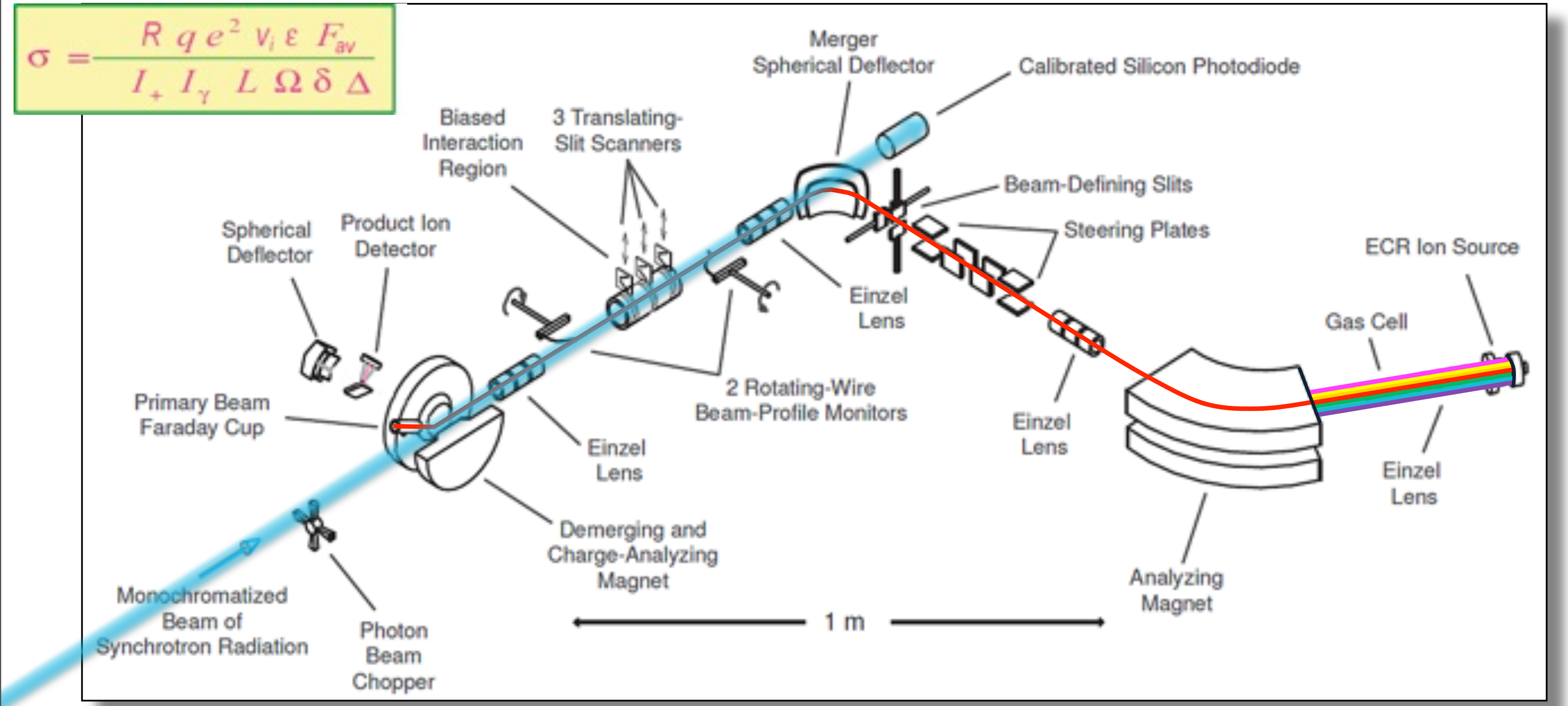

Merge the primary beam with a counter-propagating beam of photons using the merger spherical deflector.

Ion–Photon–Beam (IPB) Endstation

$$\sigma = \frac{R\, q\, e^2\, v_i\, \varepsilon\, F_{av}}{I_+\, I_\gamma\, L\, \Omega\, \delta\, \Delta}$$

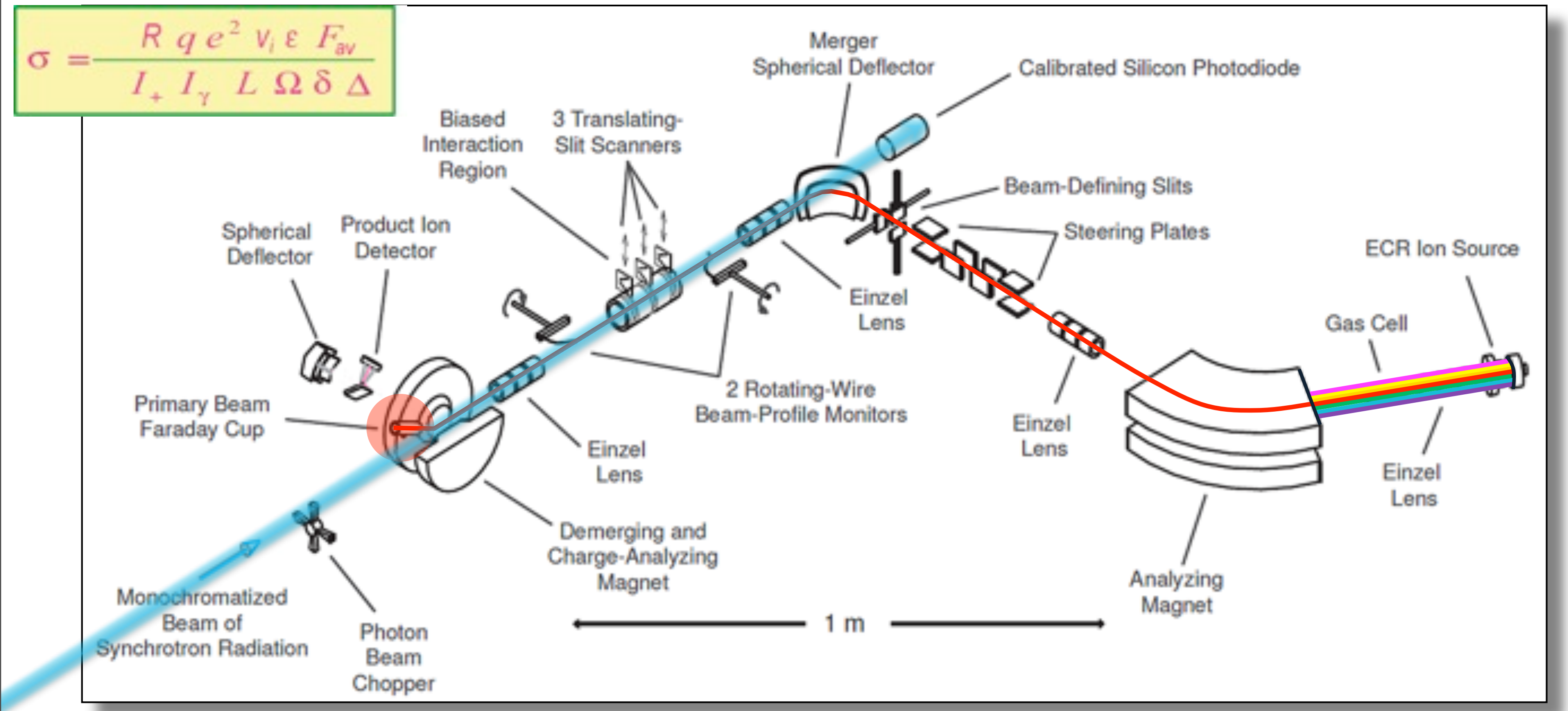

Monitor the primary beam on the beam Faraday cup.

Ion-Photon-Beam (IPB) Endstation

$$\sigma = \frac{R\, q\, e^2\, v_i\, \varepsilon\, F_{av}}{I_+\, I_\gamma\, L\, \Omega\, \delta\, \Delta}$$

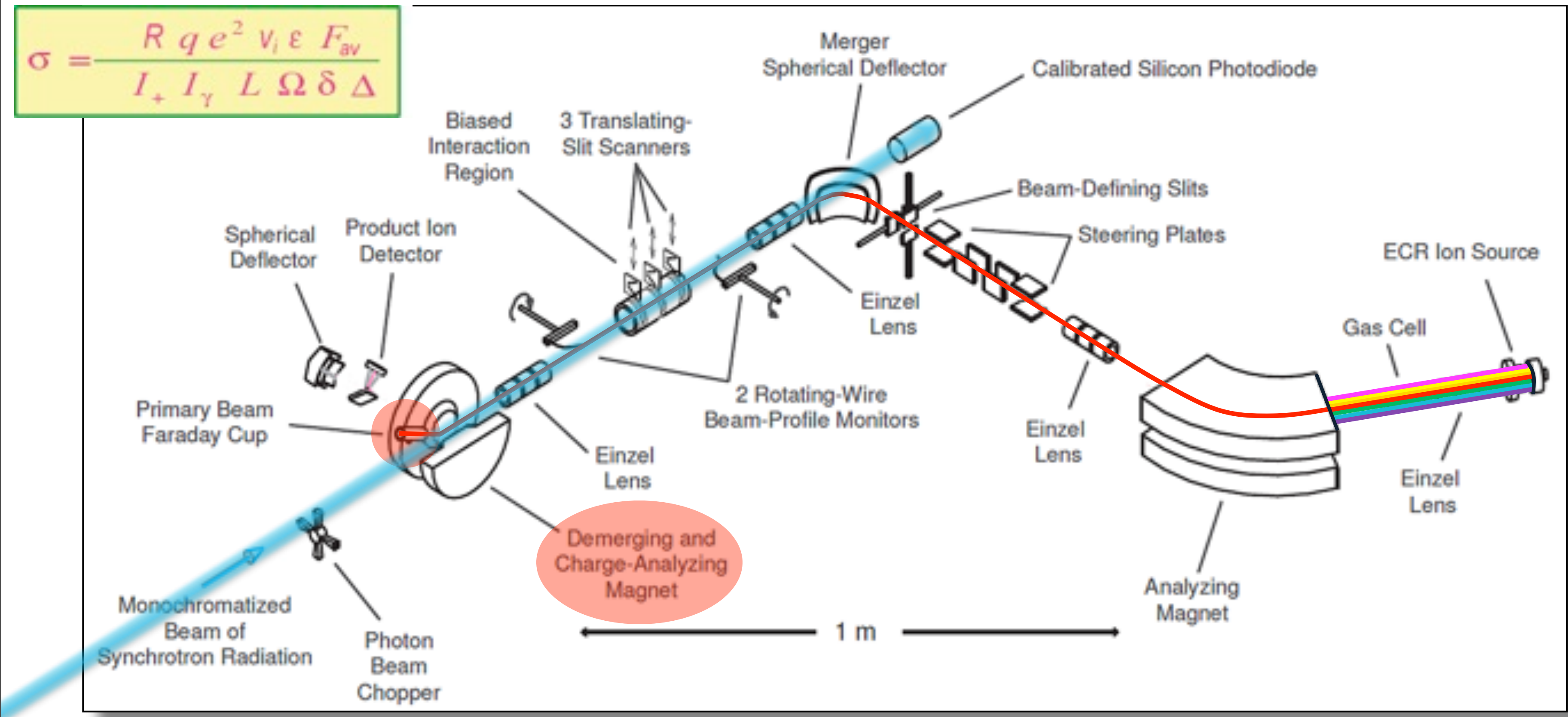

Monitor the primary beam on the beam Faraday cup.

Ion-Photon-Beam (IPB) Endstation

$$\sigma = \frac{R\, q\, e^2\, v_i\, \varepsilon\, F_{av}}{I_+\, I_\gamma\, L\, \Omega\, \delta\, \Delta}$$

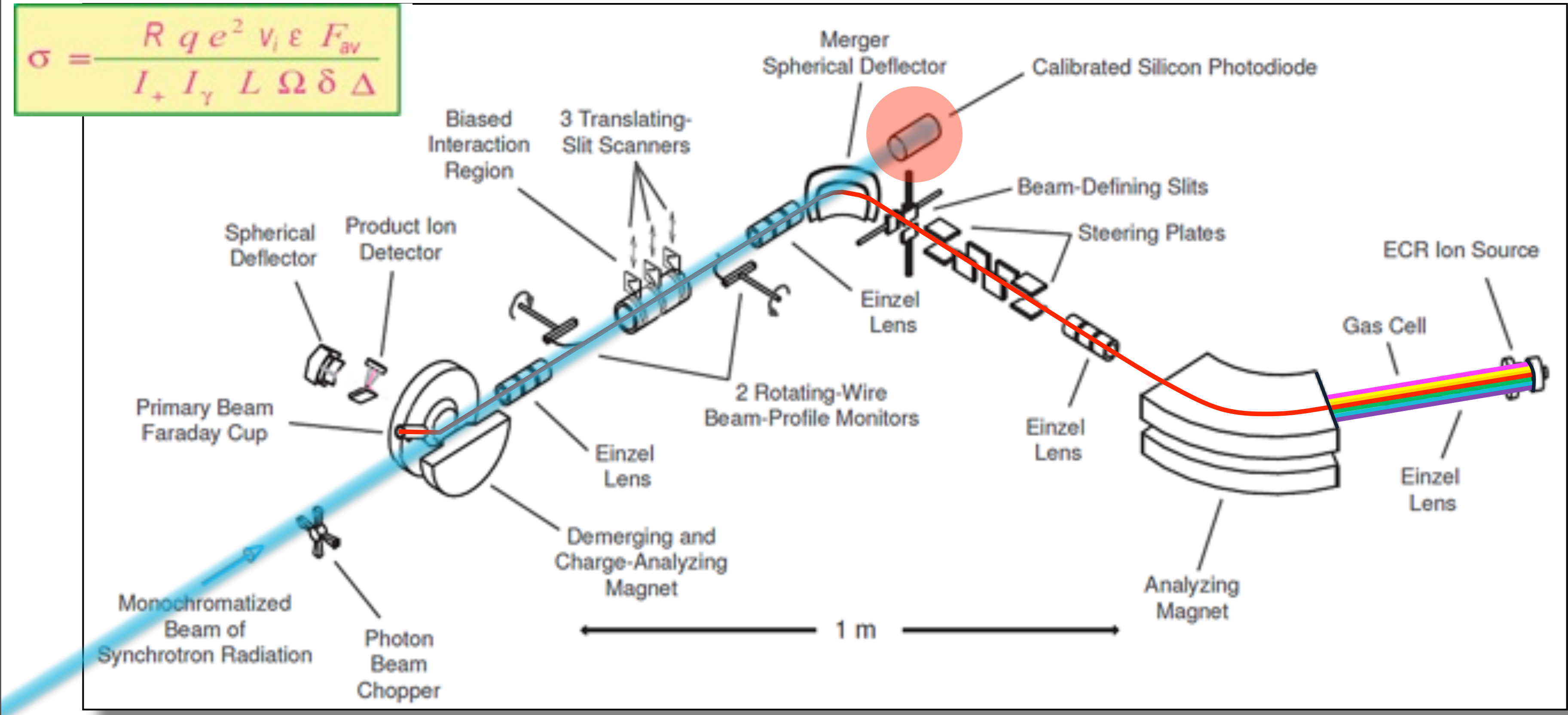

Monitor the photon flux on a calibrated silicon photodiode.

Ion–Photon–Beam (IPB) Endstation

$$\sigma = \frac{R\, q\, e^2\, v_i\, \varepsilon\, F_{av}}{I_+\, I_\gamma\, L\, \Omega\, \delta\, \Delta}$$

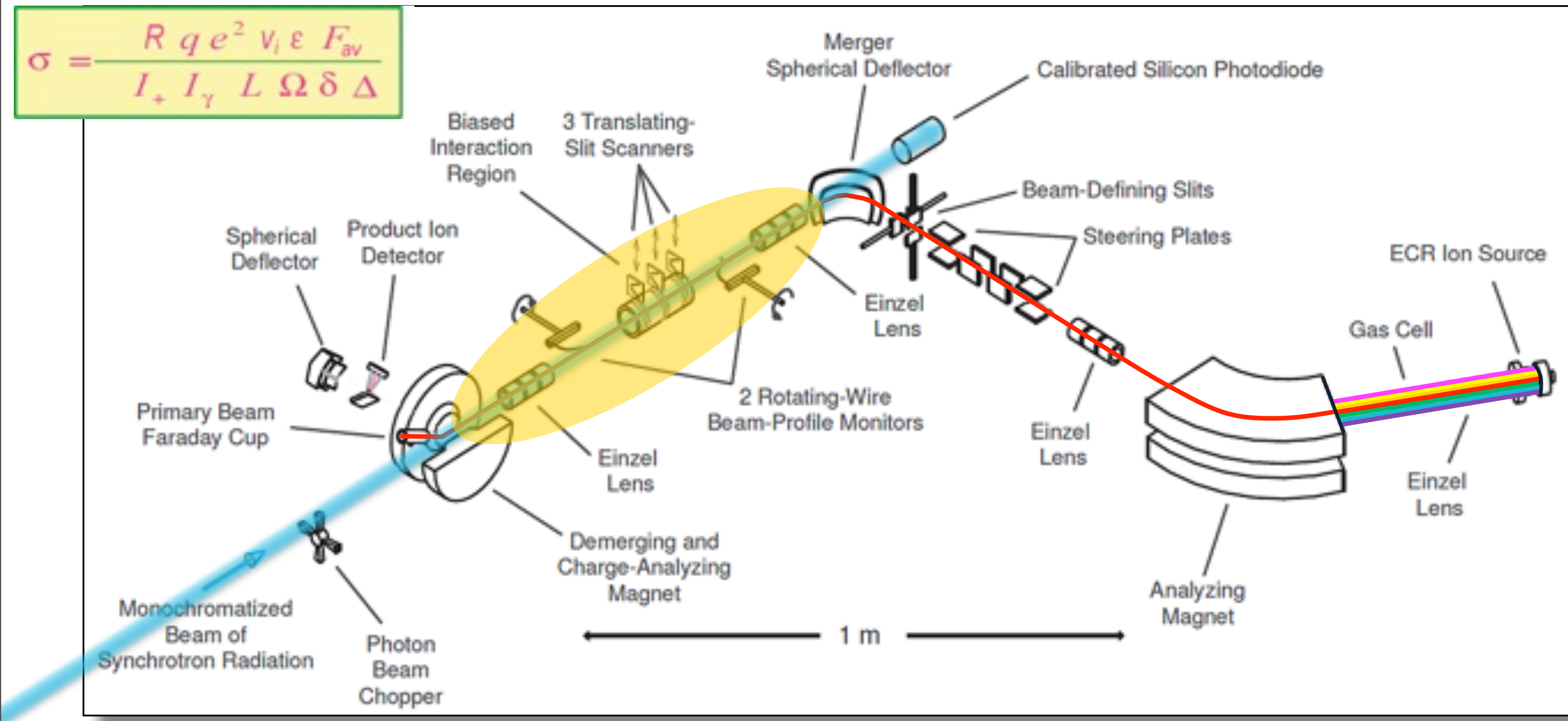

Determine the specific interaction region.

Ion-Photon-Beam (IPB) Endstation

$$\sigma = \frac{R\, q\, e^2\, v_i\, \varepsilon\, F_{av}}{I_+\, I_\gamma\, L\, \Omega\, \delta\, \Delta}$$

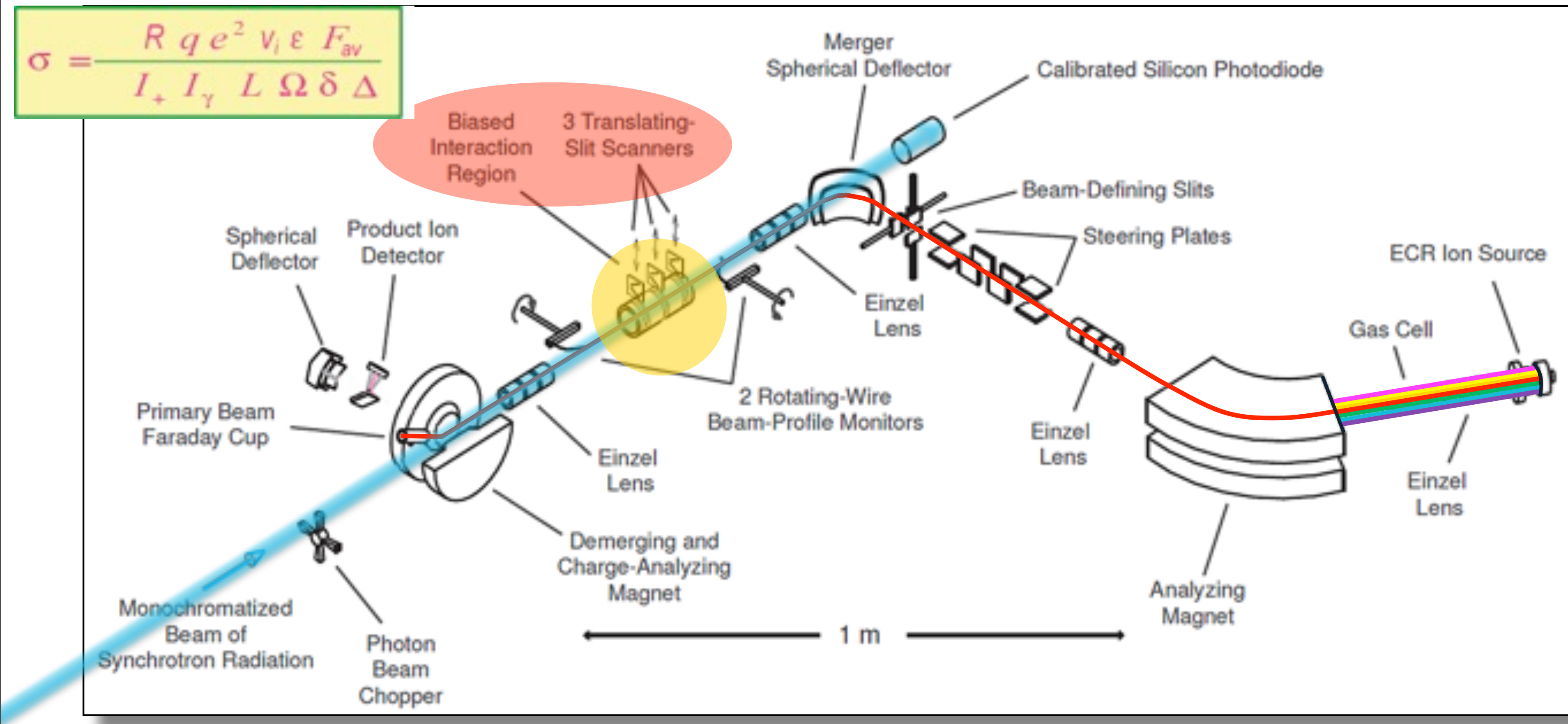

Determine the specific interaction region.

Ion-Photon-Beam (IPB) Endstation

$$\sigma = \frac{R\, q\, e^2\, v_i\, \varepsilon\, F_{av}}{I_+\, I_\gamma\, L\, \Omega\, \delta\, \Delta}$$

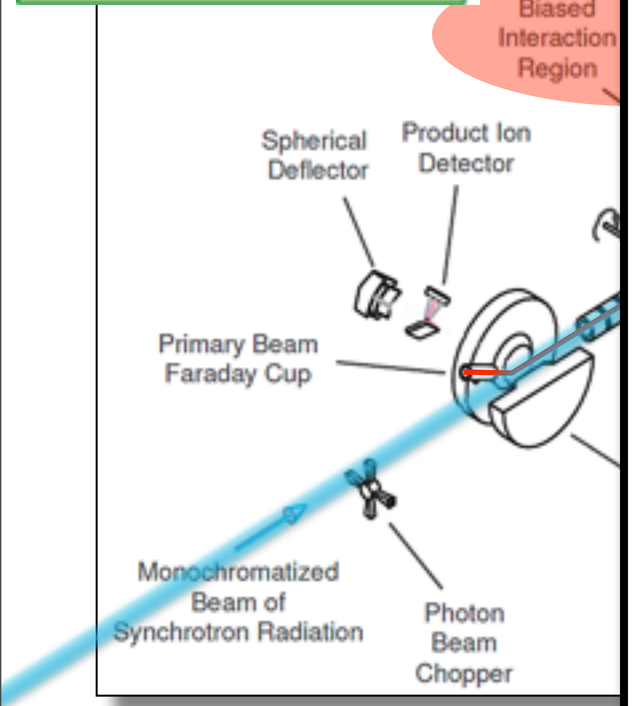

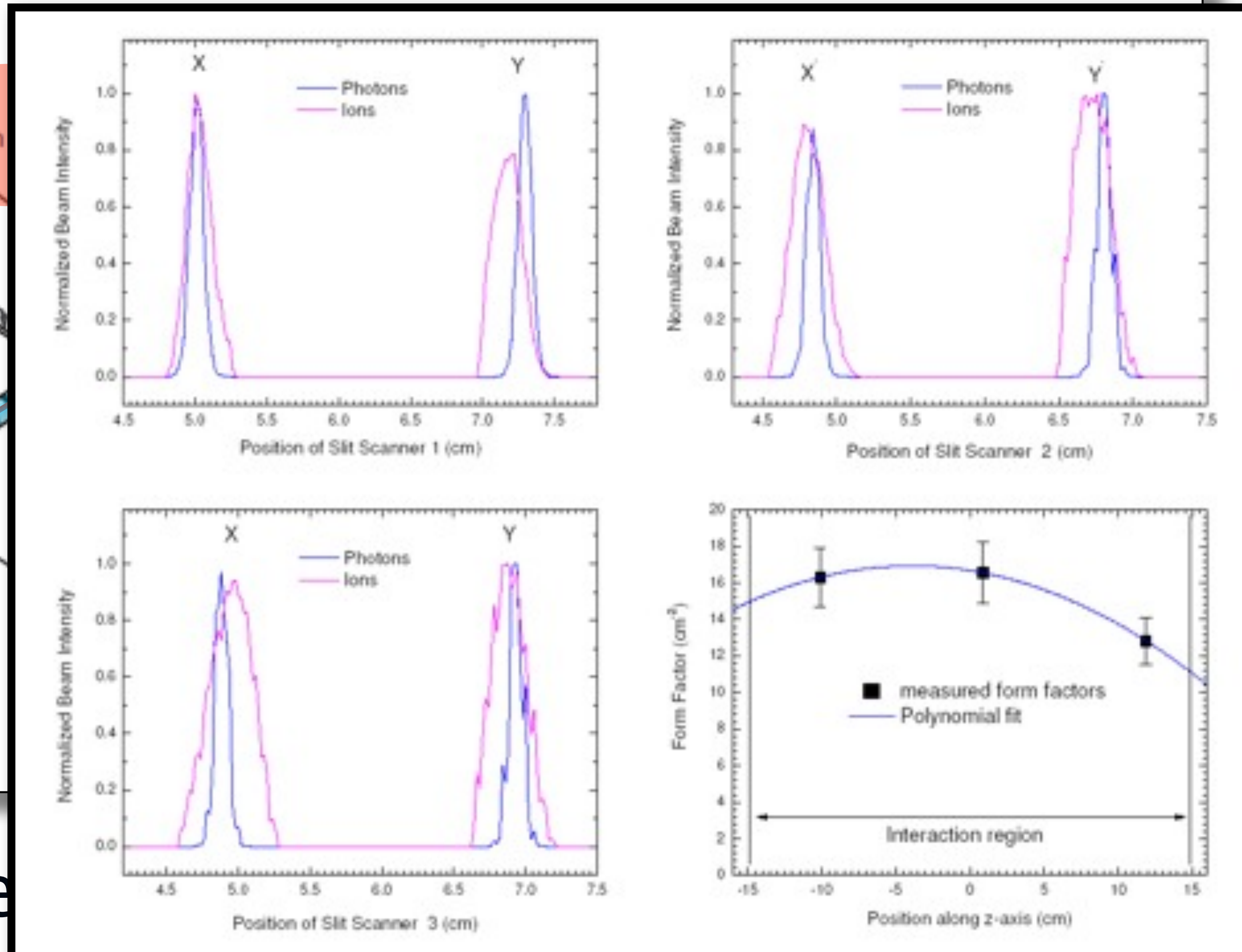

Determine the

Ion–Photon–Beam (IPB) Endstation

$$\sigma = \frac{R\, q\, e^2\, v_i\, \varepsilon\, F_{av}}{I_+\, I_\gamma\, L\, \Omega\, \delta\, \Delta}$$

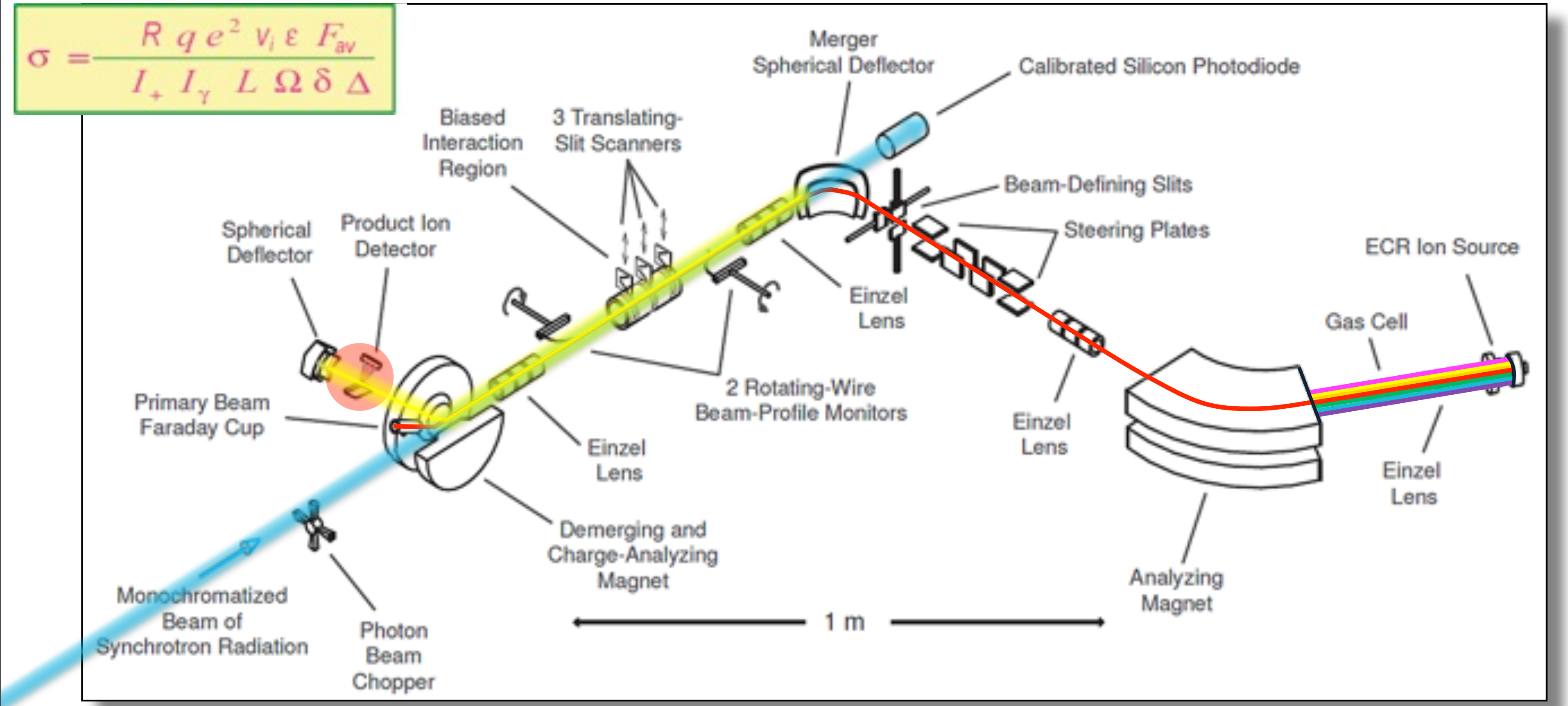

Count the photo-ions on a single particle channeltron detector.

Ion-Photon-Beam (IPB) Endstation

$$\sigma = \frac{R\, q\, e^2\, v_i\, \varepsilon\, F_{av}}{I_+\, I_\gamma\, L\, \Omega\, \delta\, \Delta}$$

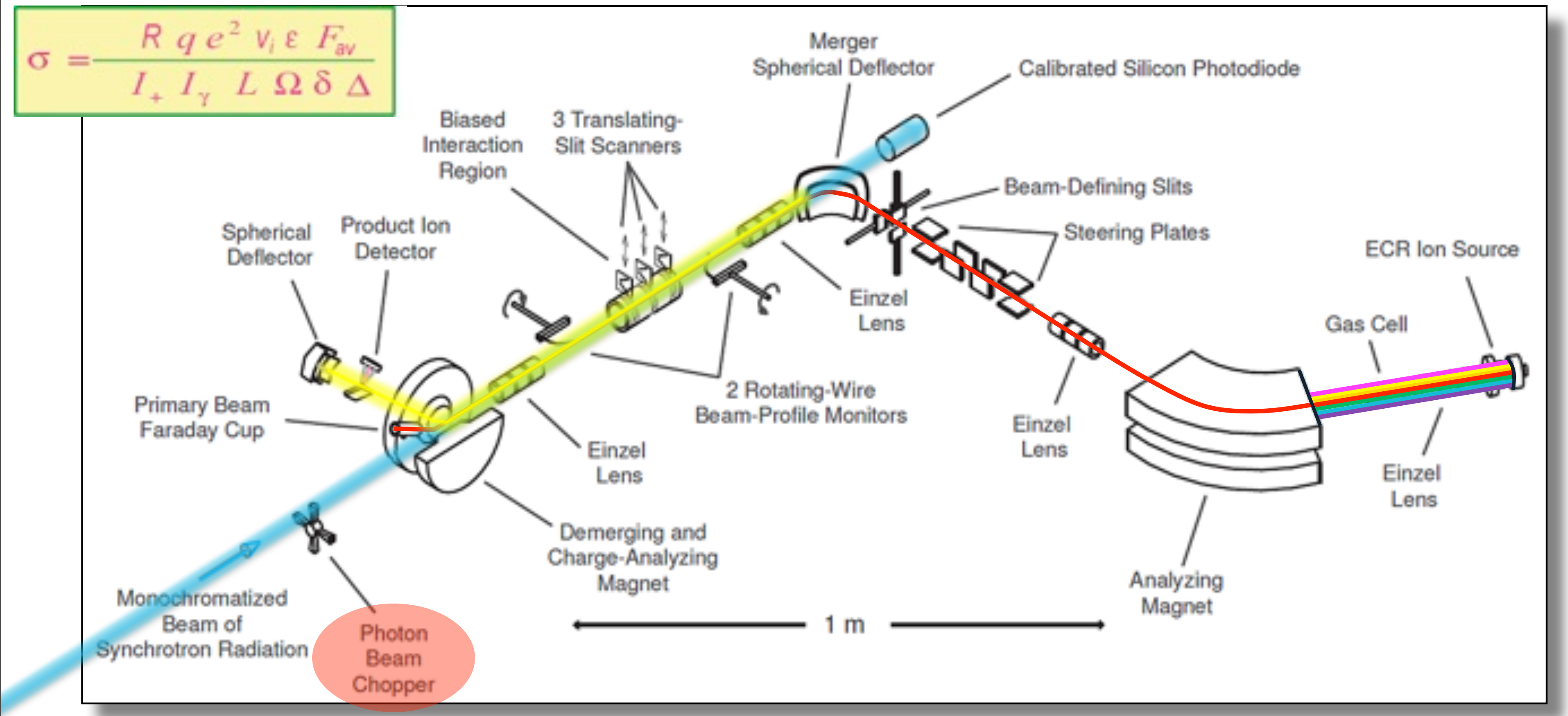

Simultaneously measure background using a mechanical photon chopper.

The Experiment

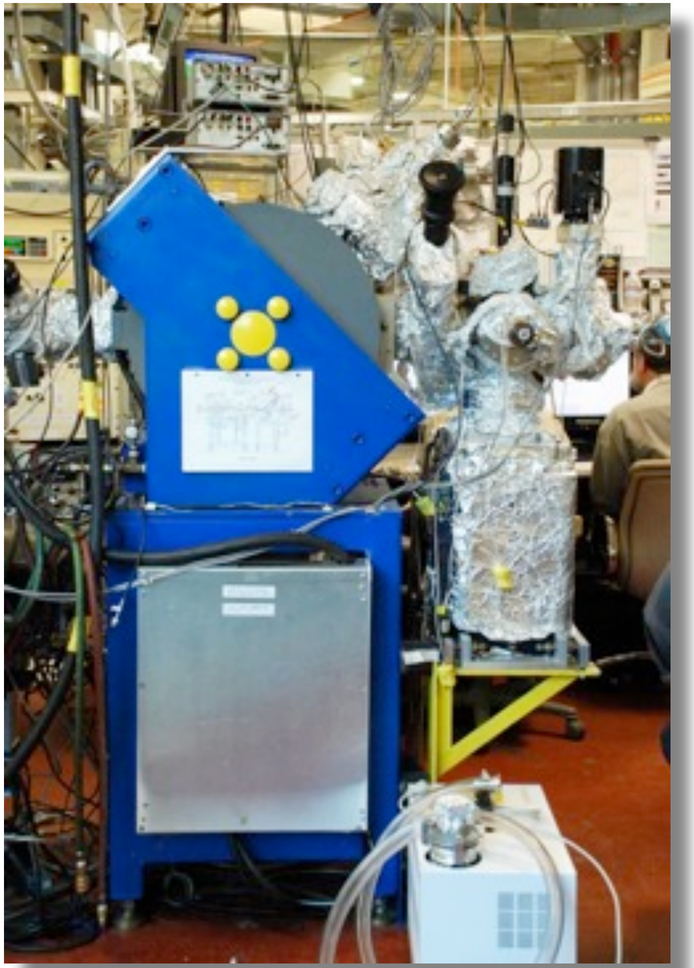

The Experiment

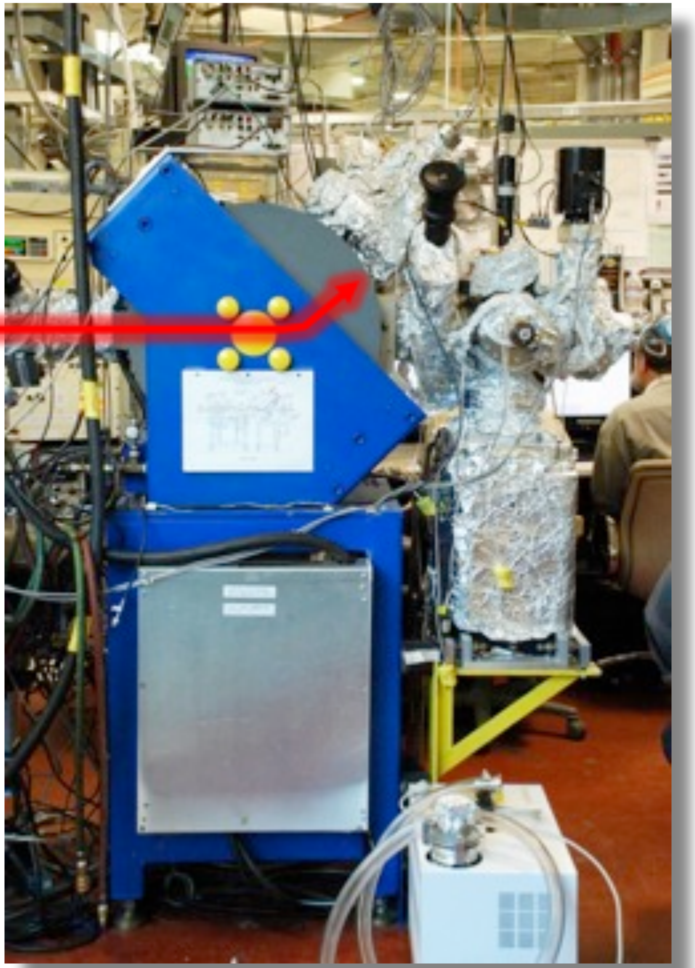

Primary Ion Beam

Se^{+}

The Experiment

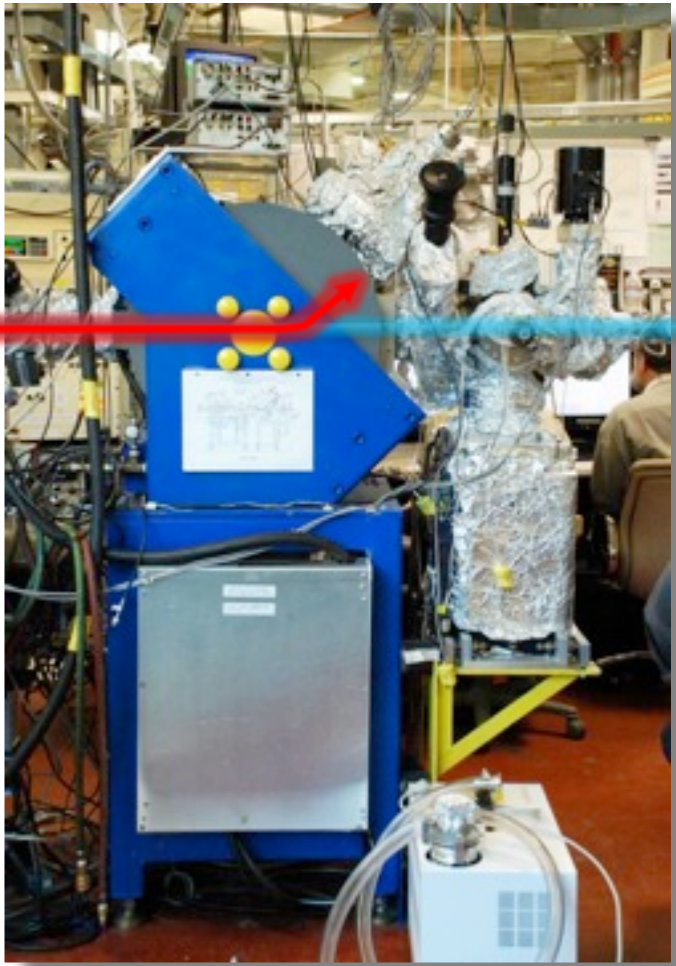

Photon Beam

Primary Ion Beam

Se^+

The Experiment

Product Photo-ion Beam

Se^{2+}

Primary Ion Beam

Se^{+}

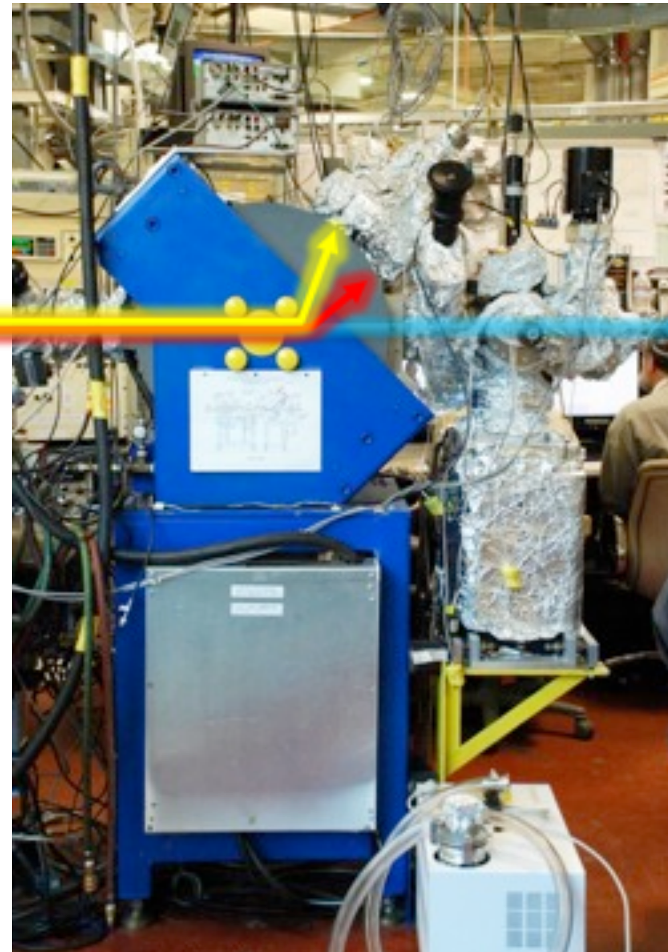

Photon Beam

IPB Endstation

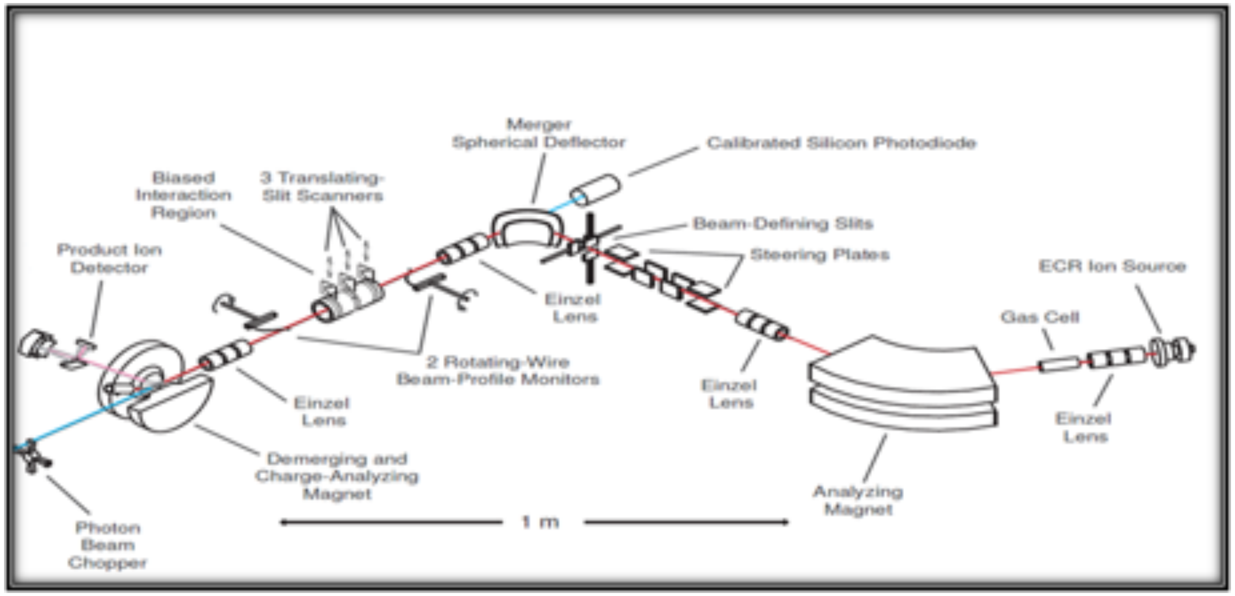

IPB Endstation

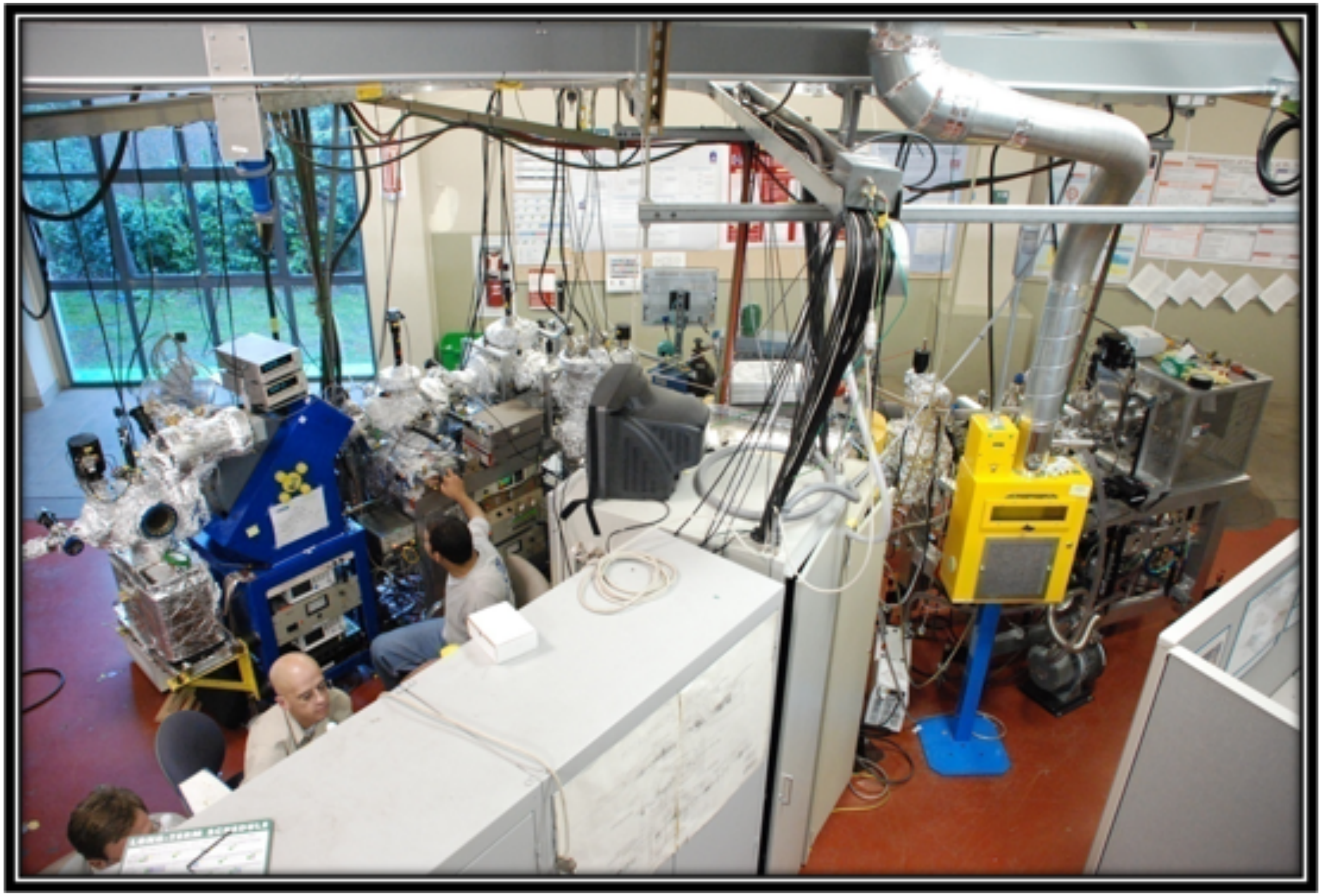

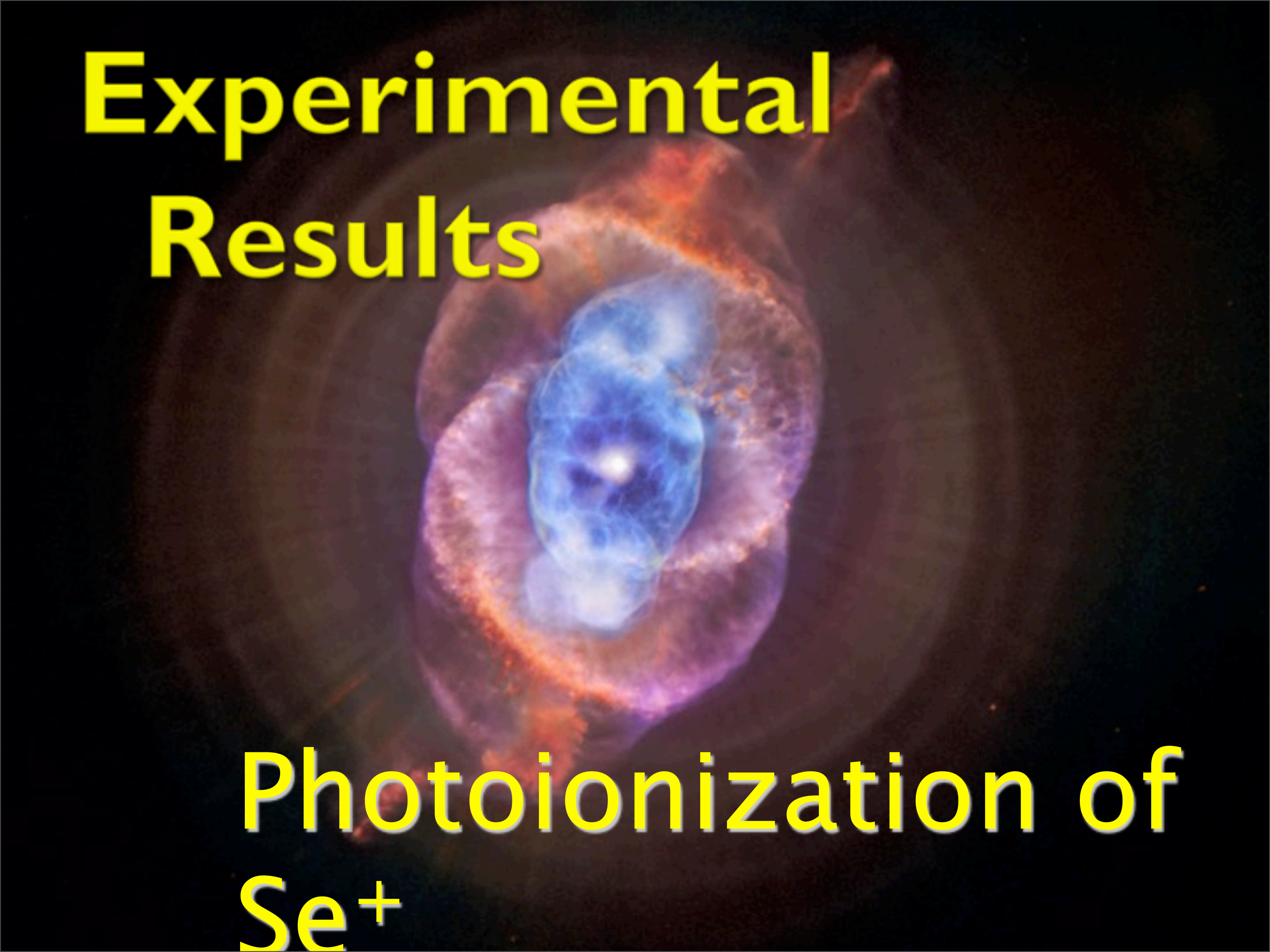
Experimental
Results
Photoionization of
Se+

Motivations

- Se, Kr, and Xe ions have been observed in several planetary nebulae (PNe, ejected envelopes of low-mass stars).
- Due to their rarity (<= 10-9 the H abundance) only 1-2 ions of these elements are usually observed.
- Their relative abundances are good tracers of neutron-capture nucleosynthesis in evolved stars.

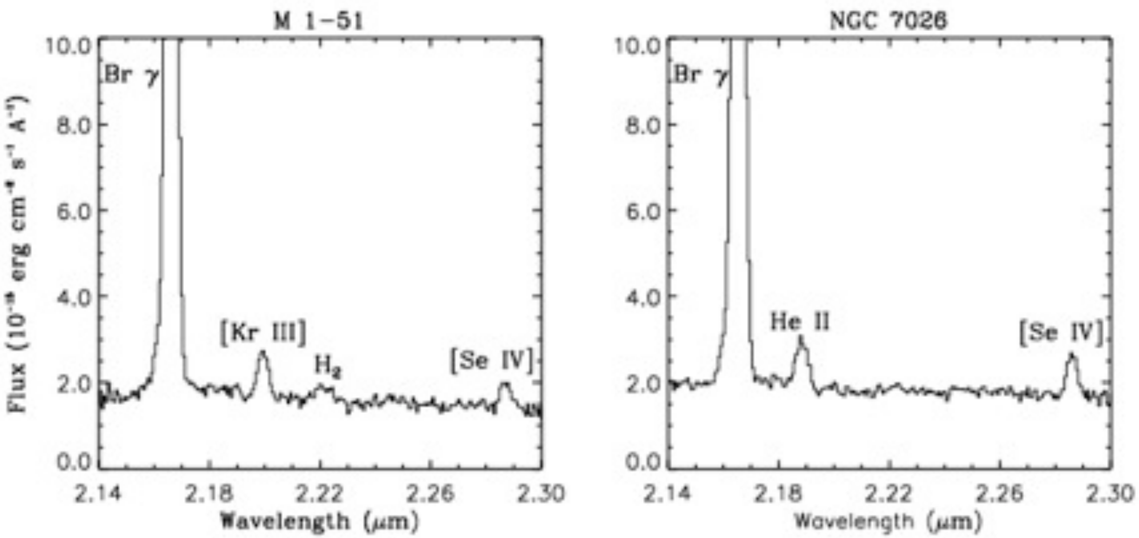

Near-infrared spectra of two planetary nebulae which exhibit [Se IV] 2.287 μm emission, obtained at the University of Texas' McDonald Observatory by Nick Sterling.

Calculations for Se^+ (Se II)

Calculations for Se^+ (Se II)

- Model **A**

  Included $4s^2 4p^2$, $4s4p^3$ and $4p^4$ configurations(3)

  Gives rise to 20 levels from (3) configurations

Calculations for Se^{+} (Se II)

- Model **A**

  Included $4s^2 4p^2$, $4s4p^3$and $4p^4$ configurations(3)

  Gives rise to 20 levels from (3) configurations

- Model **B**

  Included in addition several 3d-hole configurations $3d^9 4s^2 4p^3$; $3d^9 4s4p^4$; $3d^9 4p^5$

  Gives rise to 126 levels from (6) configurations

Calculations for Se^+ (Se II)

- Model **A**

  Included $4s^24p^2$, $4s4p^3$and $4p^4$ configurations(3)

  Gives rise to 20 levels from (3) configurations

- Model **B**

  Included in addition several 3d-hole configurations $3d^94s^24p^3$; $3d^94s4p^4$; $3d^94p^5$

  Gives rise to 126 levels from (6) configurations

- Model **C**

Calculations for Se^+ (Se II)

- Model **A**

  Included $4s^24p^2$, $4s4p^3$ and $4p^4$ configurations(3)

  Gives rise to 20 levels from (3) configurations

- Model **B**

  Included in addition several 3d-hole configurations $3d^94s^24p^3$; $3d^94s4p^4$; $3d^94p^5$

  Gives rise to 126 levels from (6) configurations

- Model **C**

  Involved a 4d orbital instead of 3d-hole. Adding the configurations $4s^24p4d$, $4s^24d^2$, $4p^24d^2$, $4s4p^24d$ and $4p^34d$

Calculations for Se^+ (Se II)

- Model **A**

  Included $4s^2 4p^2$, $4s4p^3$ and $4p^4$ configurations(3)

  Gives rise to 20 levels from (3) configurations

- Model **B**

  Included in addition several 3d-hole configurations $3d^9 4s^2 4p^3$; $3d^9 4s4p^4$; $3d^9 4p^5$

  Gives rise to 126 levels from (6) configurations

- Model **C**

  Involved a 4d orbital instead of 3d-hole. Adding the configurations $4s^2 4p4d$, $4s^2 4d^2$, $4p^2 4d^2$, $4s4p^2 4d$ and $4p^3 4d$

  Gives rise to 246 levels from (8) configurations

Se^+ Photo-ion Spectroscopy

- 27 scans
- 1 eV wide each
- Measured one-at-a-time
- Can take several hours per-scan

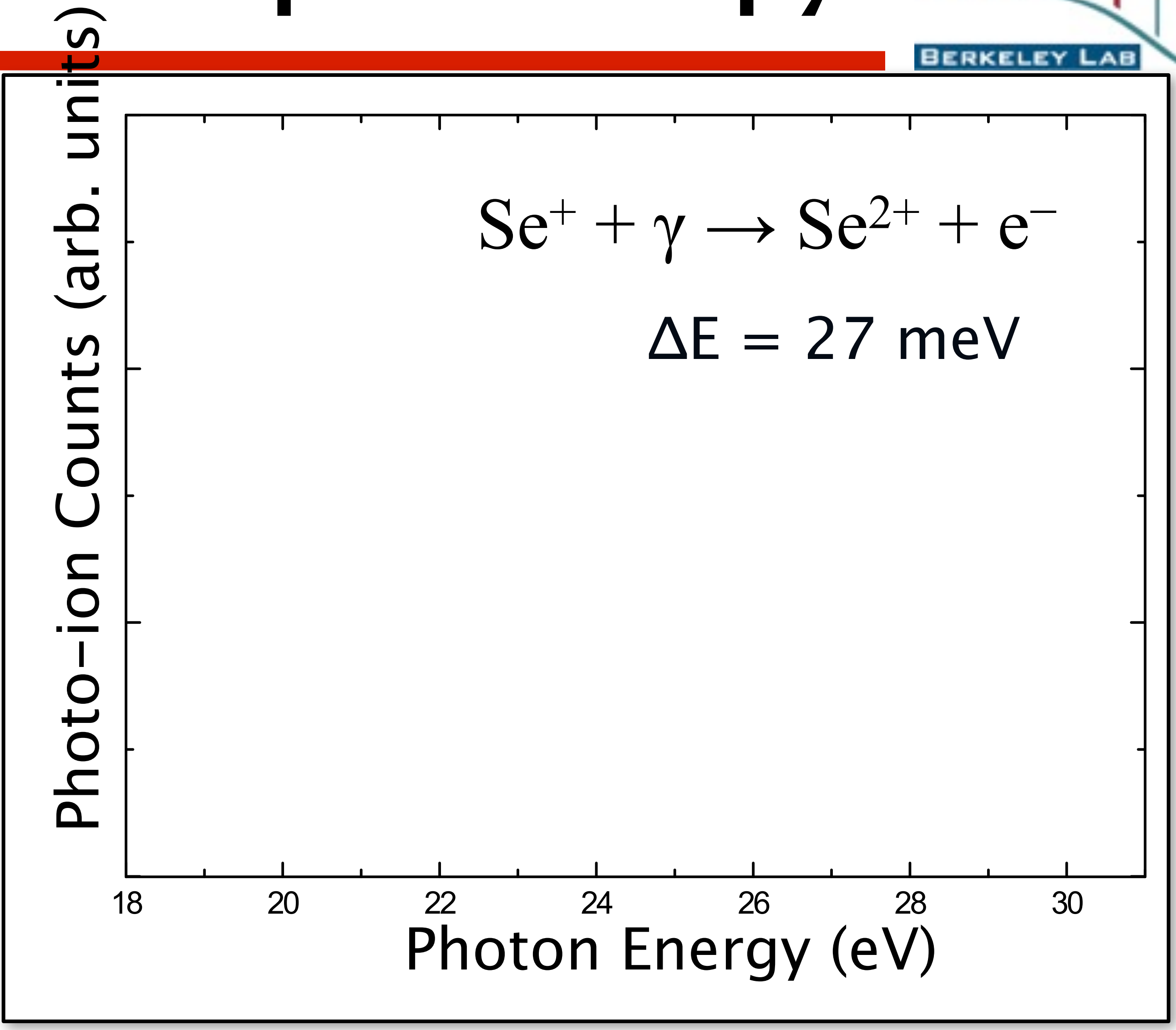

Se^+ Photo-ion Spectroscopy

- 27 scans
- 1 eV wide each
- Measured one-at-a-time
- Can take several hours per-scan

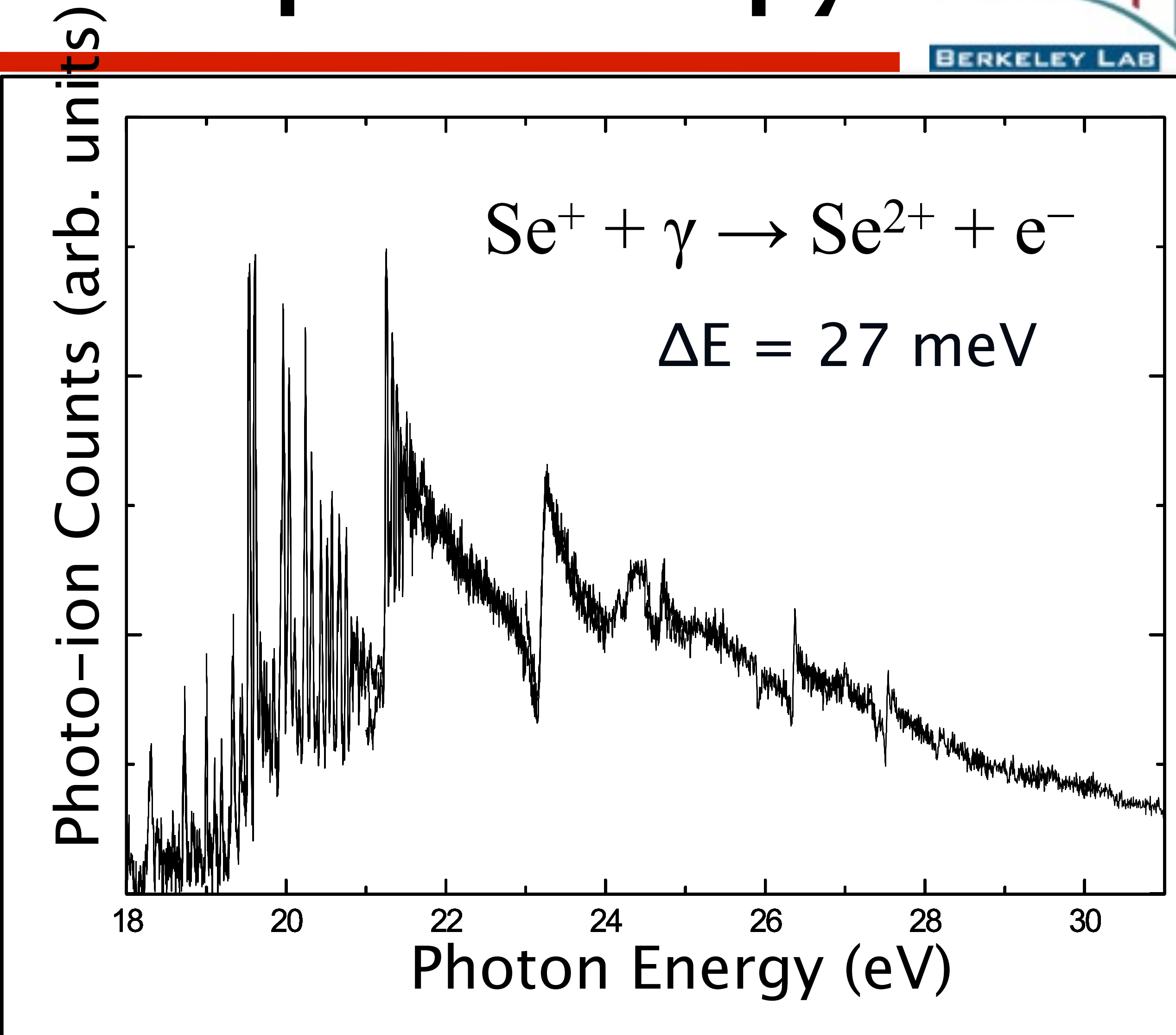

Se⁺ Photo-ion Spectroscopy

- 27 scans
- 1 eV wide each
- Measured one-at-a-time
- Can take several hours per-scan

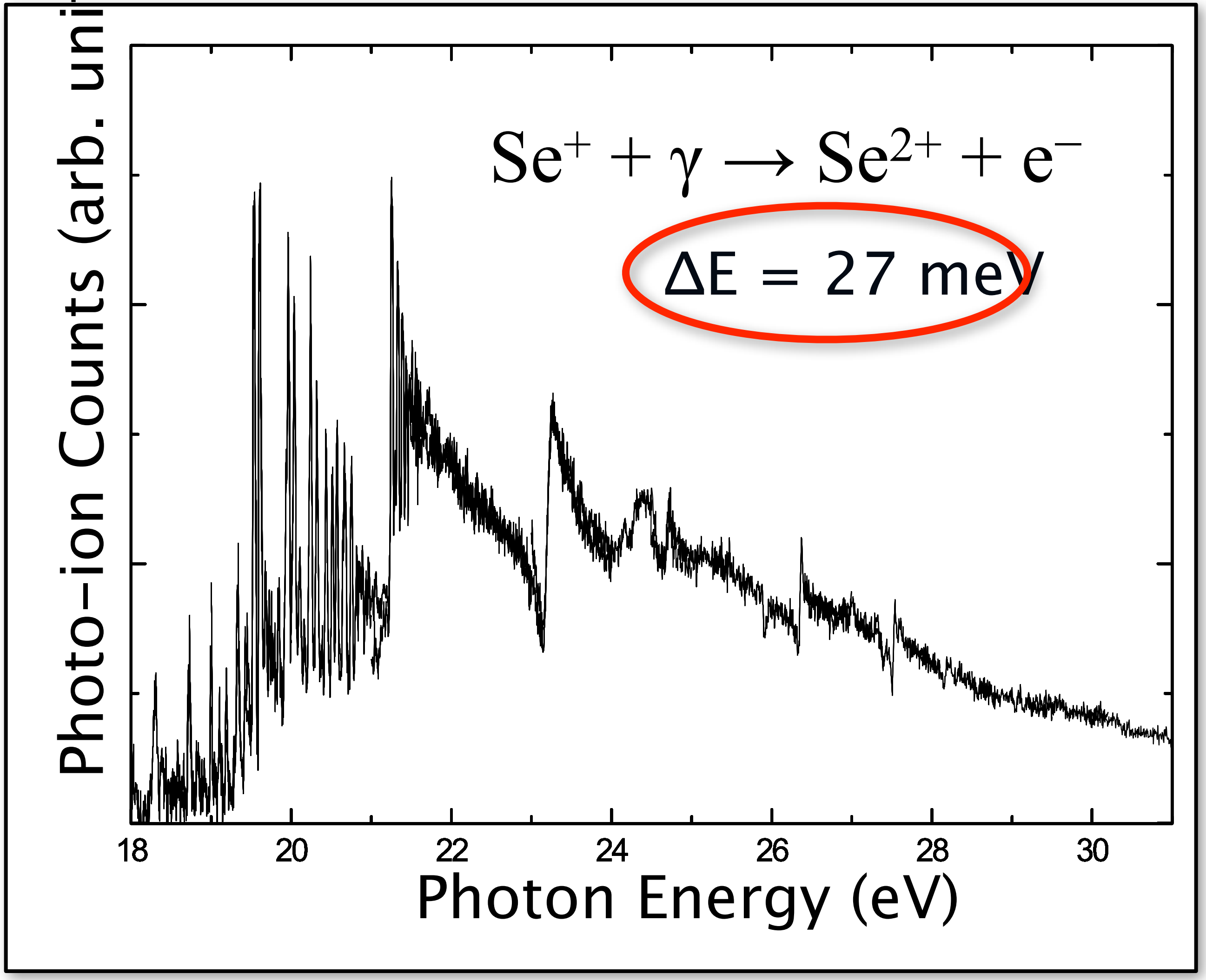

Se^+ Photo-ion Spectroscopy

- 27 scans
- 1 eV wide each
- Measured one-at-a-time
- Can take several hours per-scan

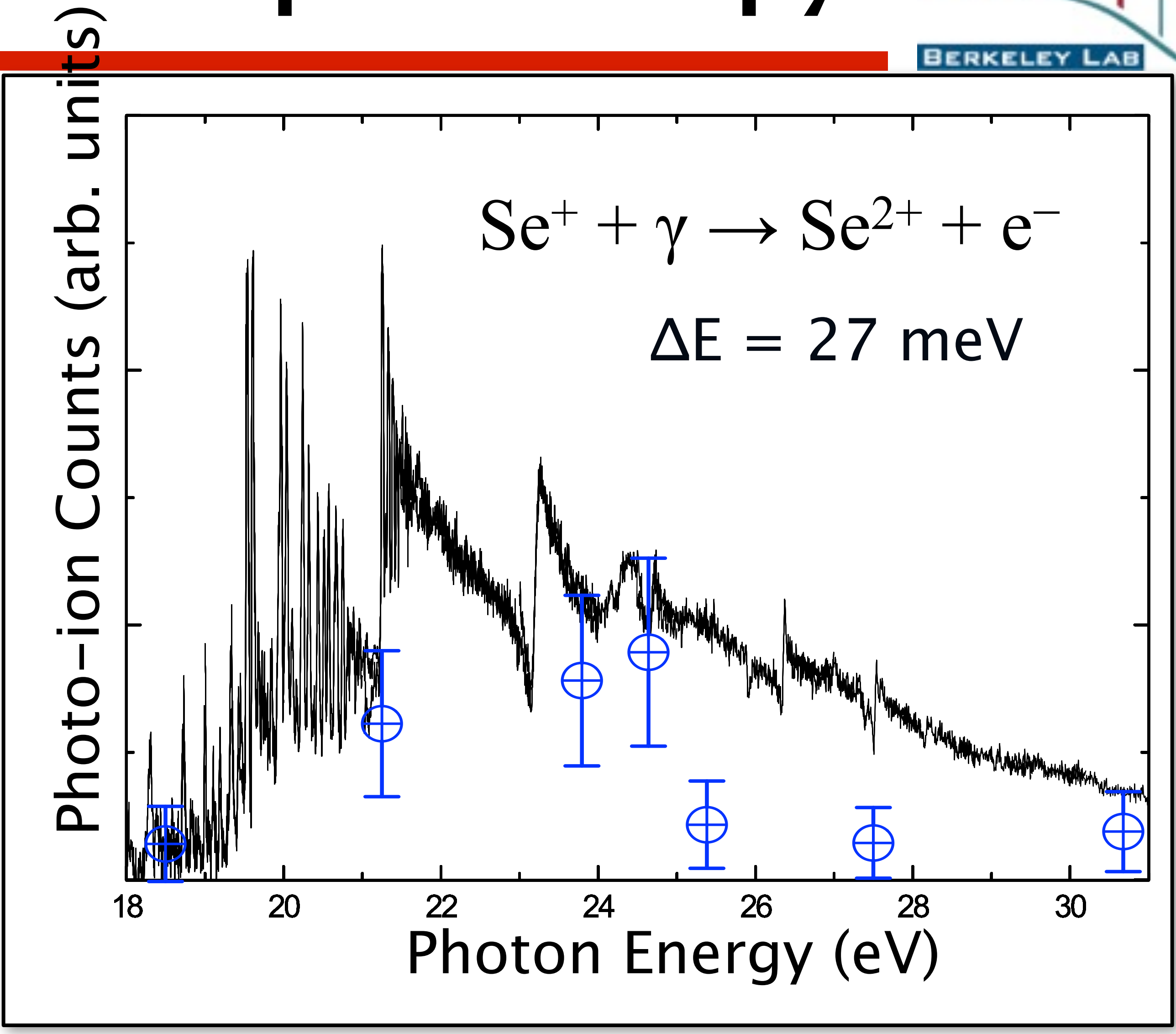

Se^+ Photo-ion Spectroscopy

- 27 scans
- 1 eV wide each
- Measured one-at-a-time
- Can take several hours per-scan

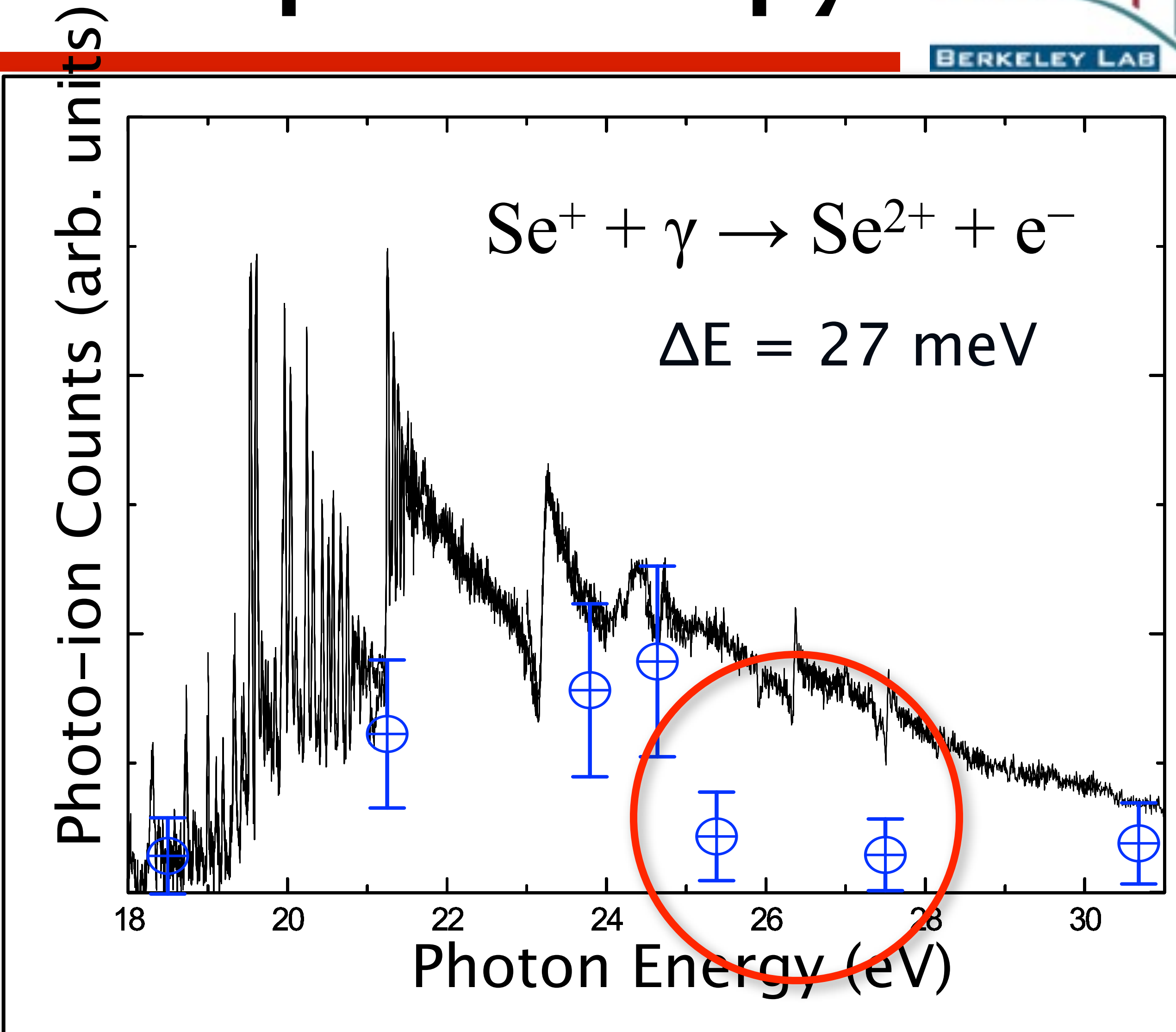

Se^+ Photo-ion Spectroscopy

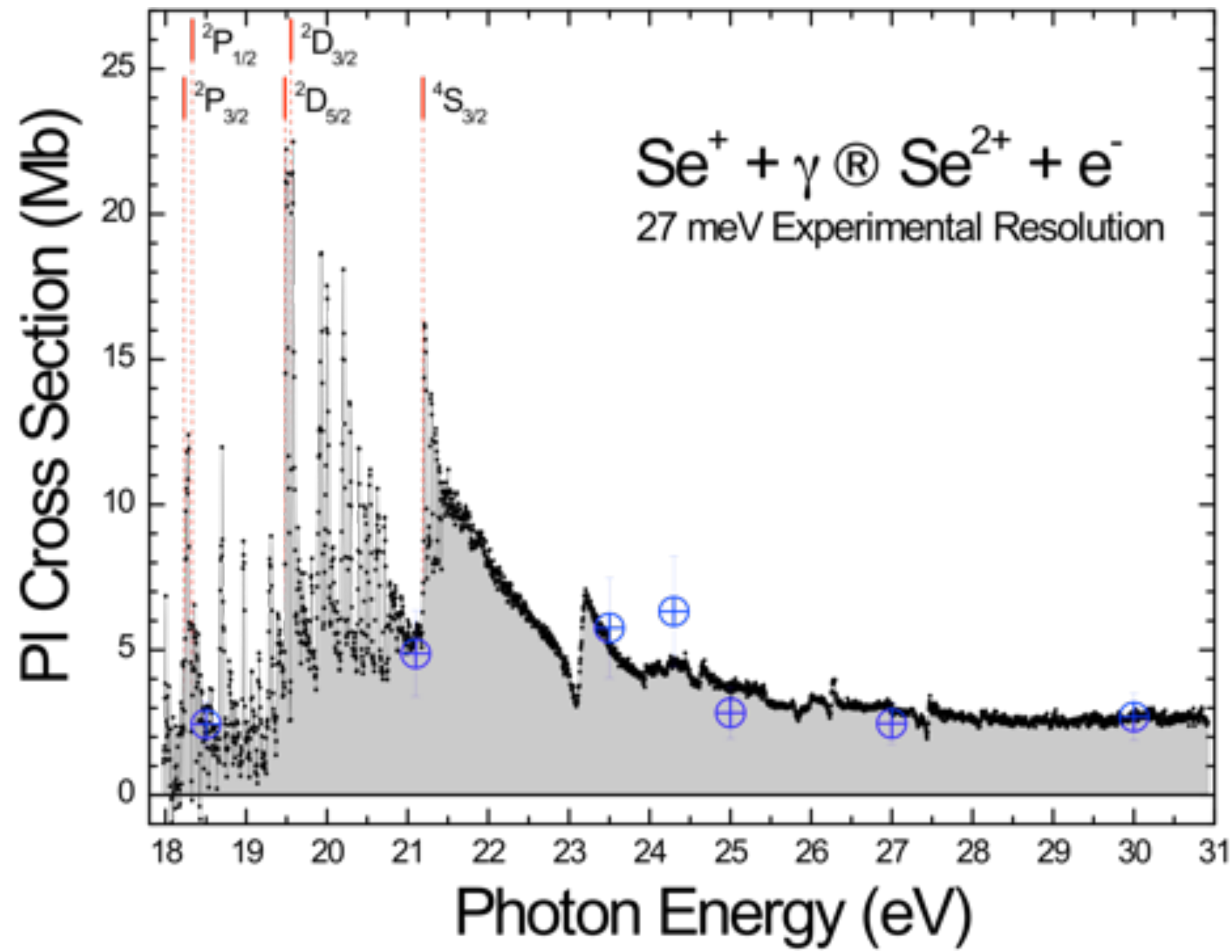

LAWRENCE BERKELEY NATIONAL LABORATORY

Se⁺ Photo–ion Spectroscopy

- Photon energy calibrated to Ar autoionizing resonances

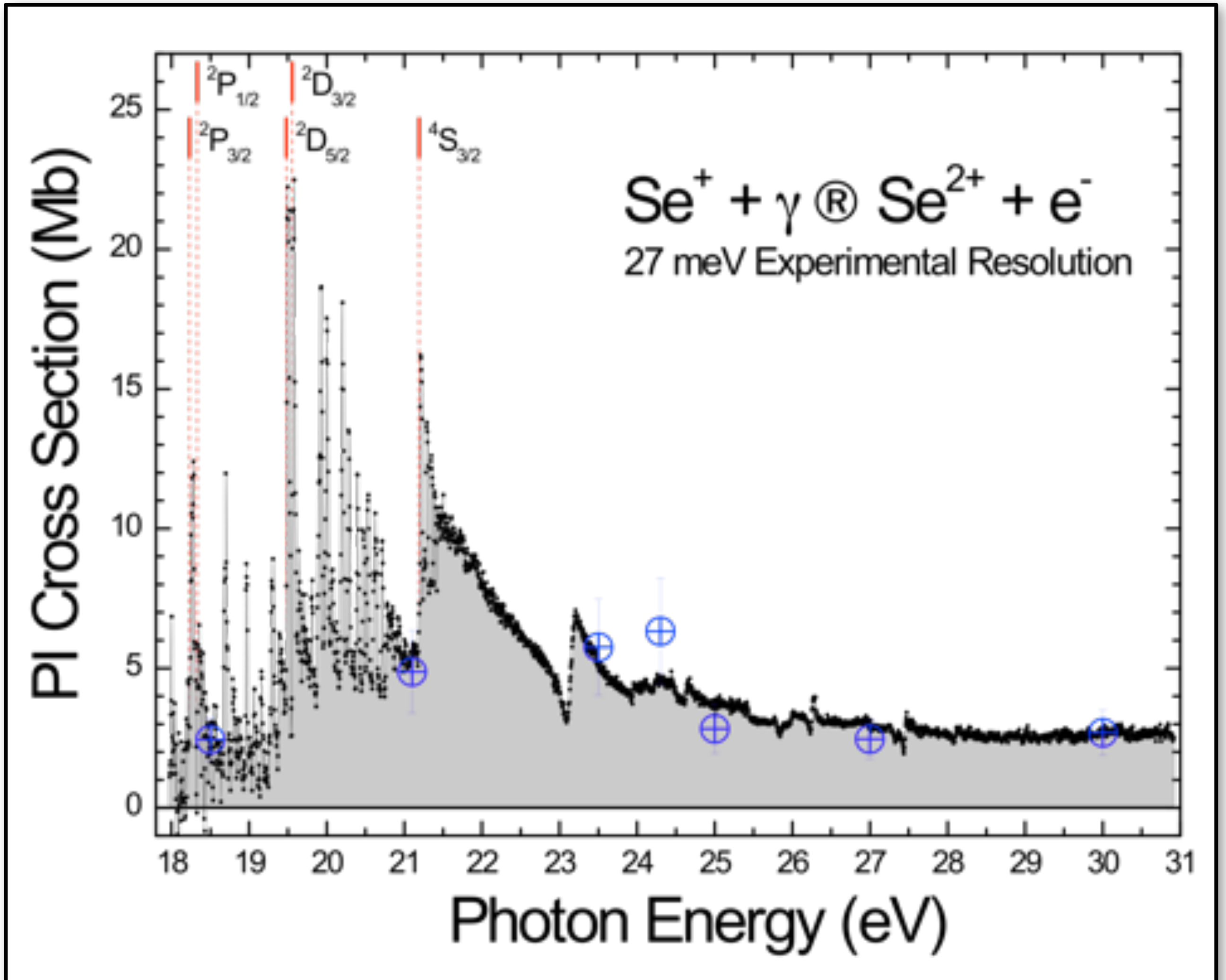

Se^+ Photo-ion Spectroscopy

- Photon energy calibrated to Ar autoionizing resonances

  (side branch gas cell)

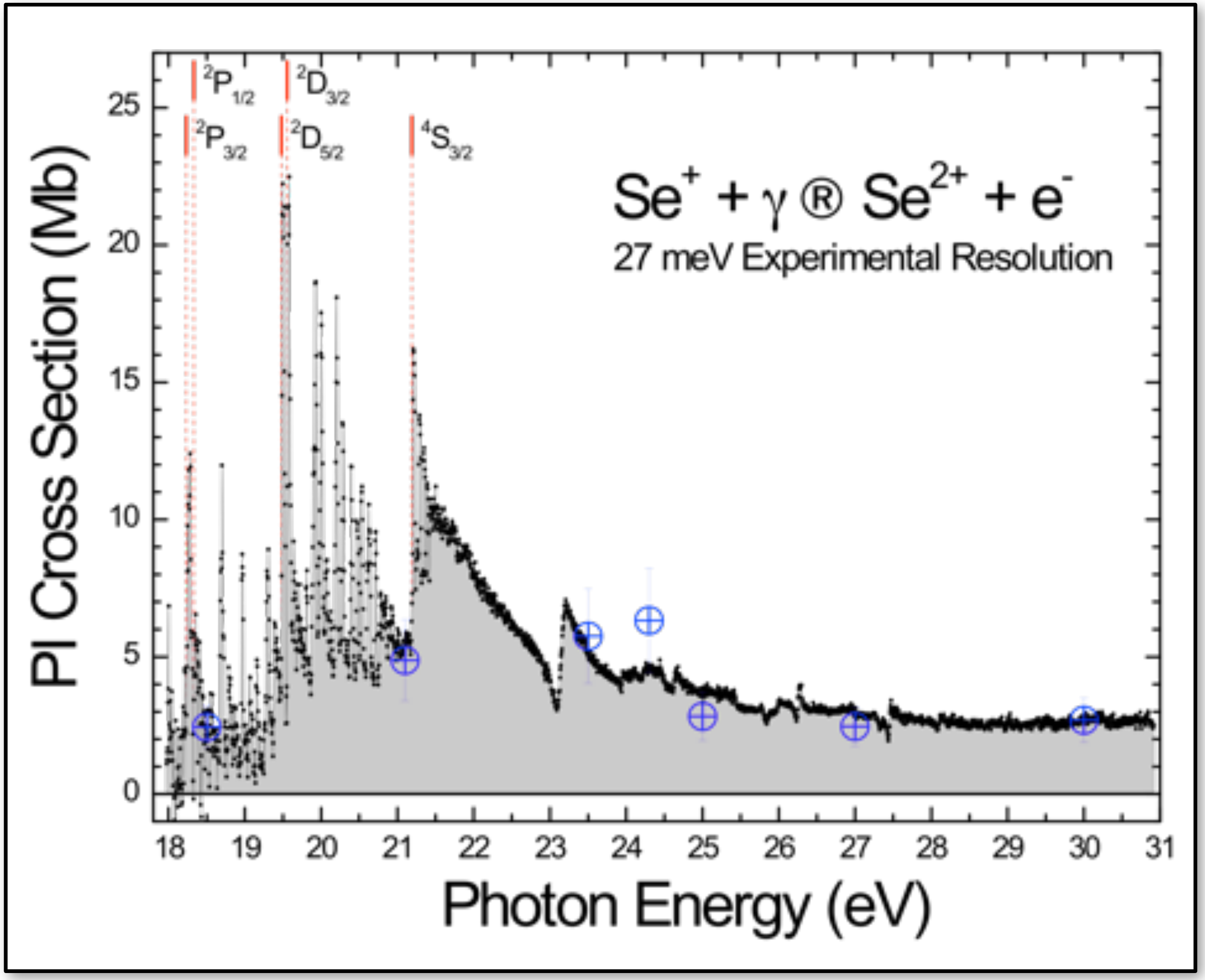

Se^+ Photo-ion Spectroscopy

- Photon energy calibrated to Ar autoionizing resonances

  (side branch gas cell)

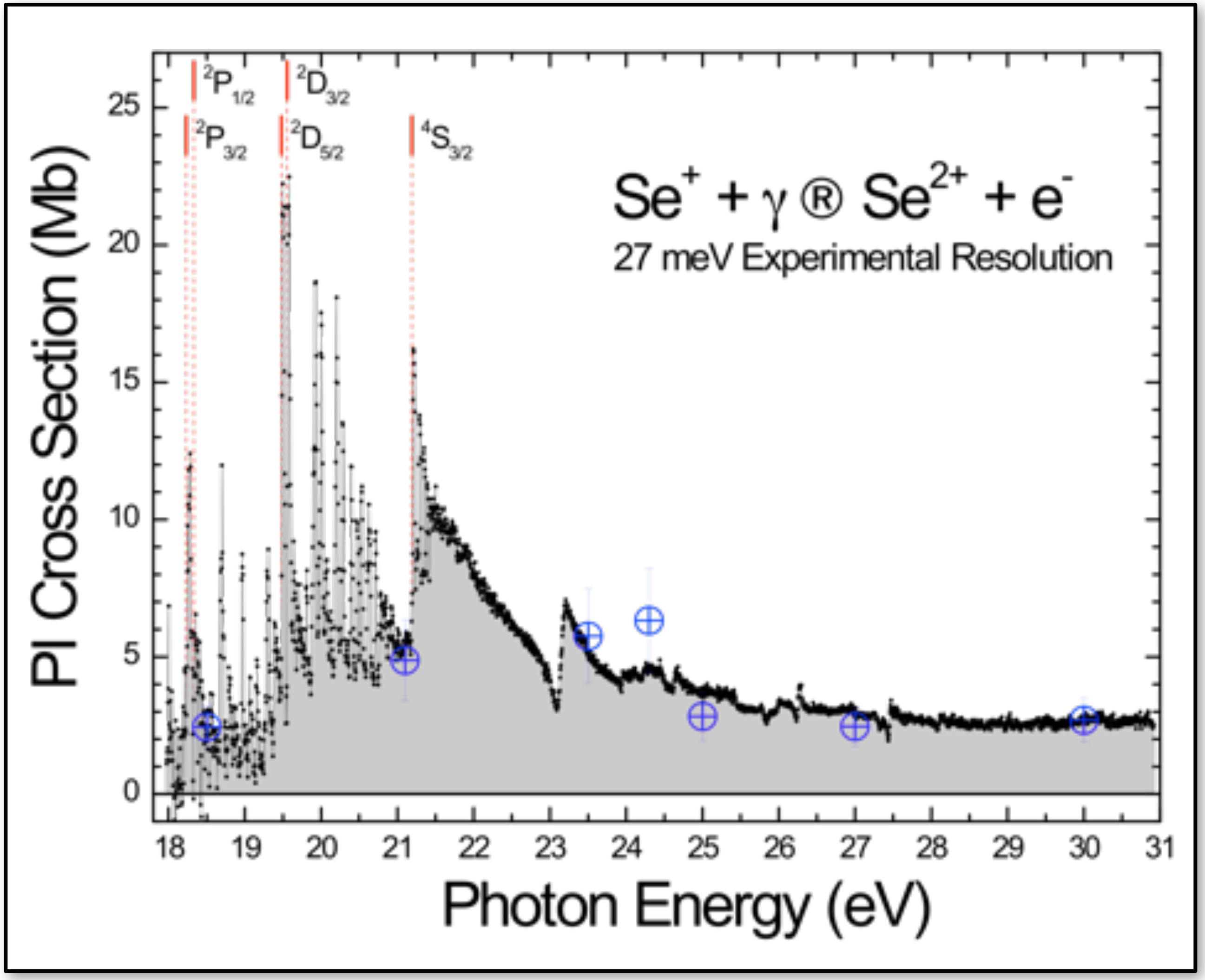

LAWRENCE BERKELEY NATIONAL LABORATORY

Se^+ Photo-ion Spectroscopy

- Photon energy calibrated to Ar autoionizing resonances

  (side branch gas cell)

- 7 absolute cross-section measurements

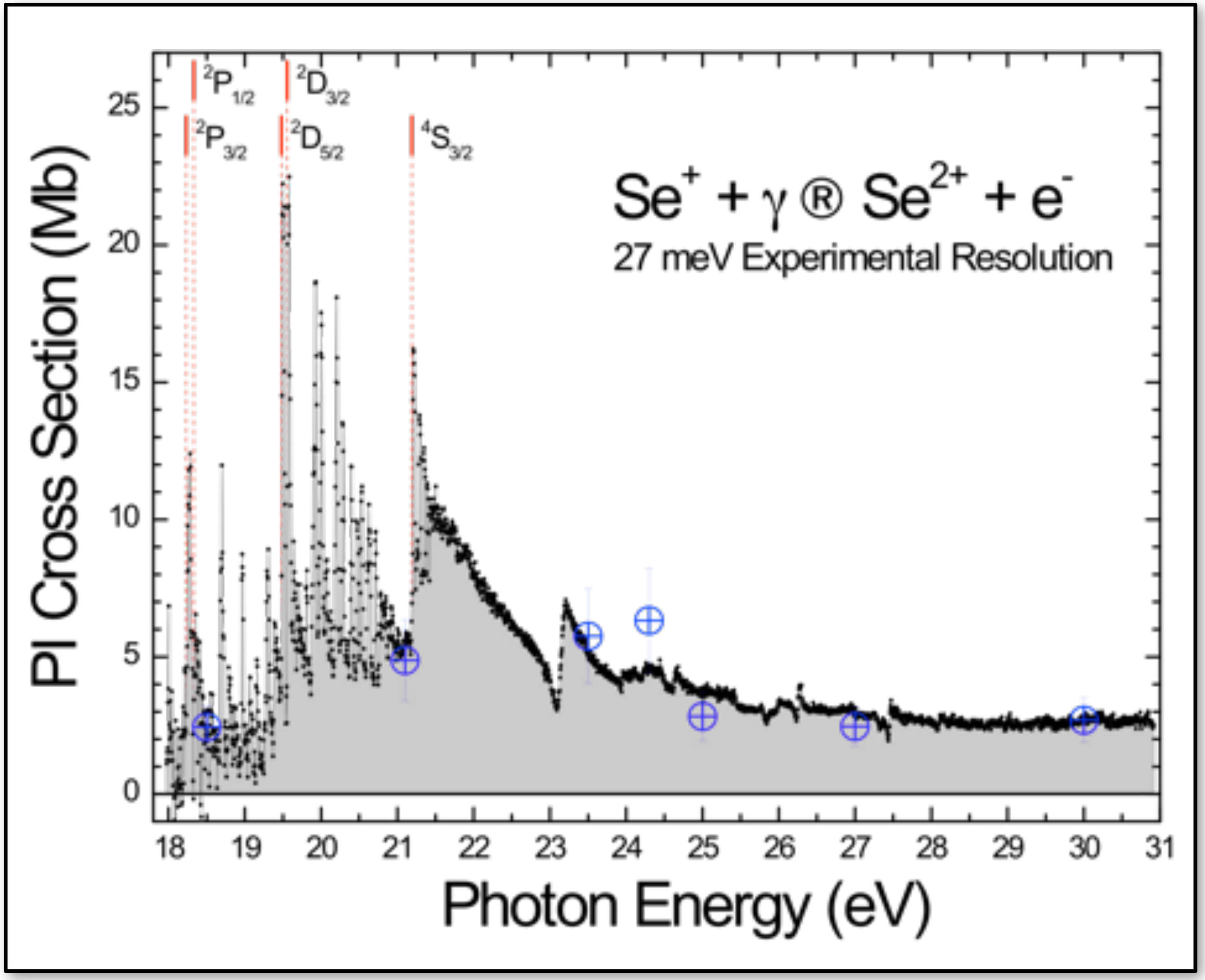

Se⁺ Photo-ion Spectroscopy

- Photon energy calibrated to Ar autoionizing resonances

  (side branch gas cell)

- 7 absolute cross-section measurements

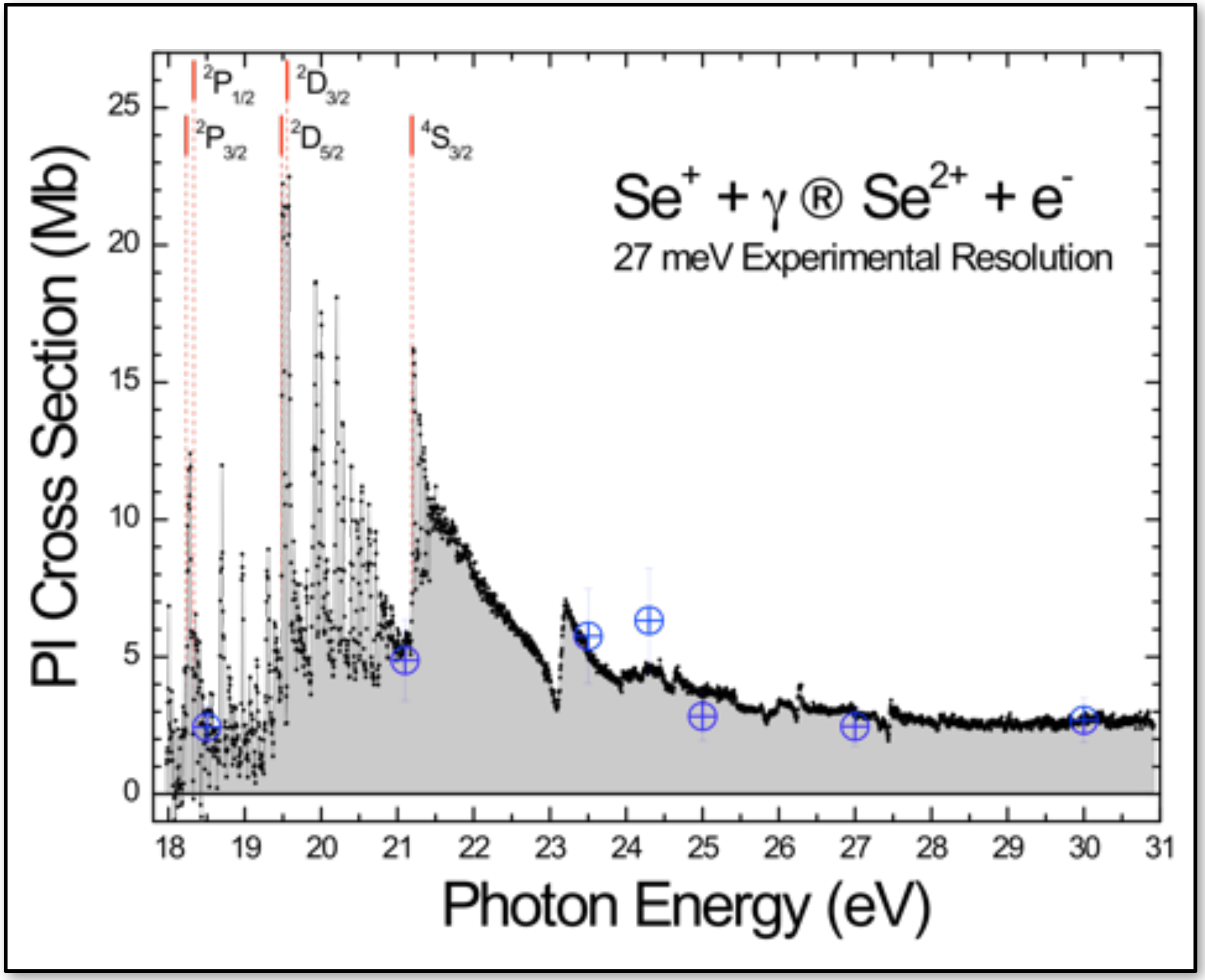

Se^+ Photo-ion Spectroscopy

- Photon energy calibrated to Ar autoionizing resonances

  (side branch gas cell)

- 7 absolute cross-section measurements

- Complex resonant structure below the ^4S ground

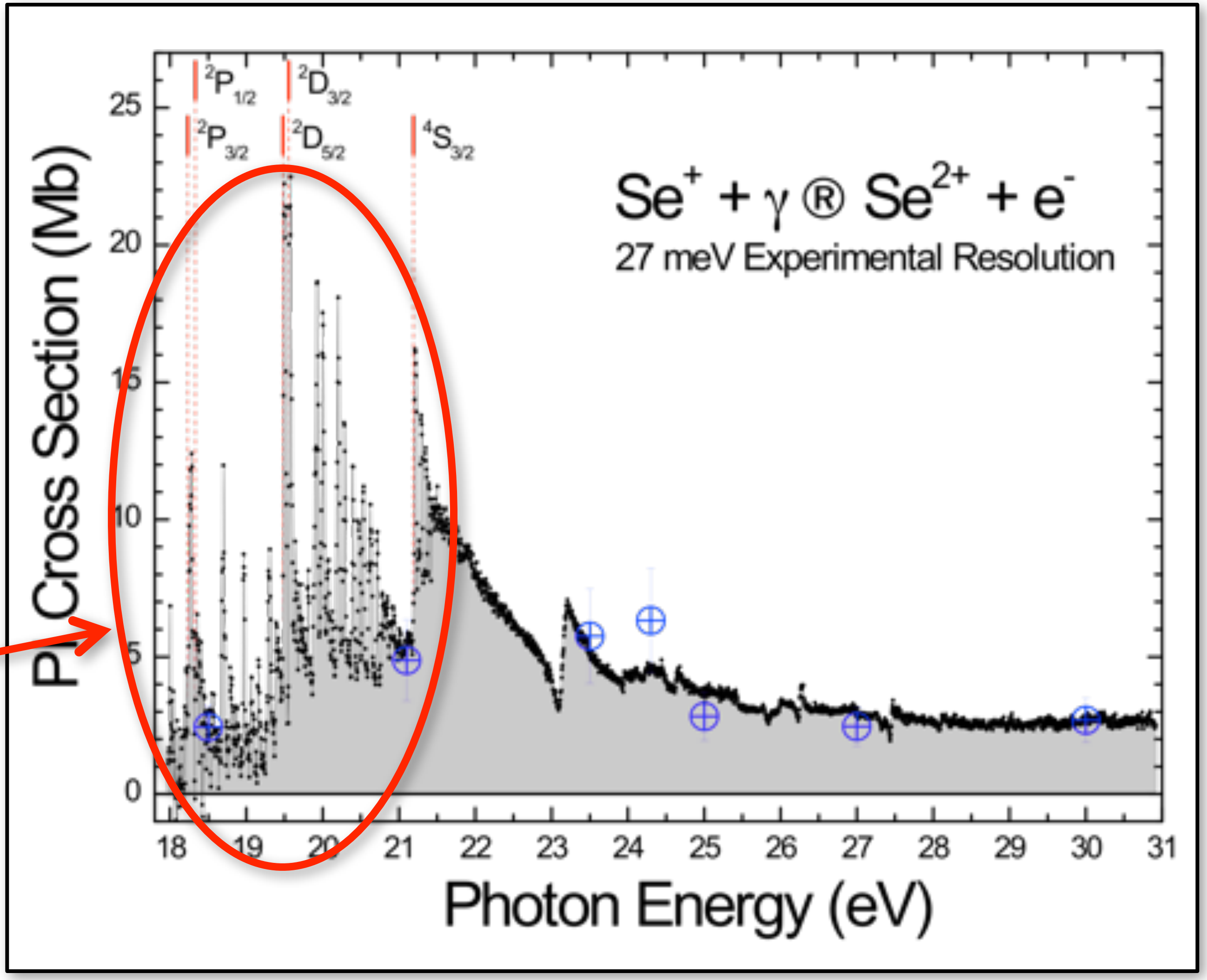

Se⁺ High-Resolution Spectroscopy

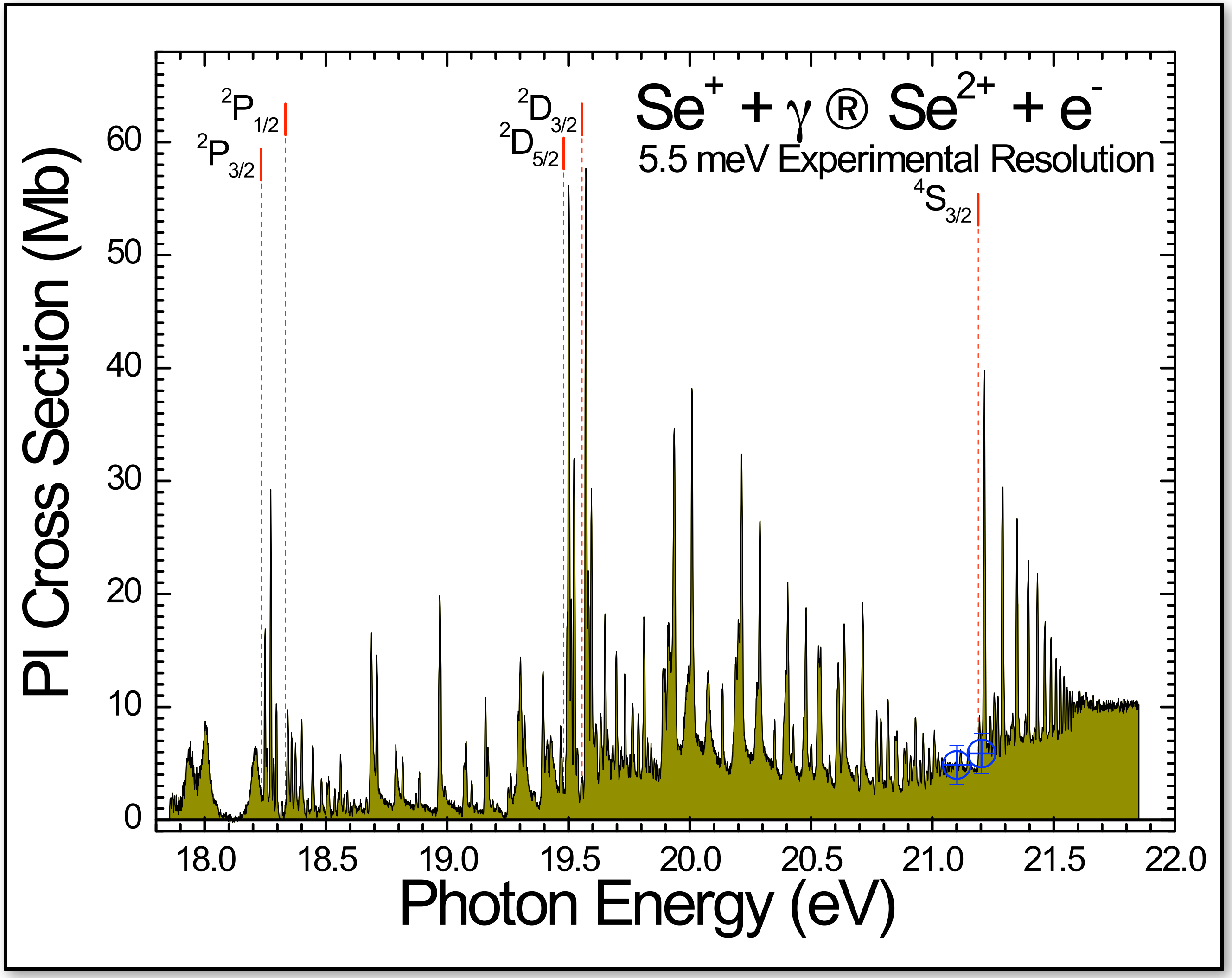

Se⁺ High-Resolution Spectroscopy

- 5.5 meV resolution

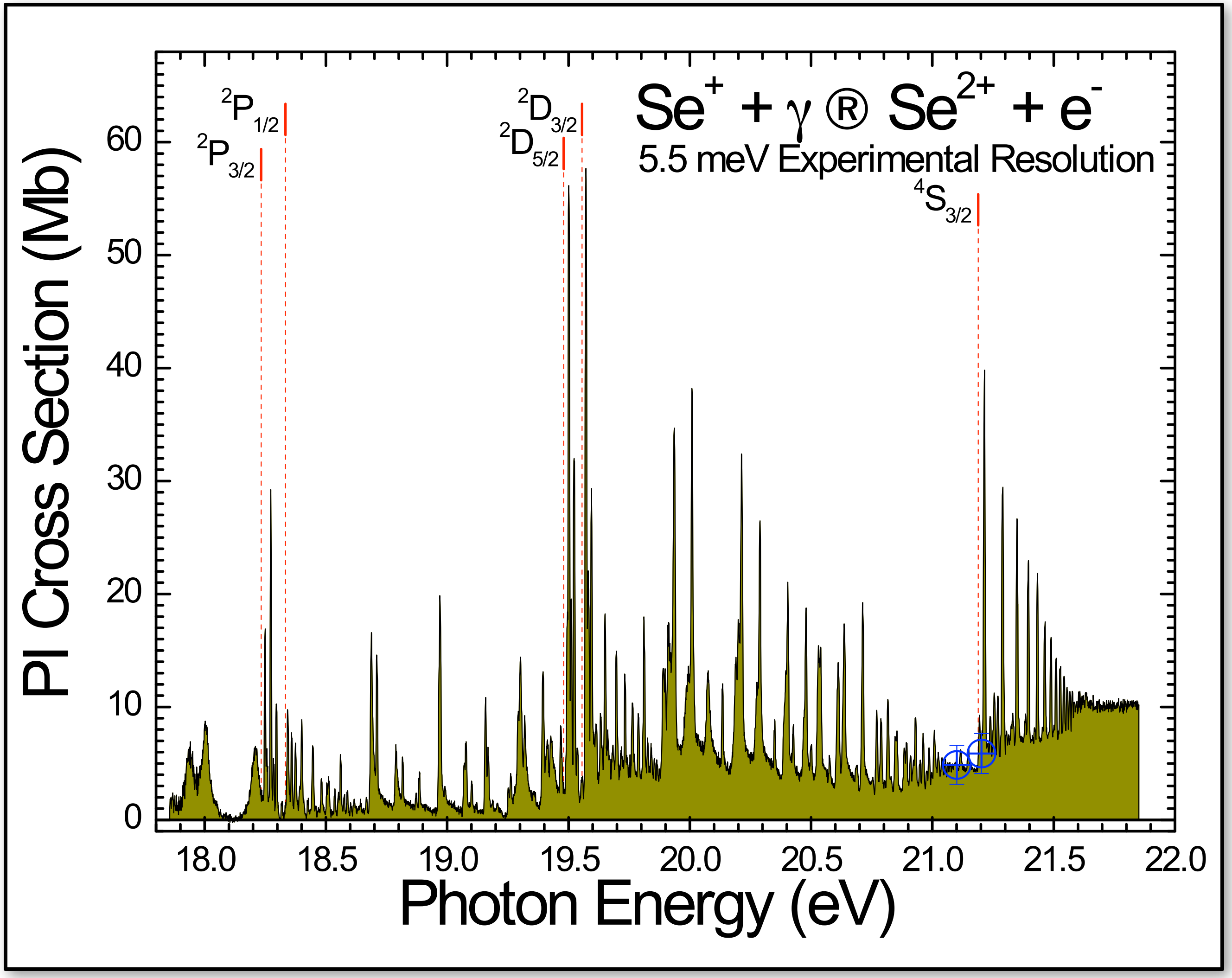

Se⁺ High-Resolution Spectroscopy

- 5.5 meV resolution
- 15 scans (0.5 eV ea)

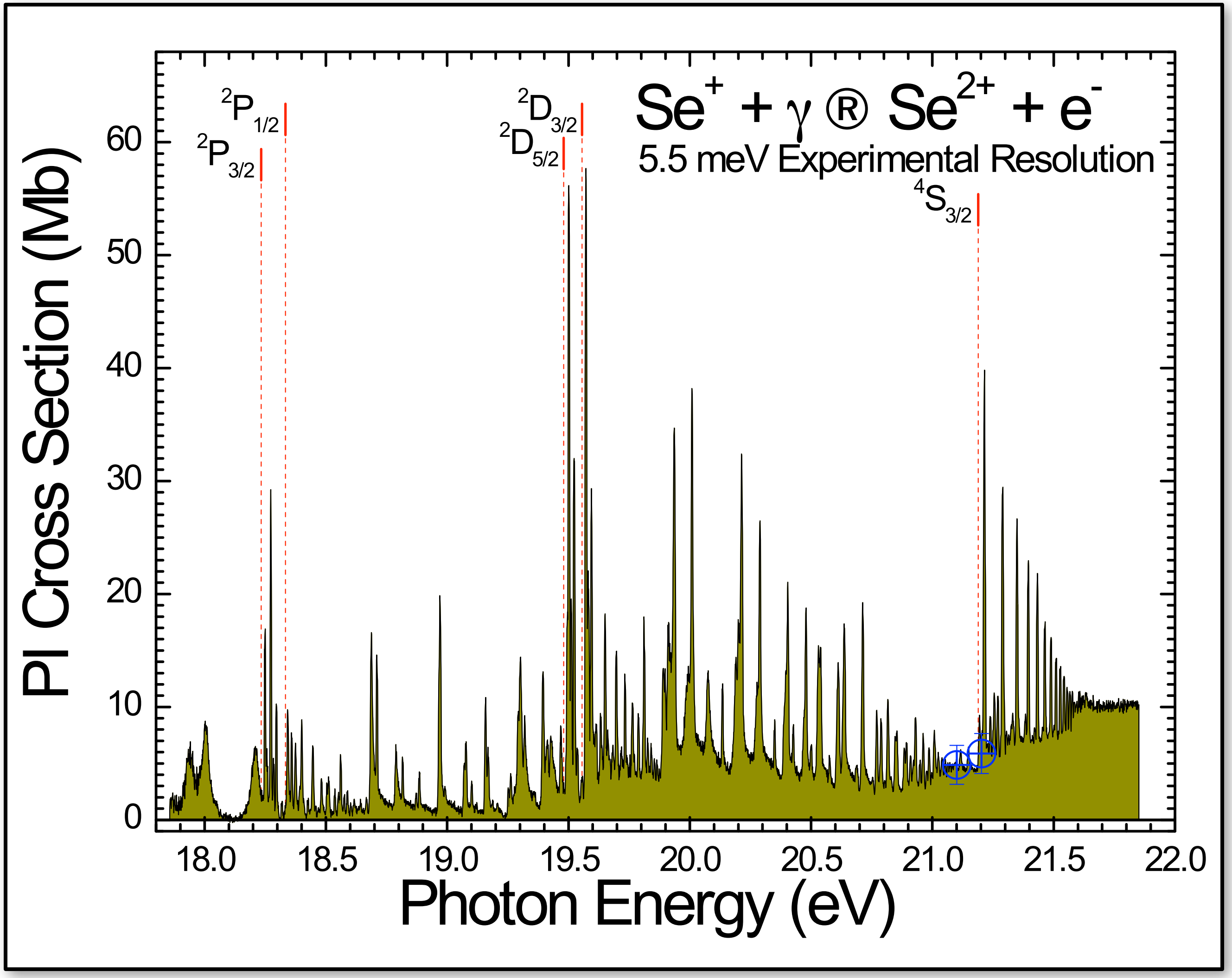

Se+ High-Resolution Spectroscopy

- 5.5 meV resolution
- 15 scans (0.5 eV ea)
- Normalized to the lo-res spectra & one absolute cross section

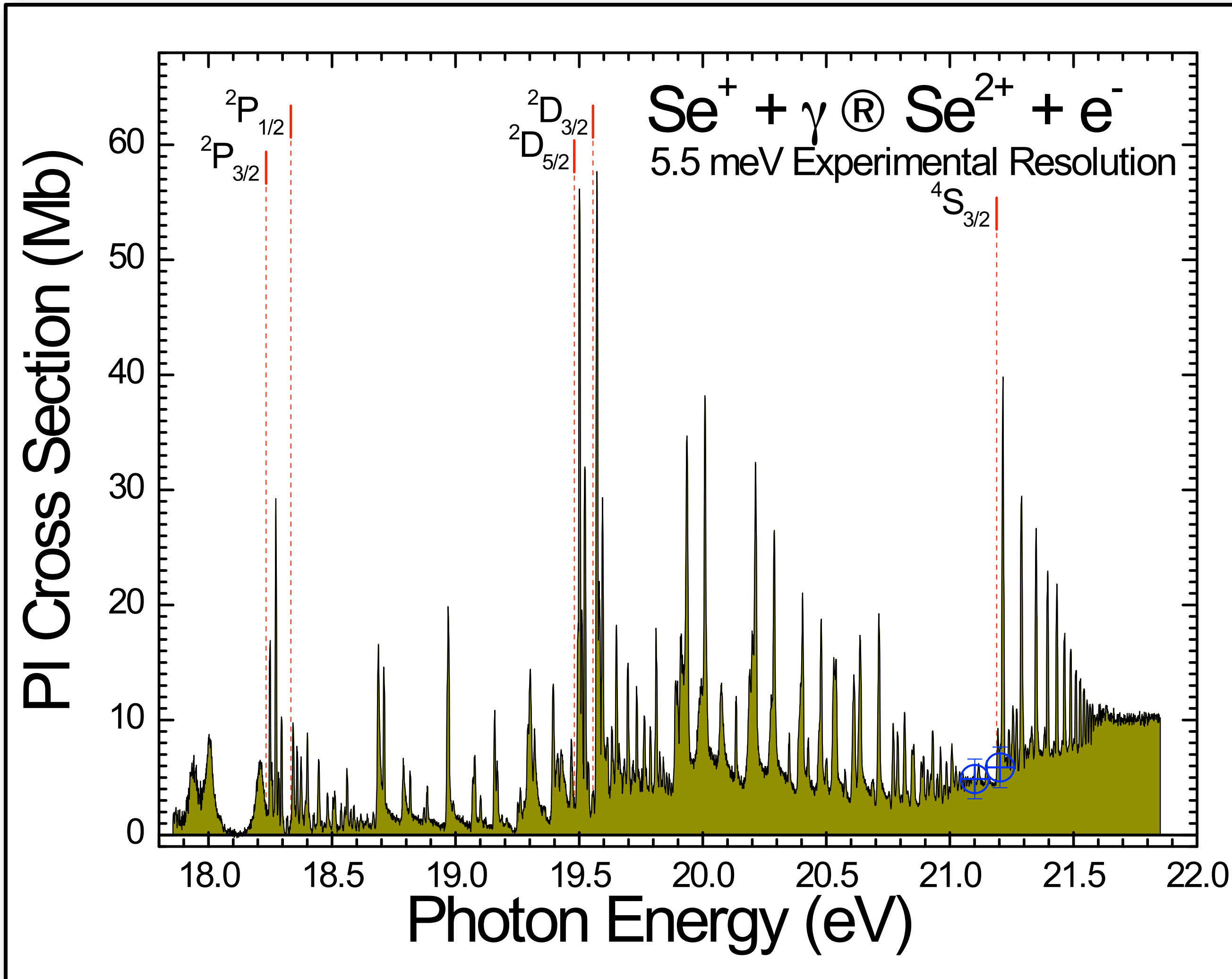

Se+ High-Resolution Spectroscopy

- 5.5 meV resolution
- 15 scans (0.5 eV ea)
- Normalized to the lo-res spectra & one absolute cross section
- Features below the $^2P_{3/2}$ metastable threshold…

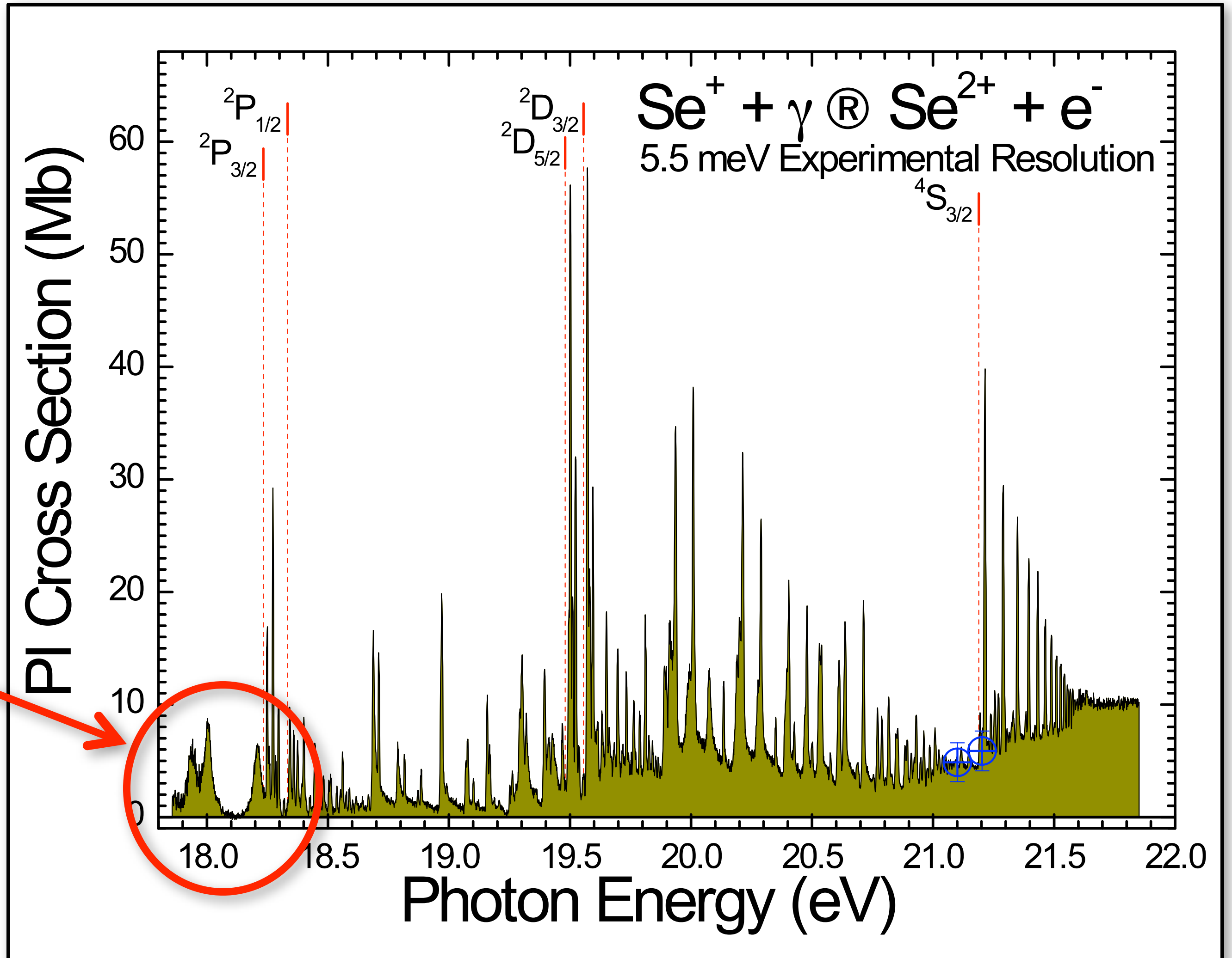

MERLIN Quasi-periodic Undulator (QEPU) Reduces Flux in Higher Harmonics

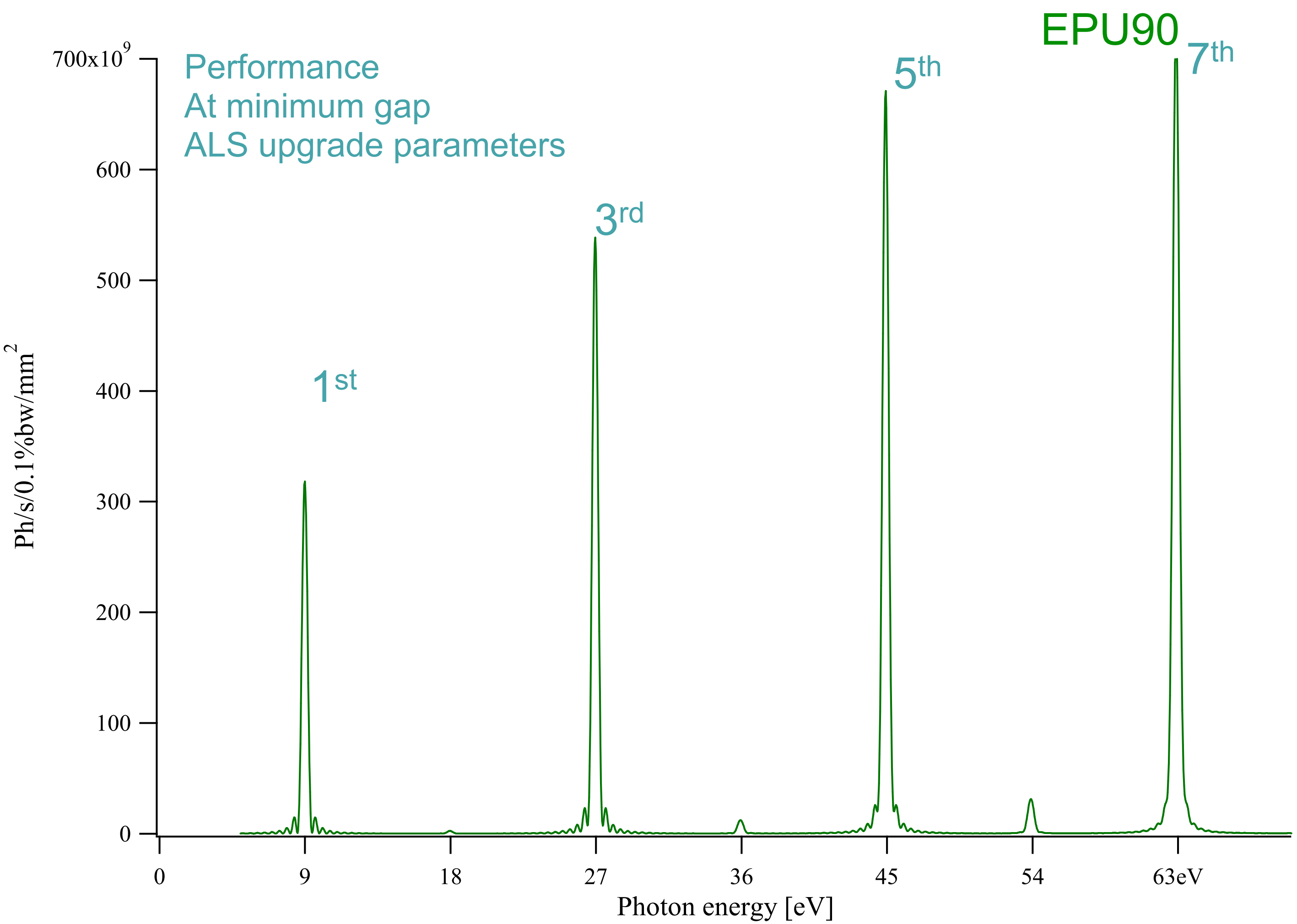

MERLIN Quasi-periodic Undulator (QEPU) Reduces Flux in Higher Harmonics

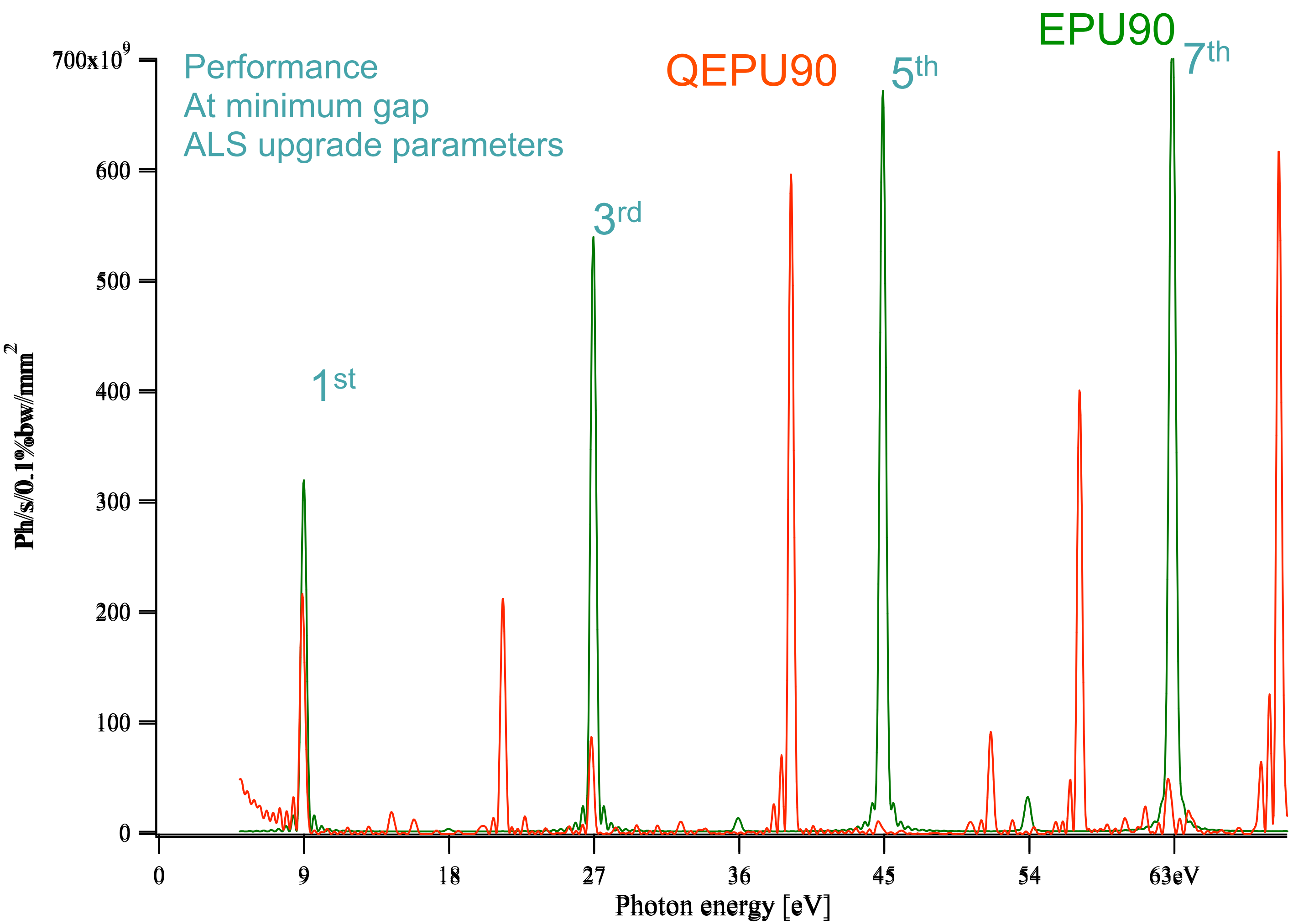

R. Schlueter, S. Prestemon, S. Marks

MERLIN Quasi-periodic Undulator (QEPU) Reduces Flux in Higher Harmonics

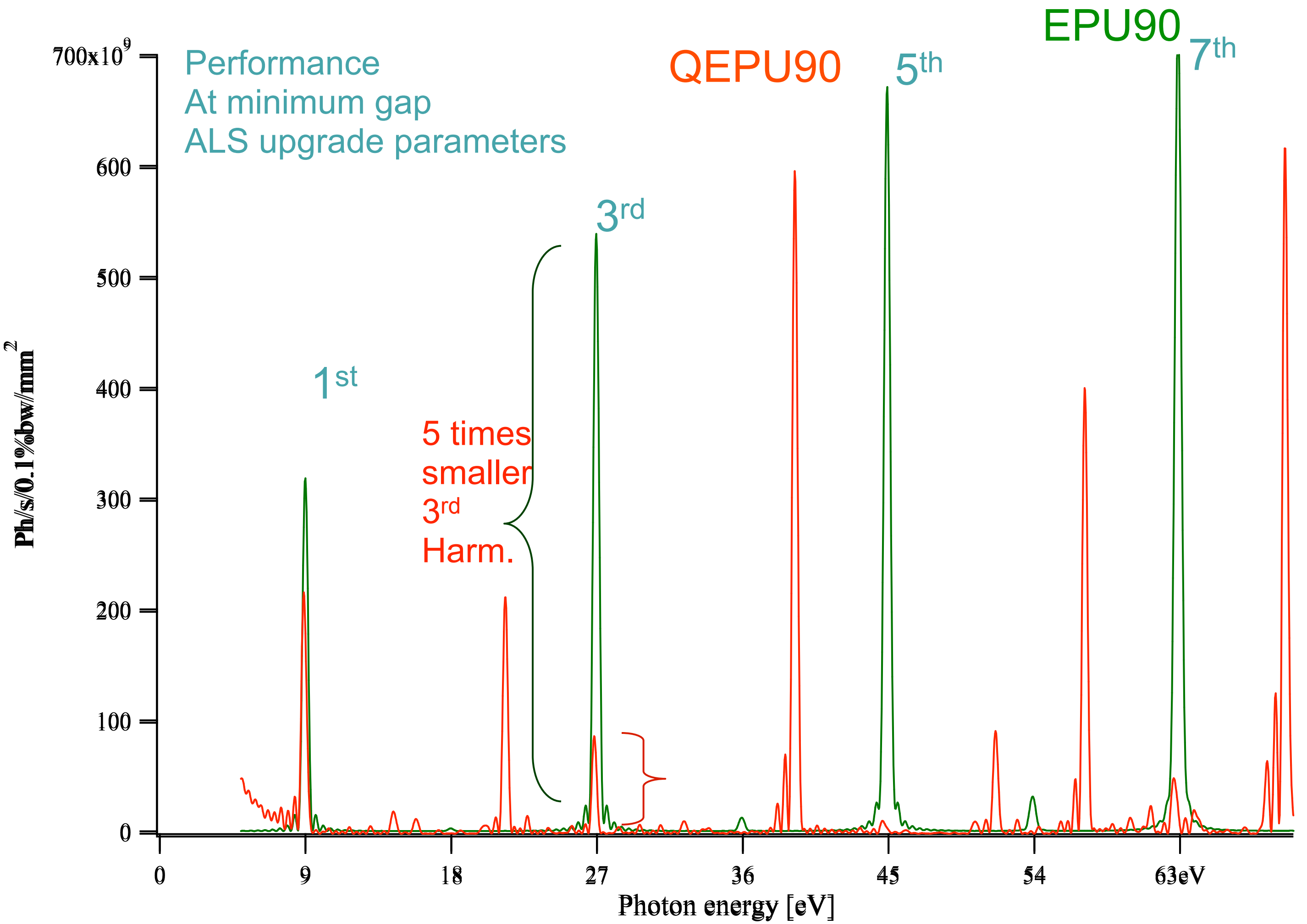

R. Schlueter, S. Prestemon, S. Marks

MERLIN Quasi-periodic Undulator (QEPU) Reduces Flux in Higher Harmonics

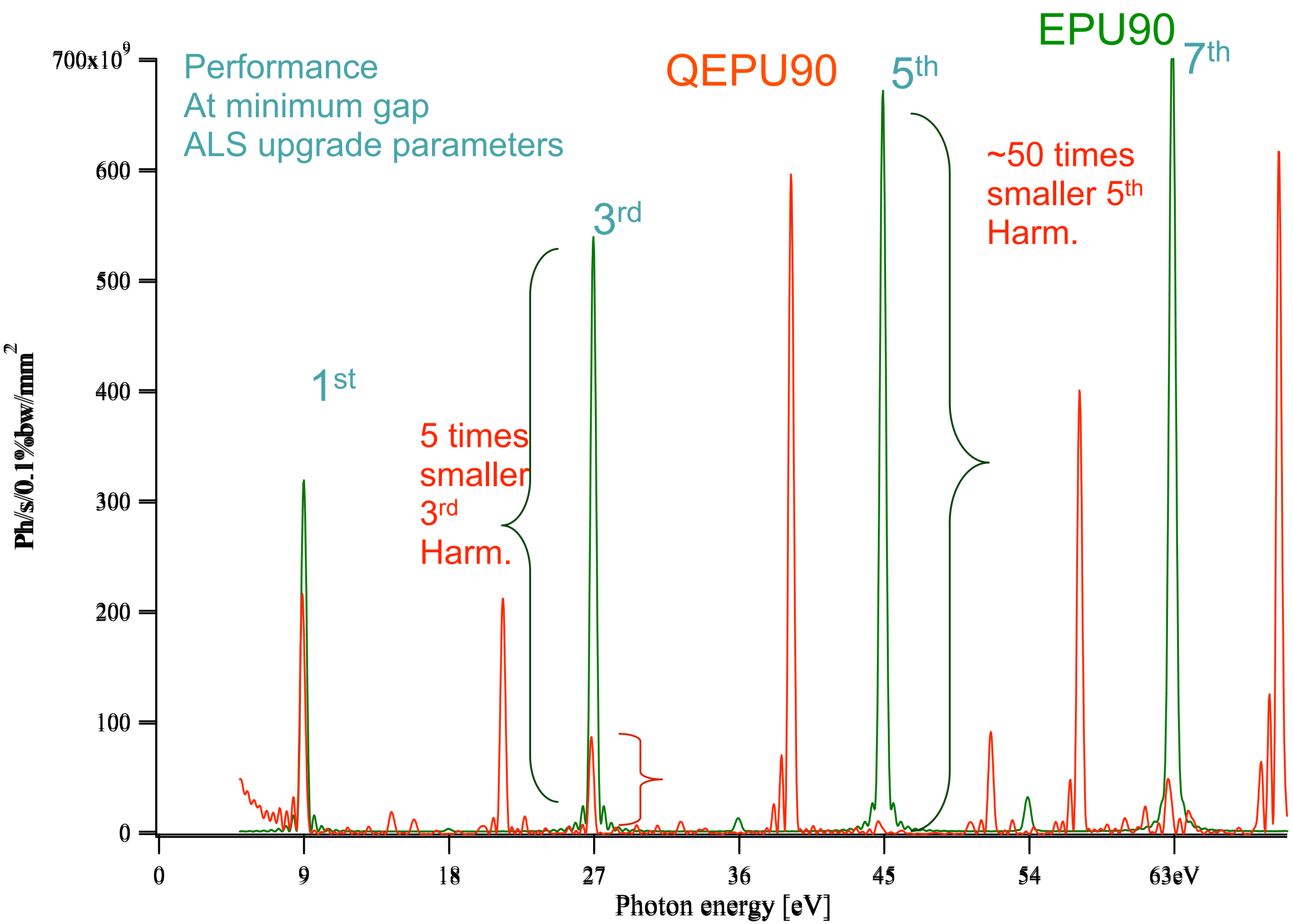

MERLIN Quasi-periodic Undulator (QEPU) Reduces Flux in Higher Harmonics

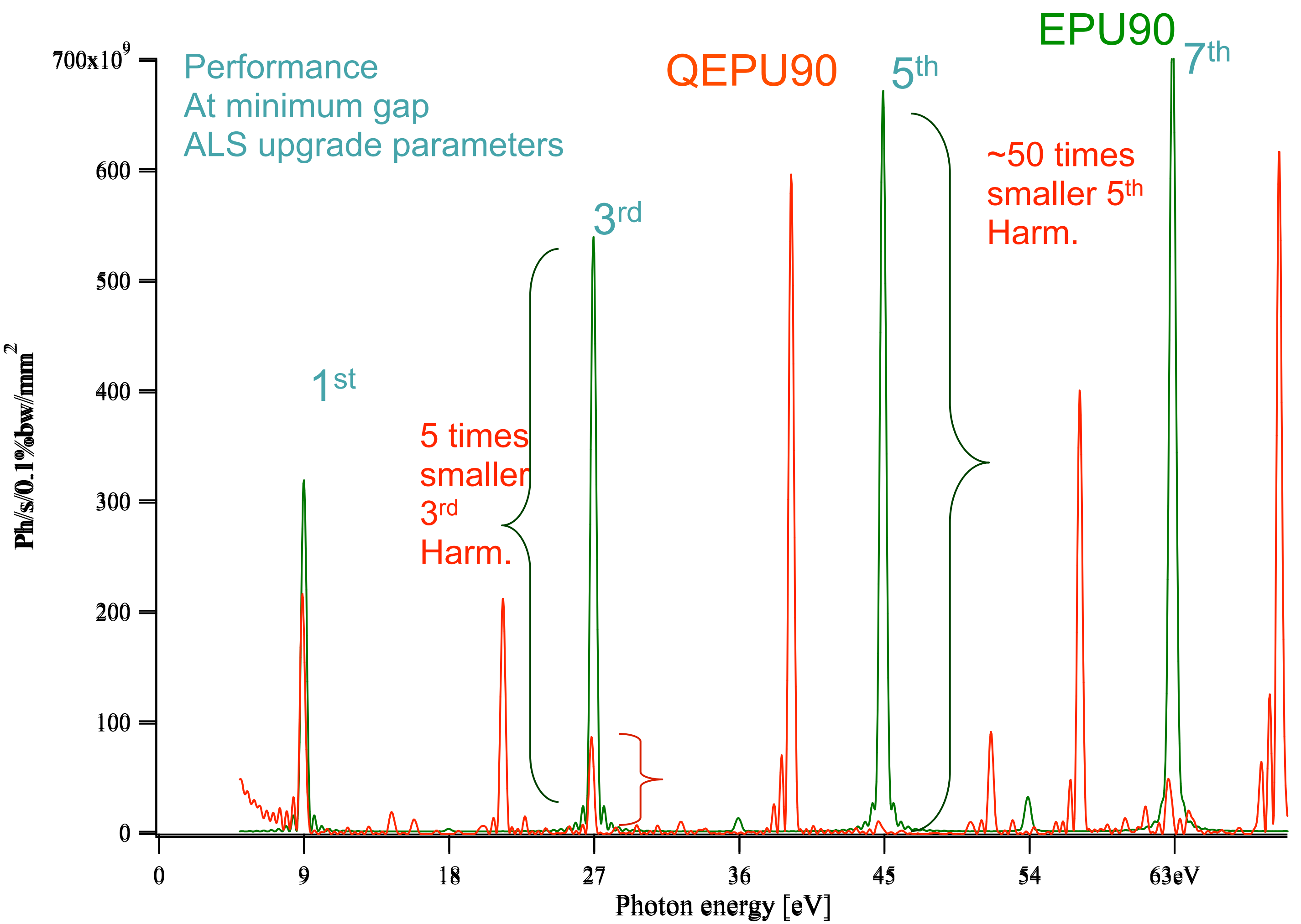

- Undulator produces multiple harmonics
- Diffraction grating disperses these in multiple orders

Se+ Higher Order Analysis

- Measurements made at 2X & 3X the energy
- Nothing at 2X
- Matching features at 3X the energy (absolute at 54.56 eV)
- Corresponding features align

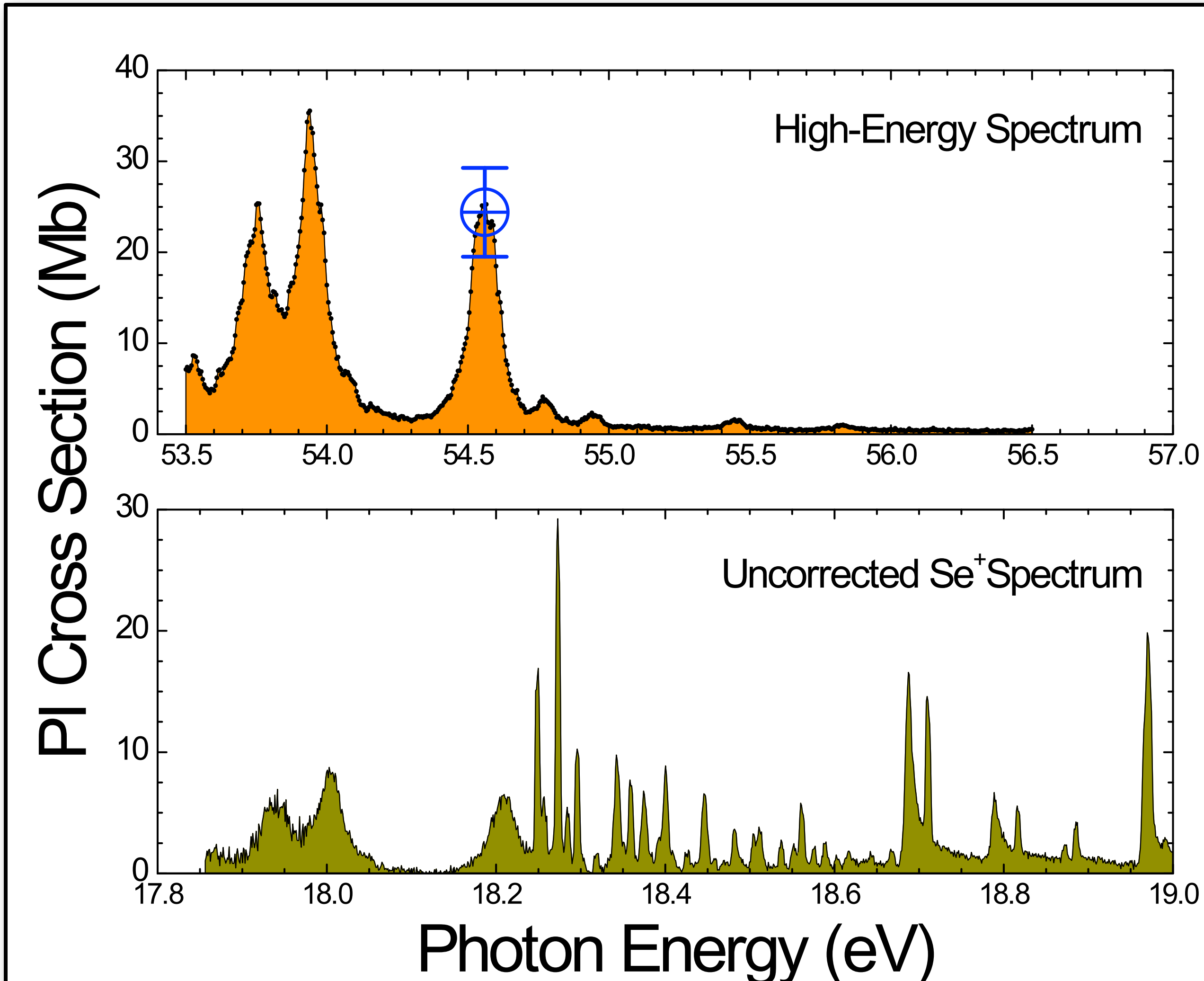

Se^+ Higher Order Analysis

- Energy scale ÷ 3, then plotted on Se^+
- Scaled to match
  (Factor = 0.211)

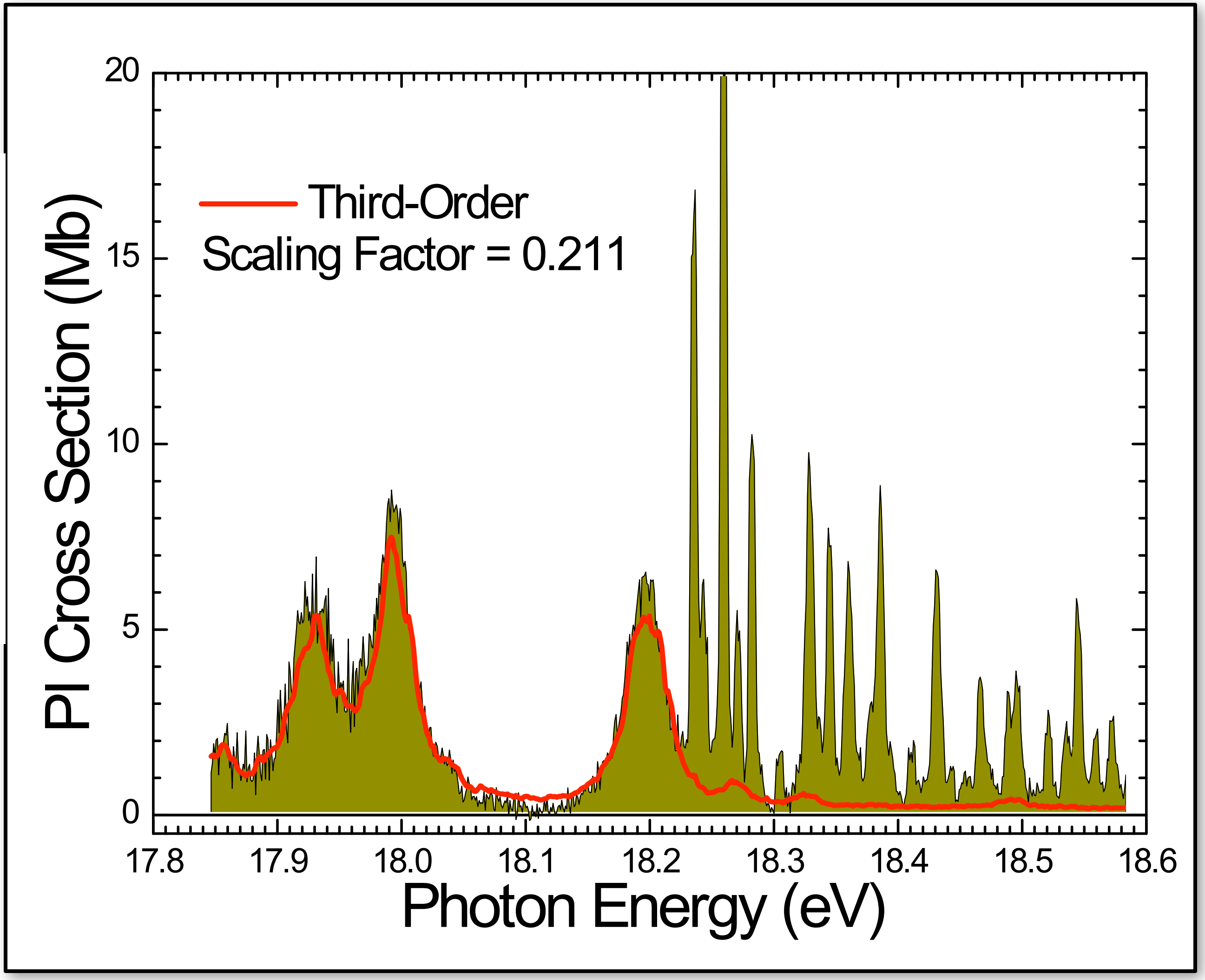

Se^+ Higher Order Analysis

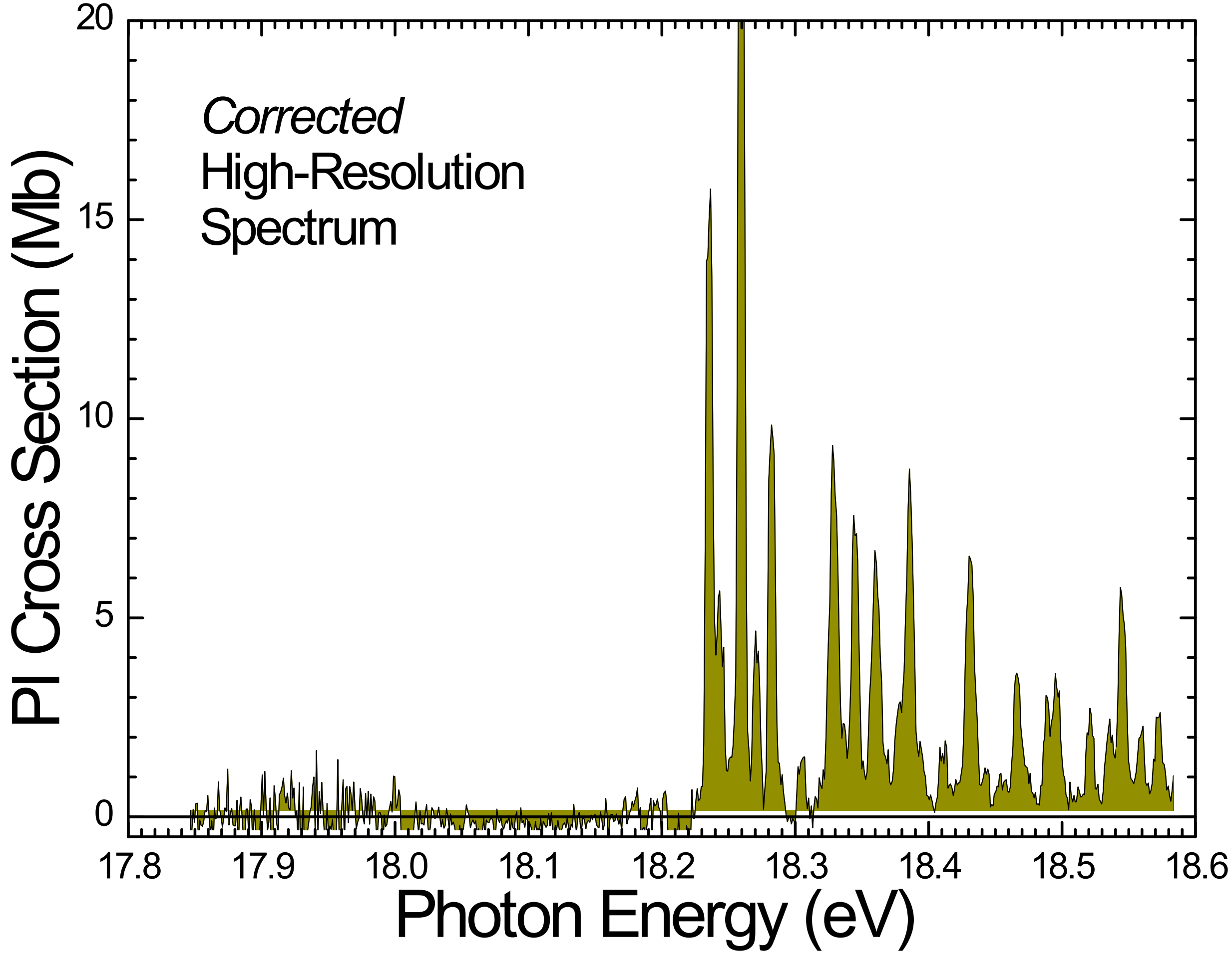

Se^+ Higher Order Analysis

- Energy scale ÷ 3, then plotted on Se^+
- Scaled to match

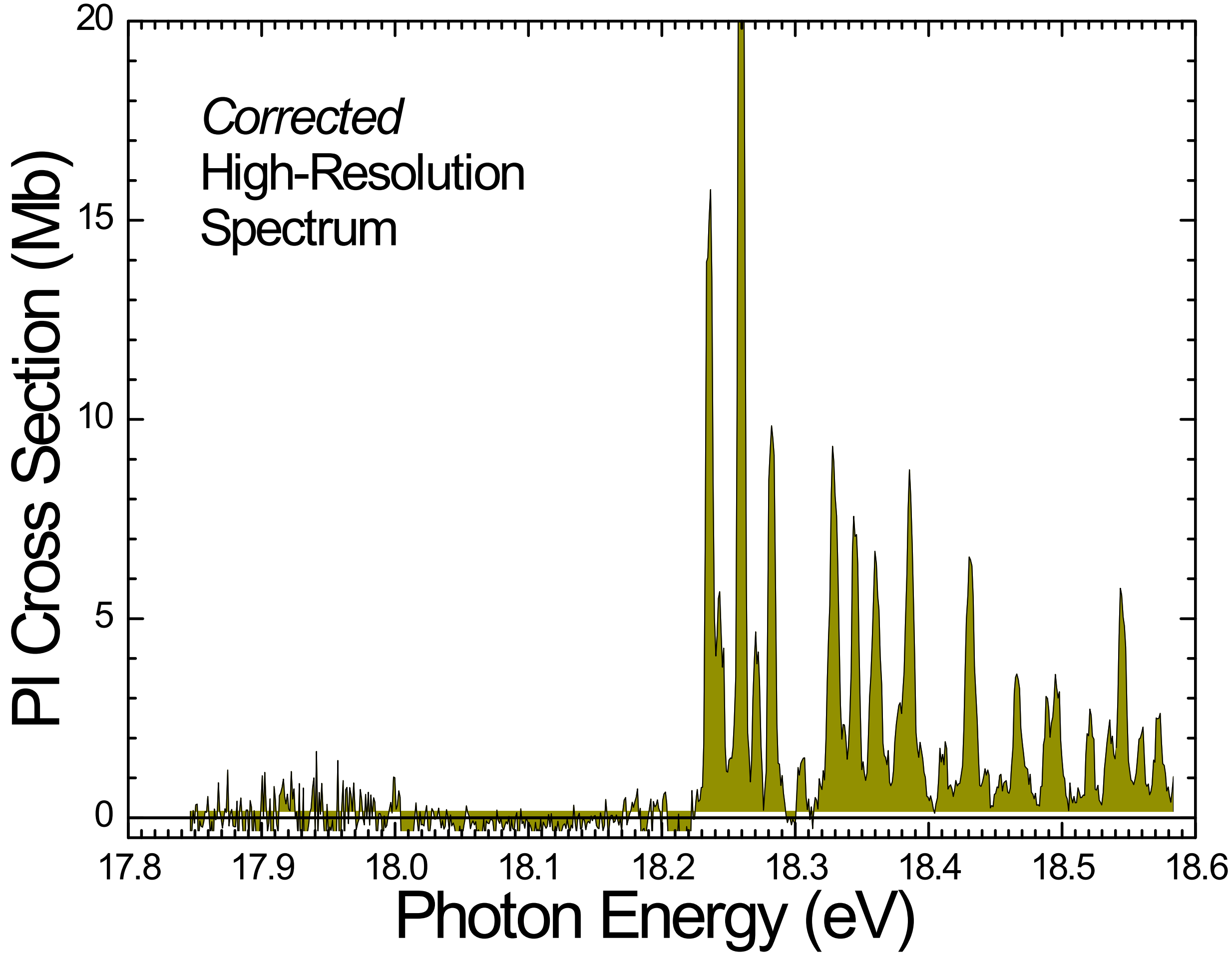

Se⁺ Higher Order Analysis

- Energy scale ÷ 3, then plotted on Se⁺
- Scaled to match (Factor = 0.211)

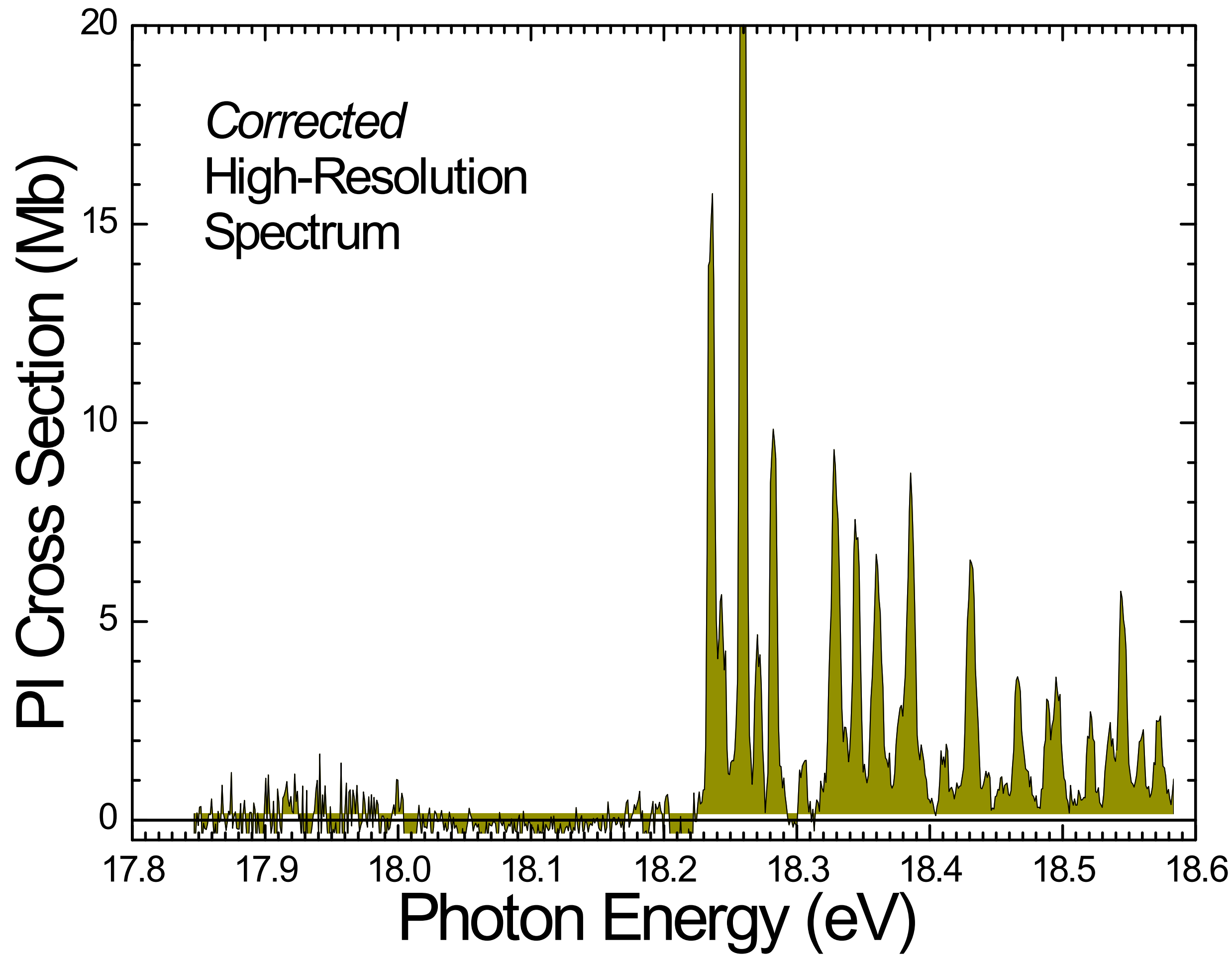

Se^+ Higher Order Analysis

- Energy scale ÷ 3, then plotted on Se^+
- Scaled to match
  (Factor = 0.211)

Estimated third order fraction

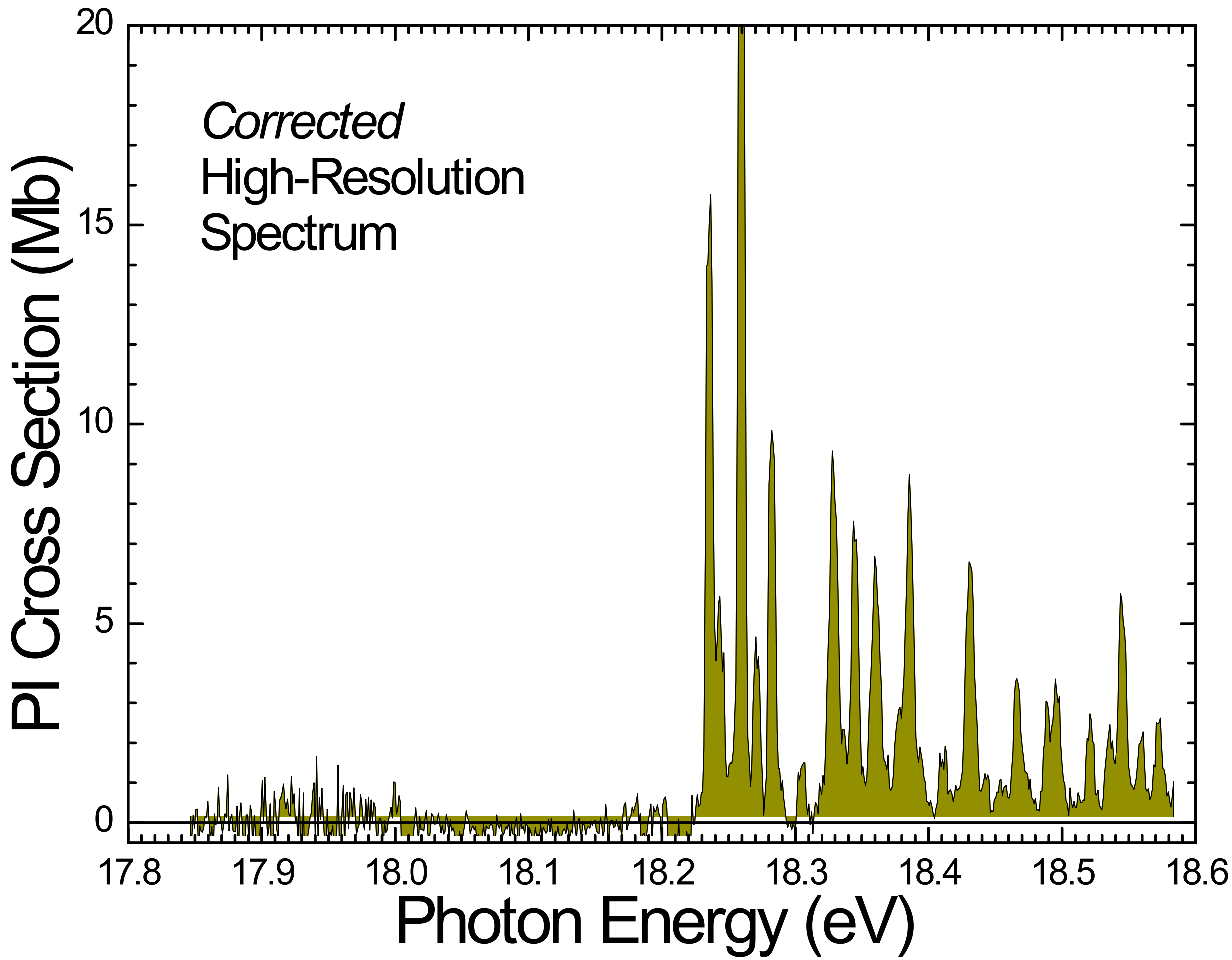

Se^+ Higher Order Analysis

- Energy scale ÷ 3, then plotted on Se^+
- Scaled to match (Factor = 0.211)

Estimated third order fraction 5.5%

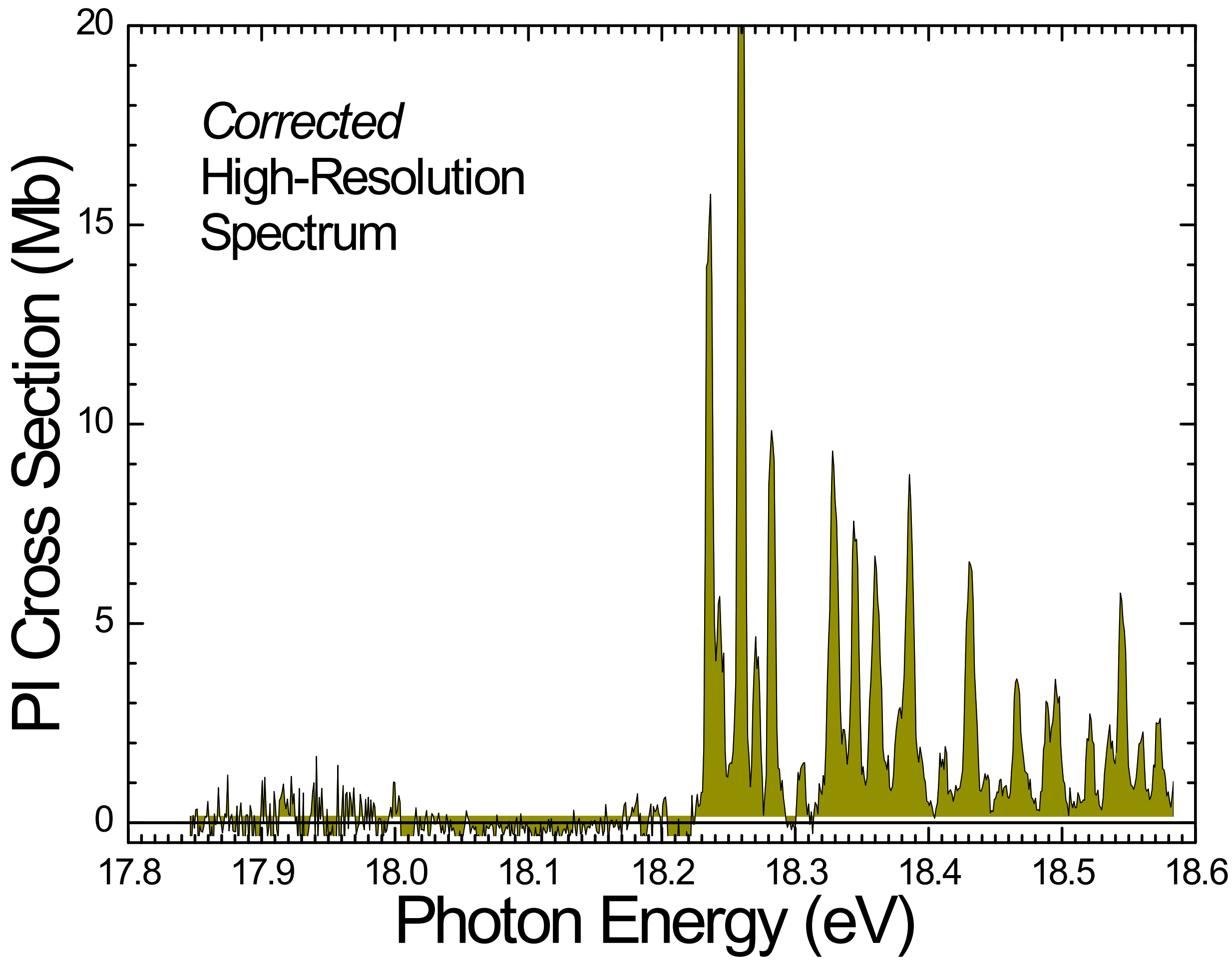

Se^+ Higher Order Analysis

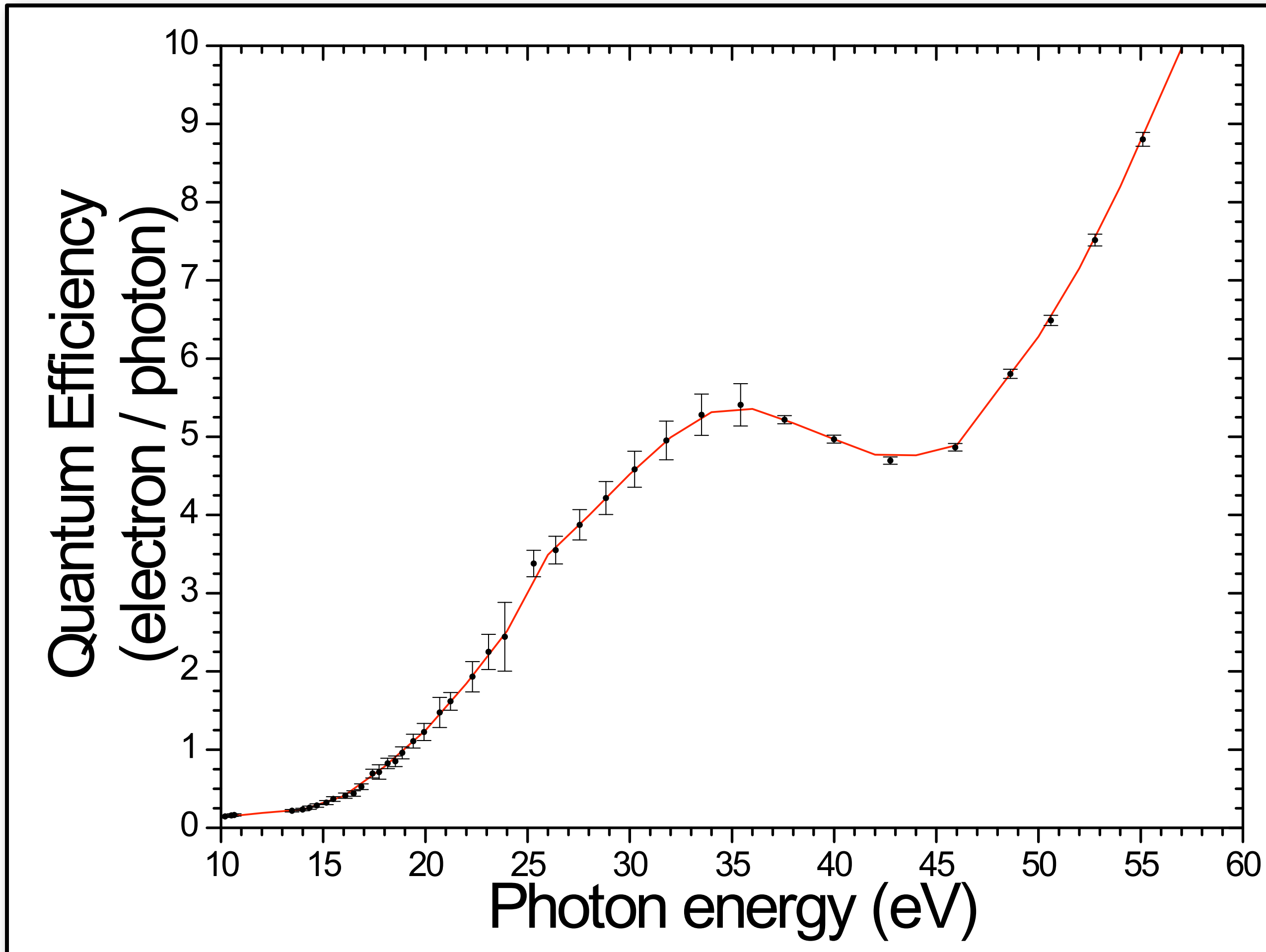

$$\sigma = \frac{R\, q\, e^2\, v_i\, \varepsilon\, F_{av}}{I_+\, I_\gamma\, L\, \Omega\, \delta\, \Delta}$$

Se^+ Higher Order Analysis

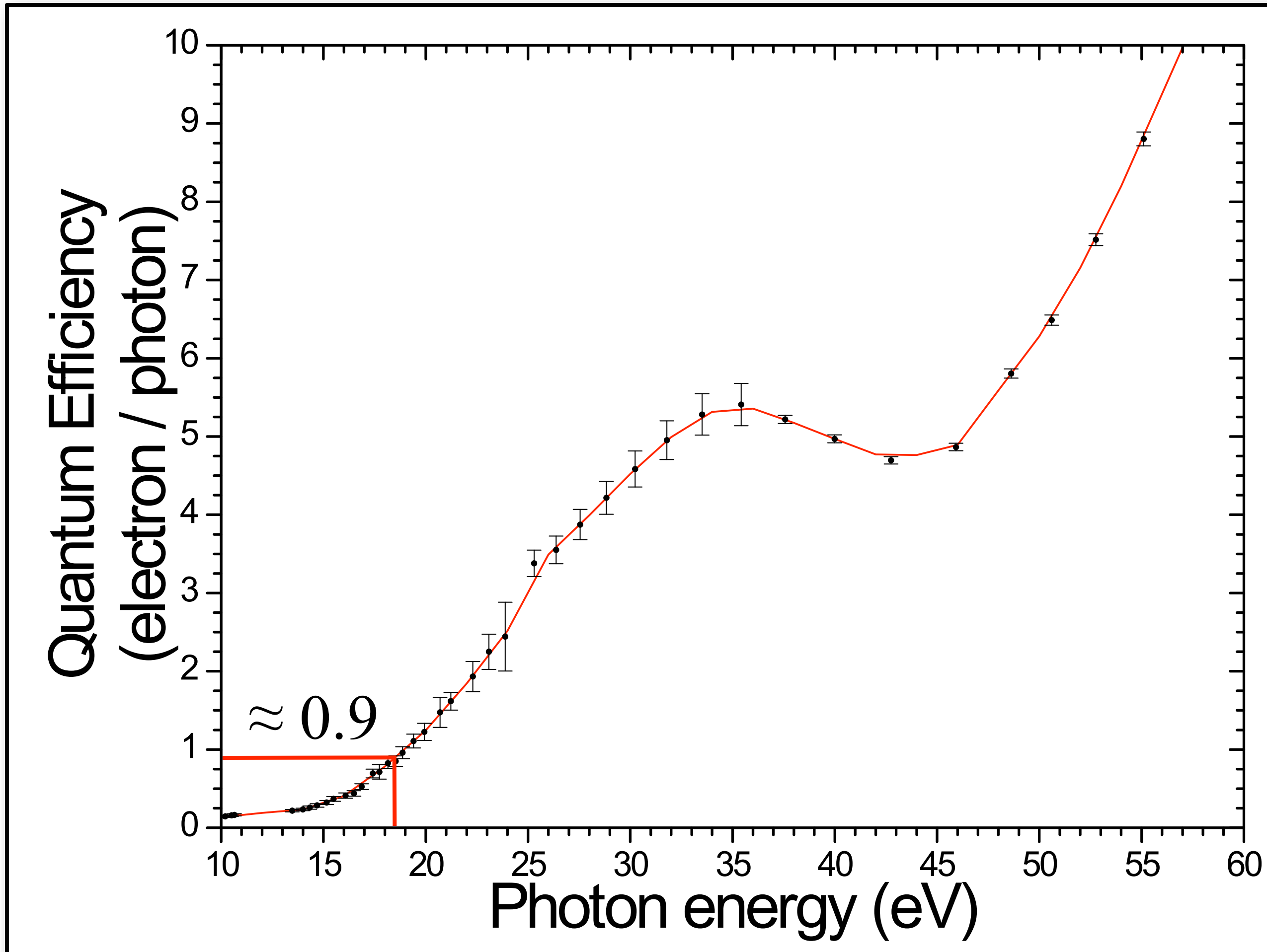

$$\sigma = \frac{R\, q\, e^2\, v_i\, \varepsilon\, F_{av}}{I_+\, I_\gamma\, L\, \Omega\, \delta\, \Delta}$$

Se^{+} Higher Order Analysis

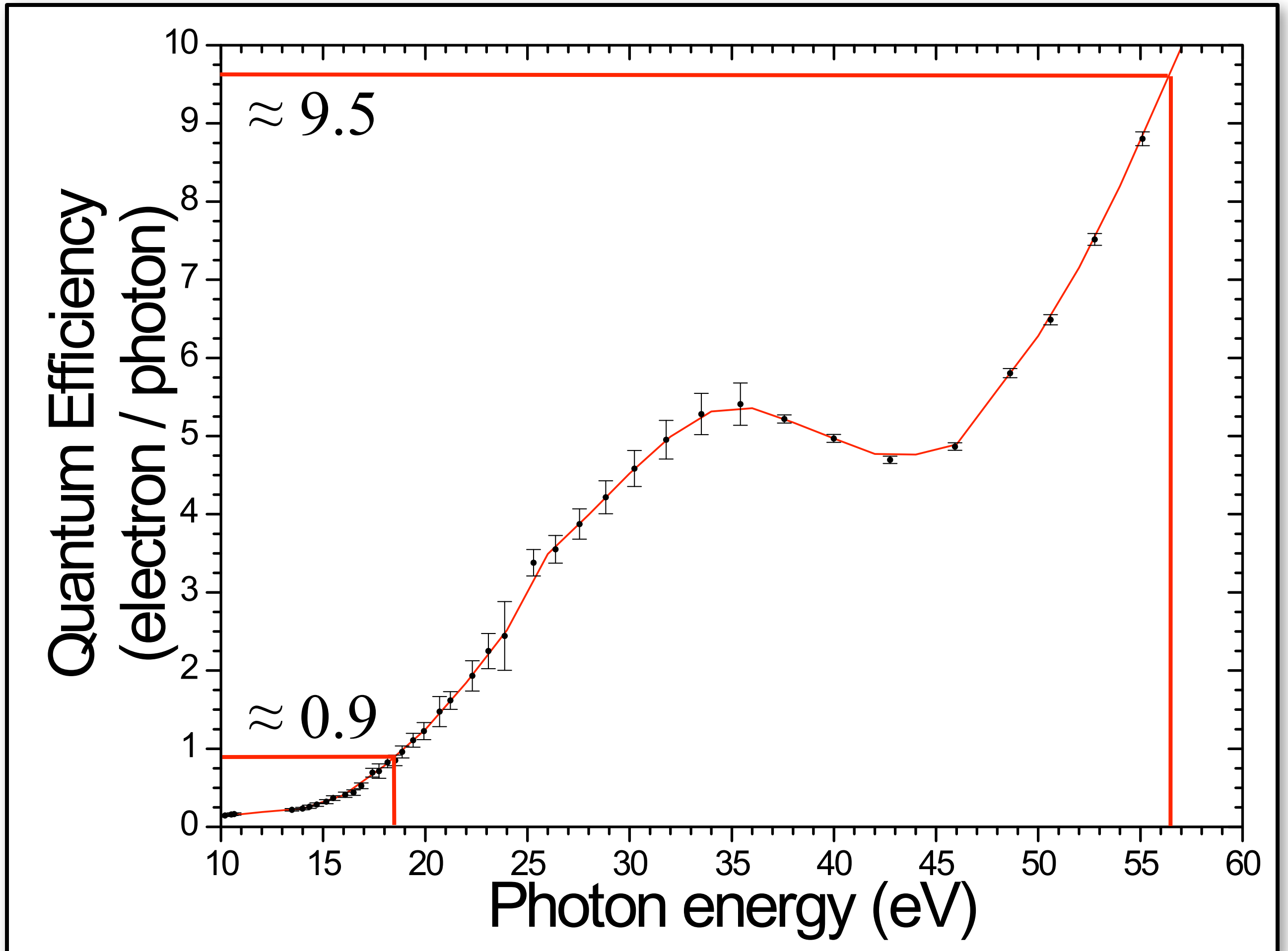

$$\sigma = \frac{R\, q\, e^2\, v_i\, \varepsilon\, F_{av}}{I_+\, I_\gamma\, L\, \Omega\, \delta\, \Delta}$$

Se^+ Higher Order Analysis

- Quantum Efficiency (electrons/photon)

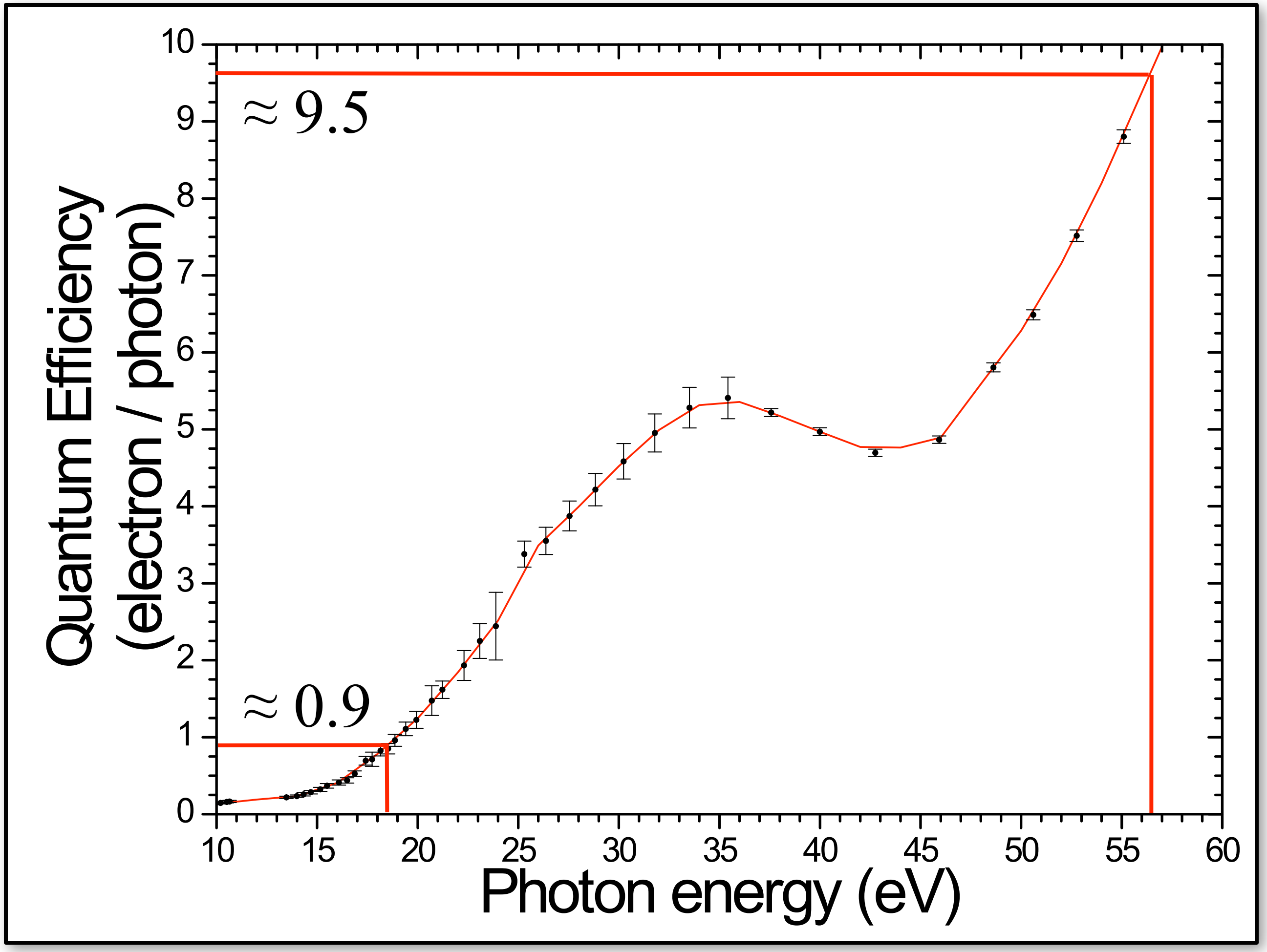

$$\sigma = \frac{R\, q\, e^2\, v_i\, \varepsilon\, F_{av}}{I_+\, I_\gamma\, L\, \Omega\, \delta\, \Delta}$$

Se^+ Higher Order Analysis

- Quantum Efficiency (electrons/photon)

$$\sigma = \frac{R\, q\, e^2\, v_i\, \varepsilon\, F_{av}}{I_+\, I_\gamma\, L\, \Omega\, \delta\, \Delta}$$

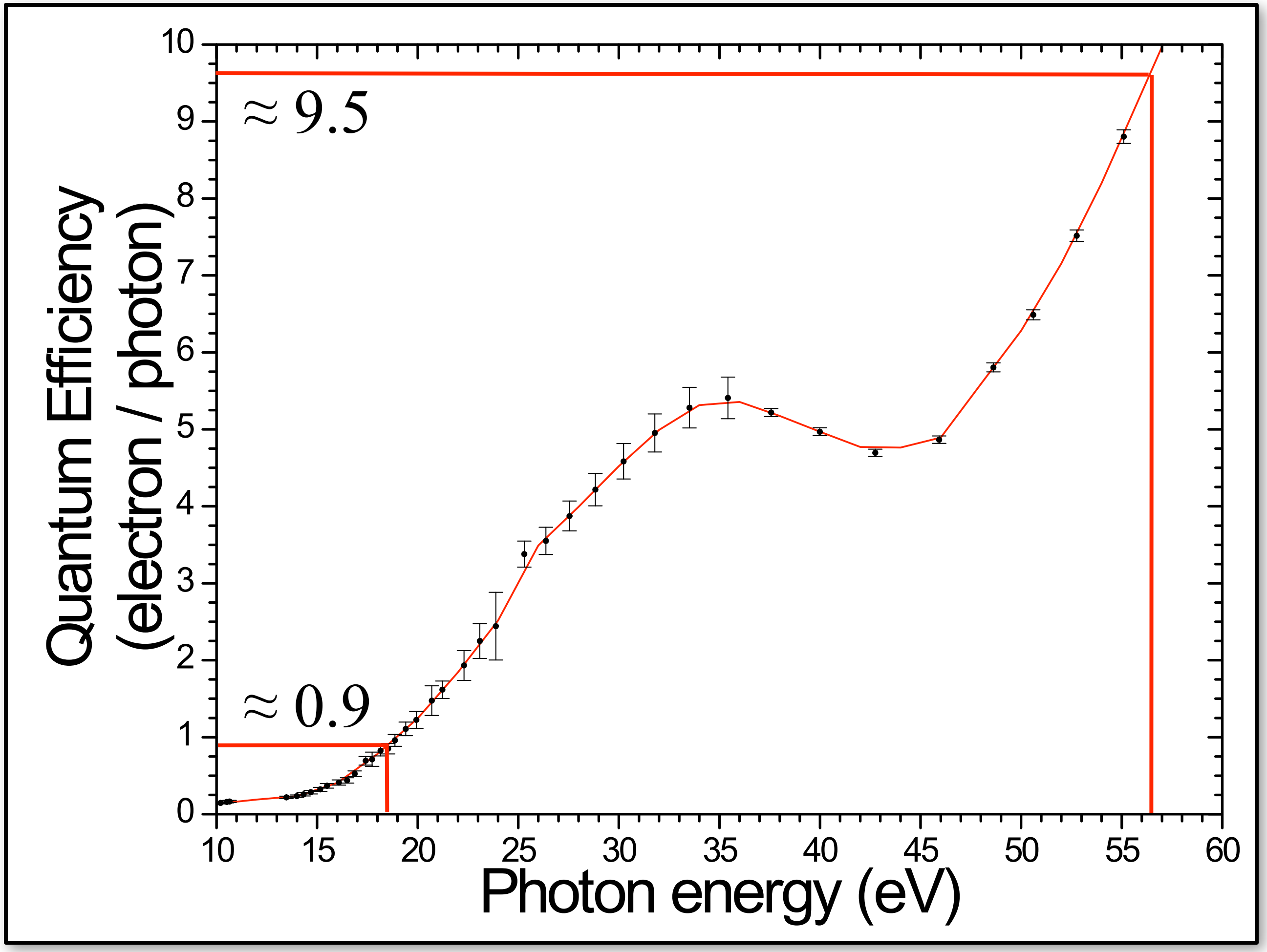

Se+ Higher Order Analysis

- Quantum Efficiency (electrons/photon)
- Inefficient < 20 eV

$$\sigma = \frac{R\, q\, e^2\, v_i\, \varepsilon\, F_{av}}{I_+\, I_\gamma\, L\, \Omega\, \delta\, \Delta}$$

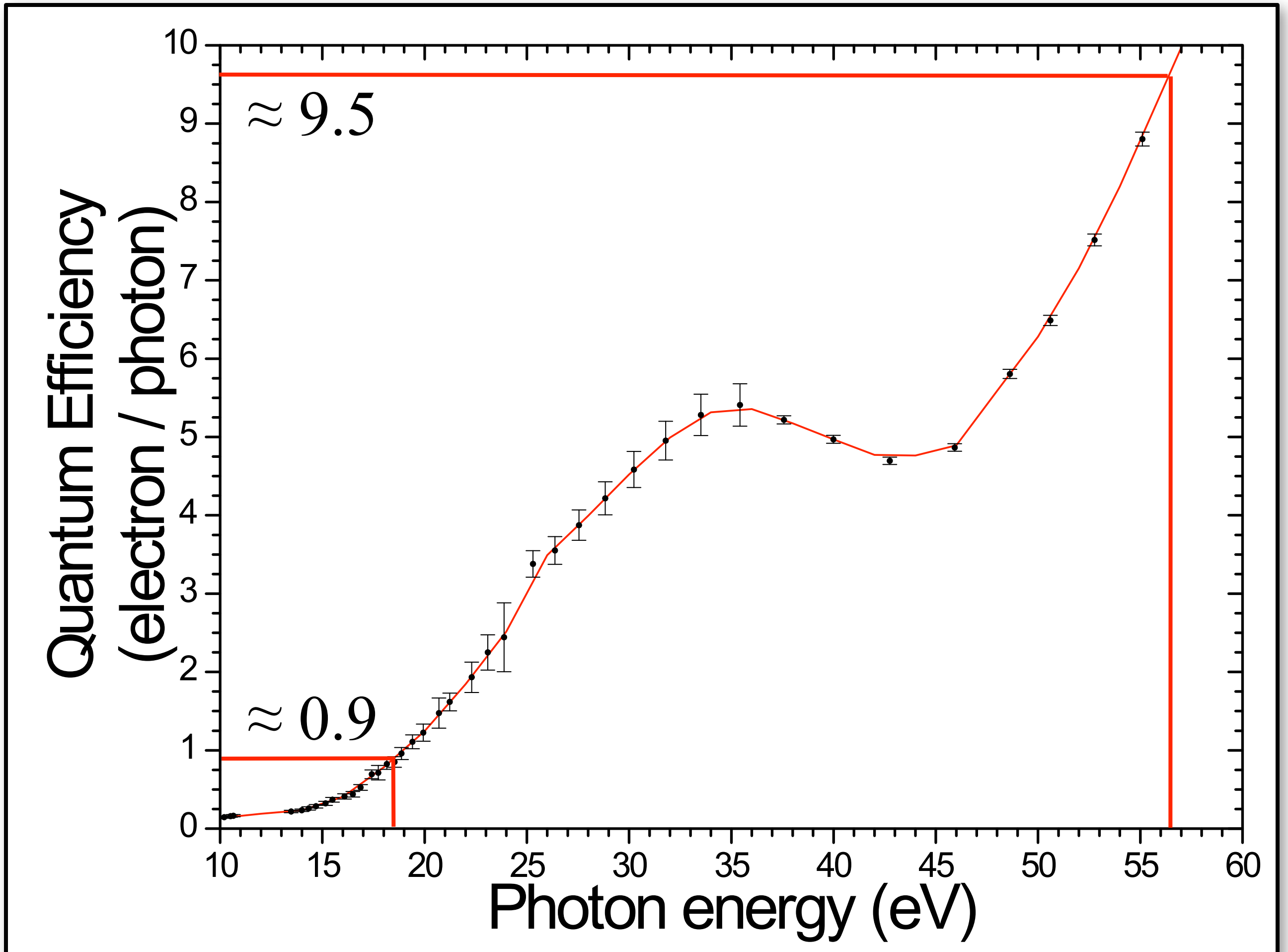

Se^+ Higher Order Analysis

- Quantum Efficiency (electrons/photon)
- Inefficient < 20 eV

$$\sigma = \frac{R\, q\, e^2\, v_i\, \varepsilon\, F_{av}}{I_+\, I_\gamma\, L\, \Omega\, \delta\, \Delta}$$

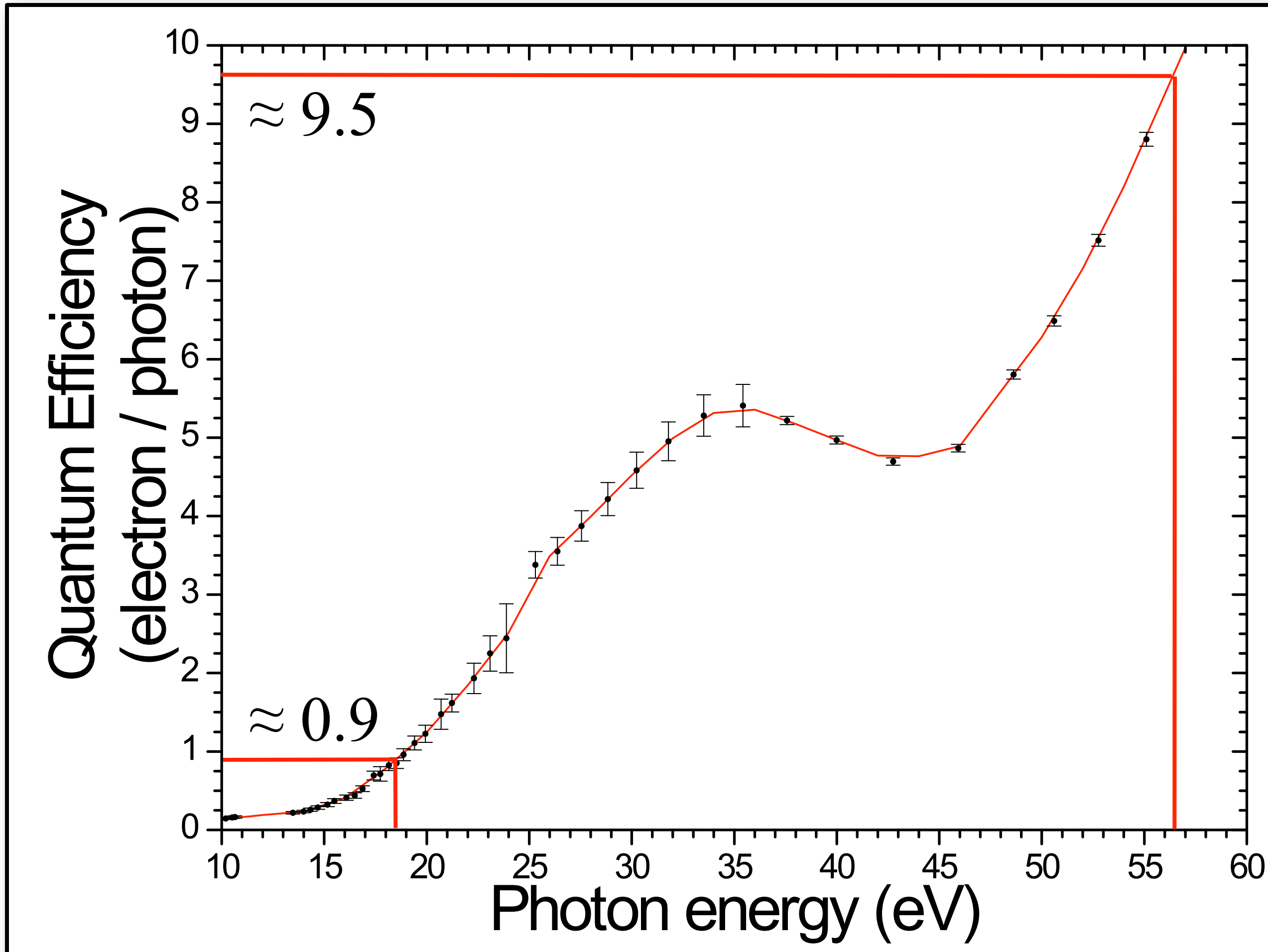

Se^+ Higher Order Analysis

- Quantum Efficiency (electrons/photon)
- Inefficient < 20 eV
- Rapidly increases with energy

$$\sigma = \frac{R\, q\, e^2\, v_i\, \varepsilon\, F_{av}}{I_+\, I_\gamma\, L\, \Omega\, \delta\, \Delta}$$

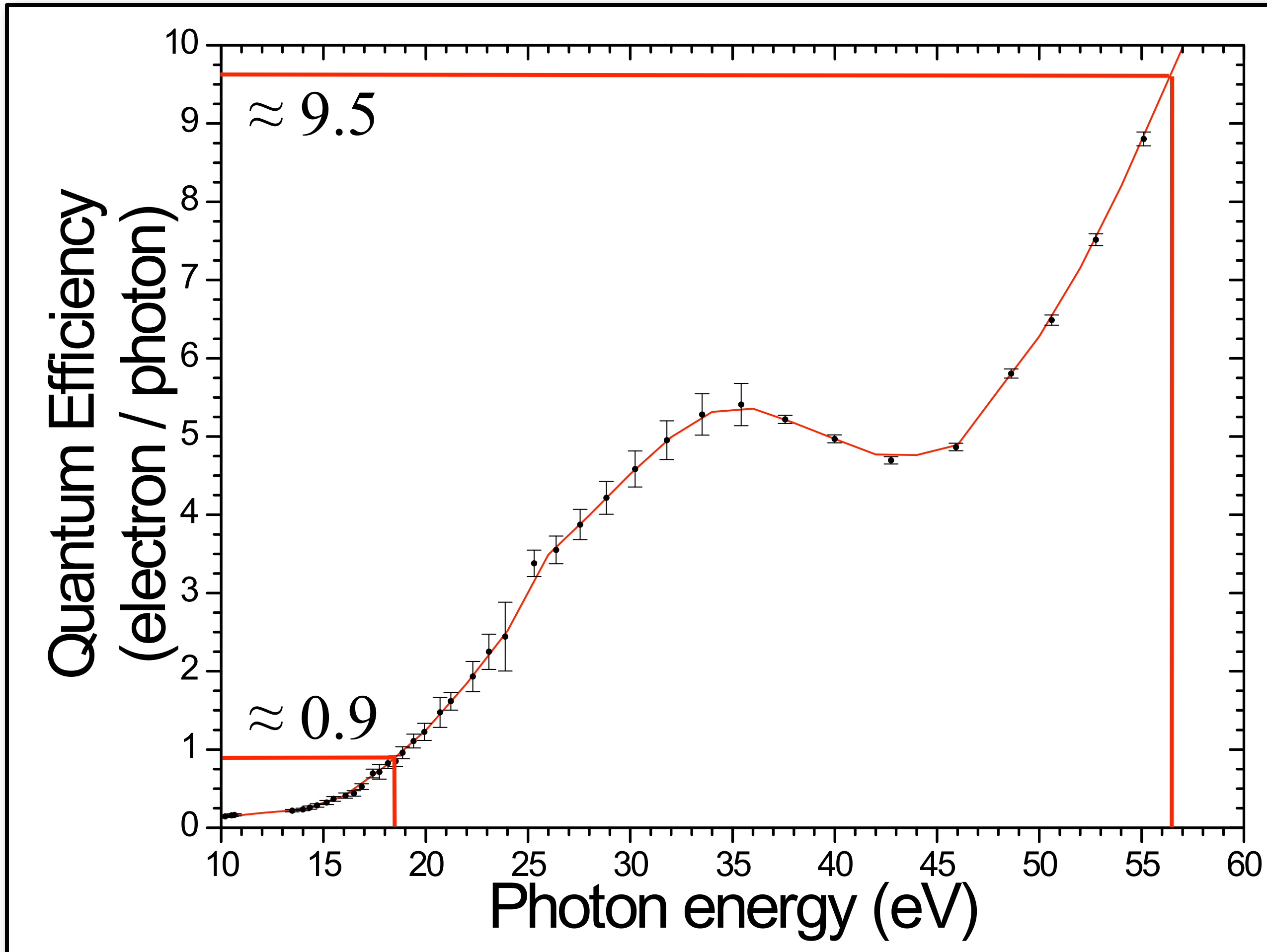

Se^+ Higher Order Analysis

- Quantum Efficiency (electrons/photon)
- Inefficient < 20 eV
- Rapidly increases with energy

$$\sigma = \frac{R\, q\, e^2\, v_i\, \varepsilon\, F_{av}}{I_+\, I_\gamma\, L\, \Omega\, \delta\, \Delta}$$

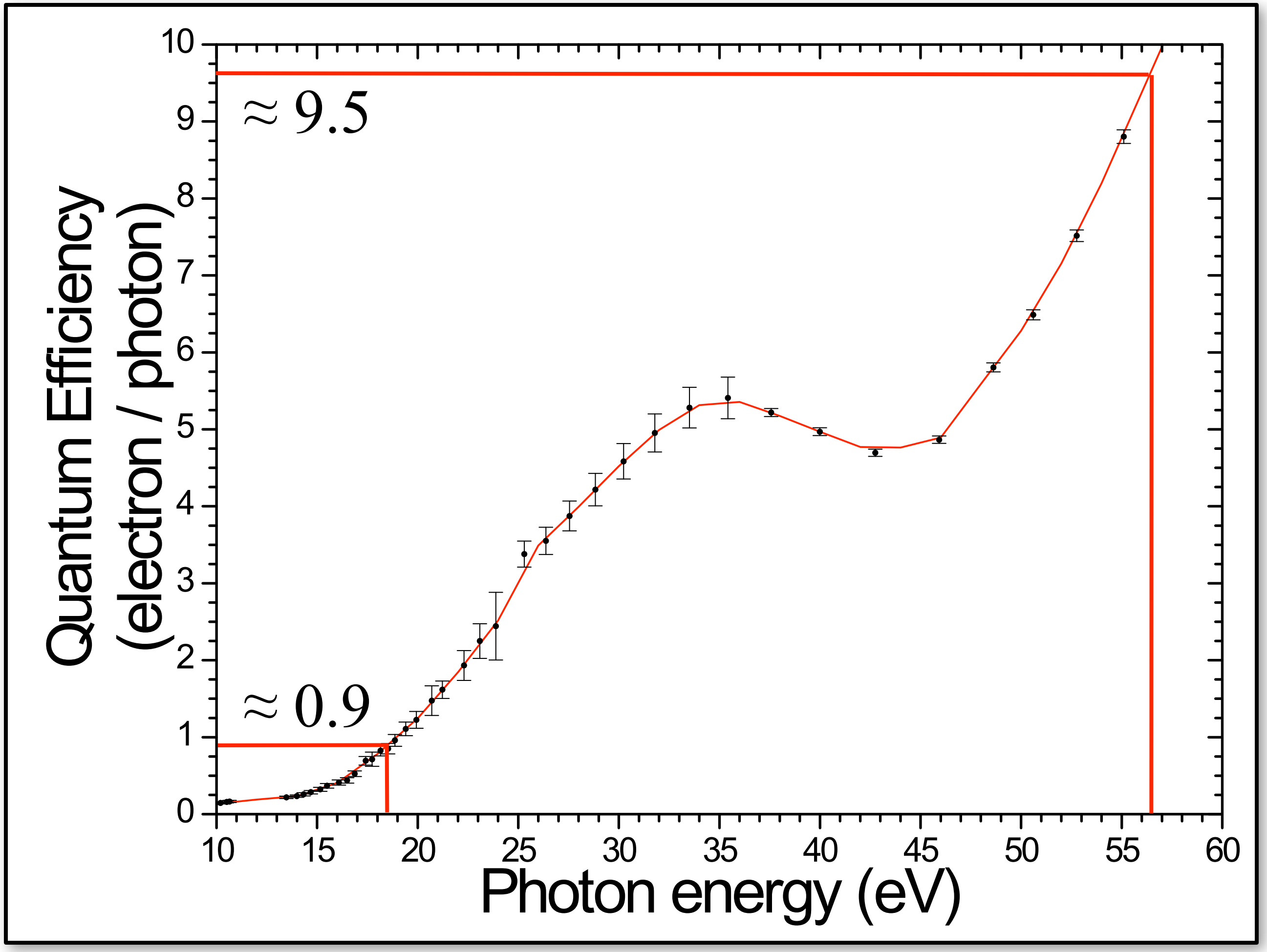

Se⁺ Higher Order Analysis

- Quantum Efficiency (electrons/photon)
- Inefficient < 20 eV
- Rapidly increases with energy
- Diode is ≈ 10X more efficient at 56.5 eV than at 18.5 eV

$$\sigma = \frac{R\, q\, e^2\, v_i\, \varepsilon\, F_{av}}{I_+\, I_\gamma\, L\, \Omega\, \delta\, \Delta}$$

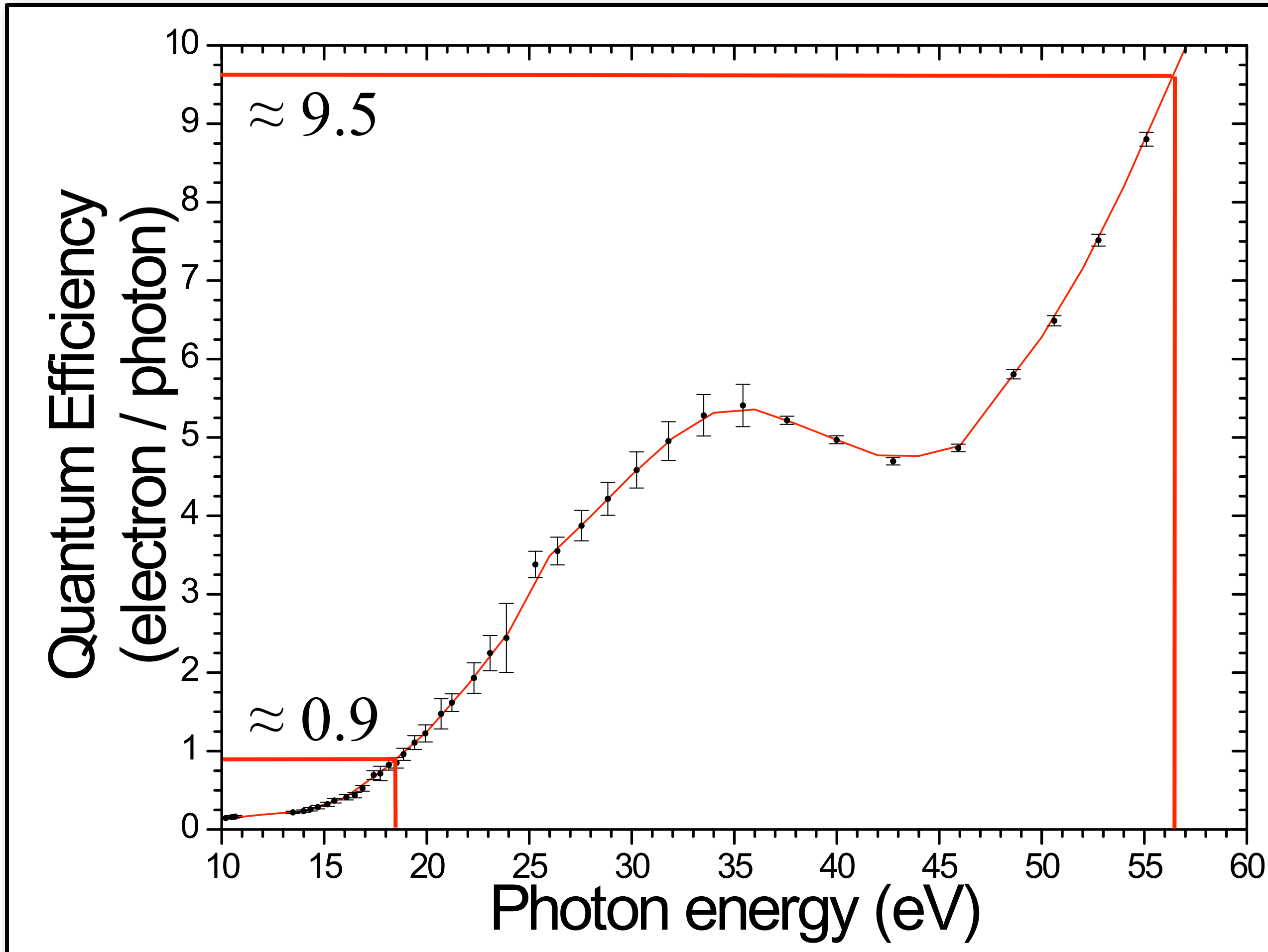

Se^+ Hi-Res Rydberg Series Analysis

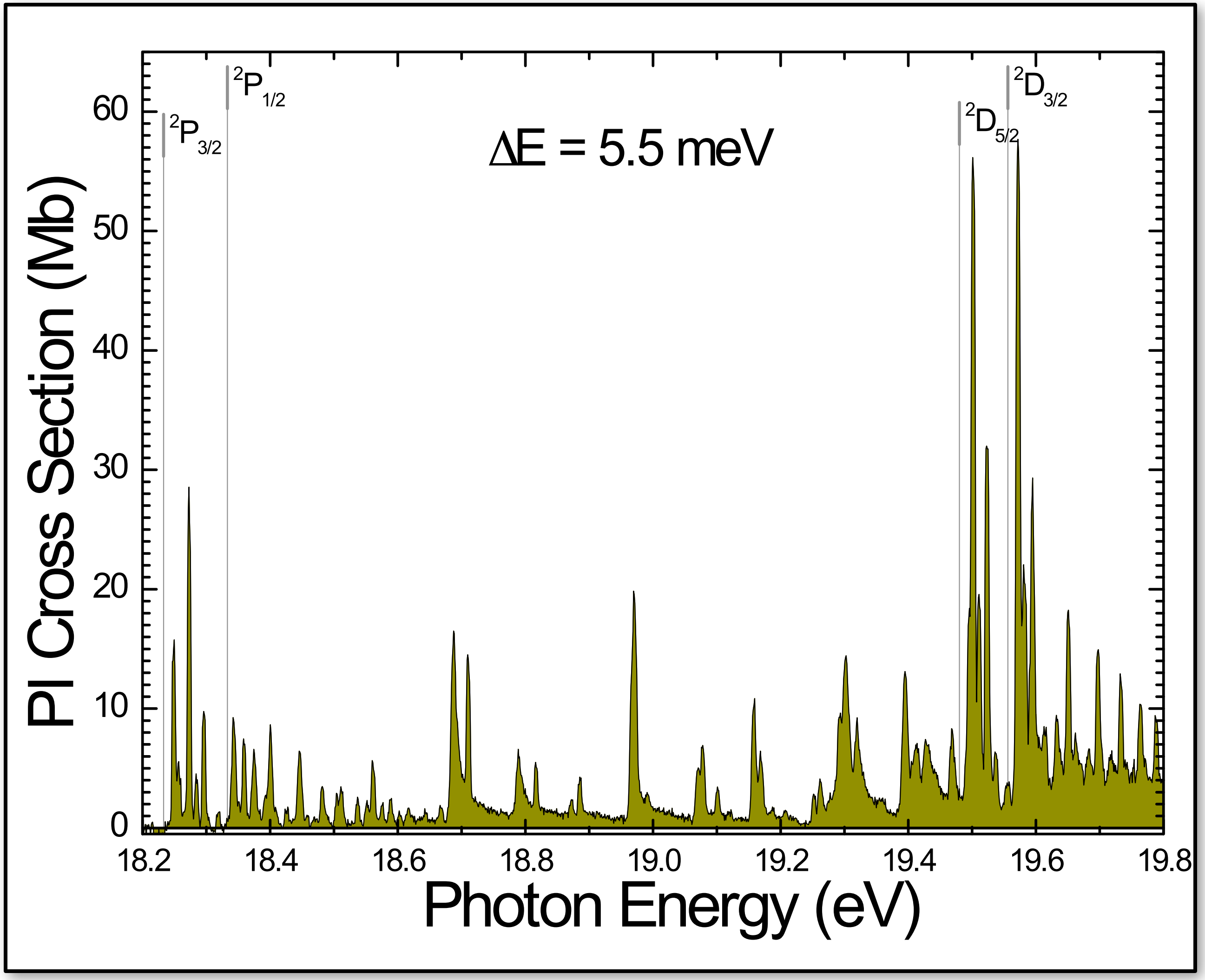

Se+ Hi–Res Rydberg Series Analysis

^2P metastable energy region

$^2P_{3/2} \rightarrow 4s^24p^2\ (^1S)\ nd\ (^2D)$

$^2P_{1/2} \rightarrow 4s^24p^2\ (^1S)\ nd\ (^2D)$

$^2P_{3/2} \rightarrow 4s^24p^2\ (^1D)\ nd\ (^2P)$

$^2P_{3/2} \rightarrow 4s^24p^2\ (^1D)\ nd\ (^2S)$

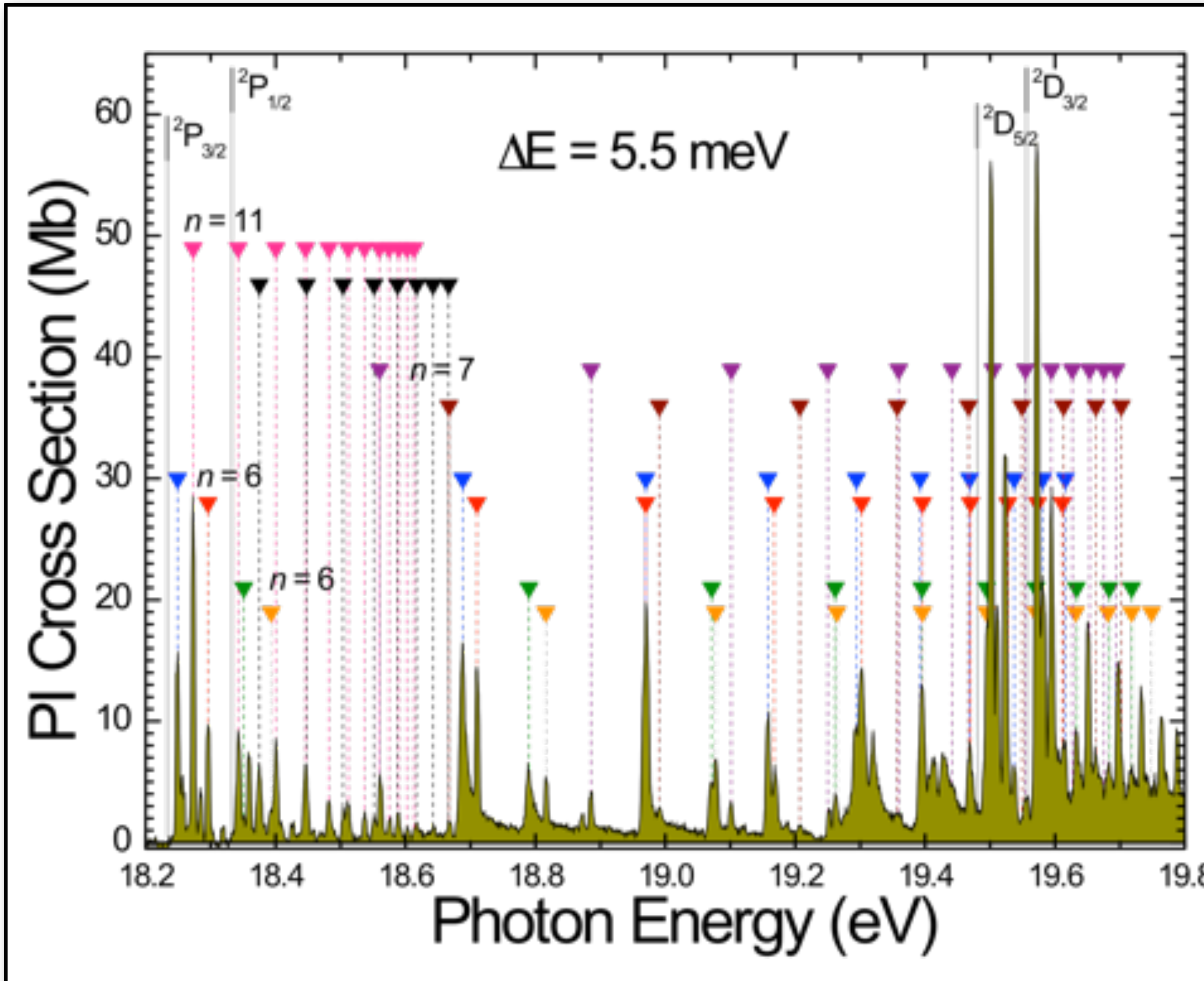

Se^+ Hi-Res Rydberg Series Analysis

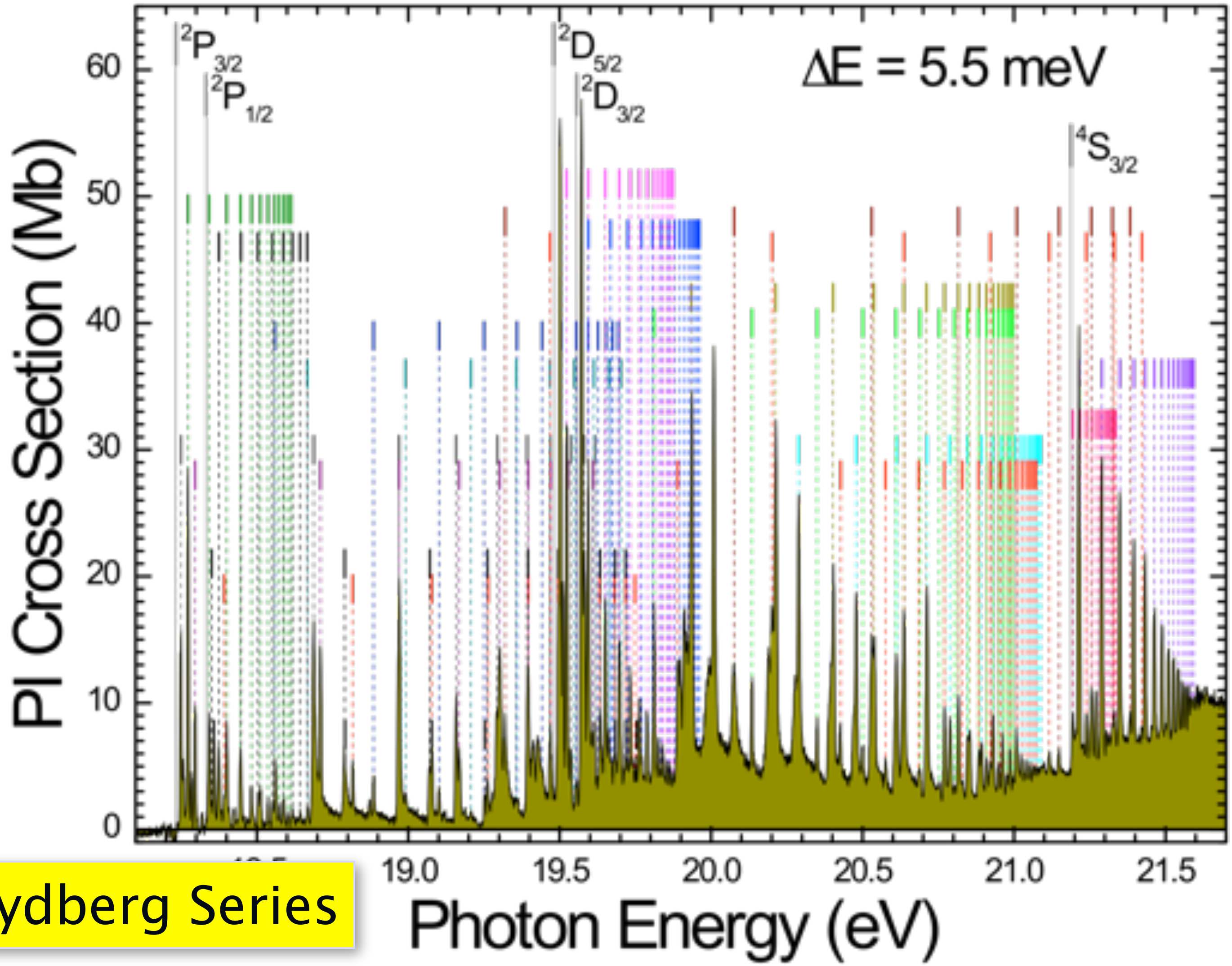

17 Rydberg Series

Theoretical Analysis, Se^+

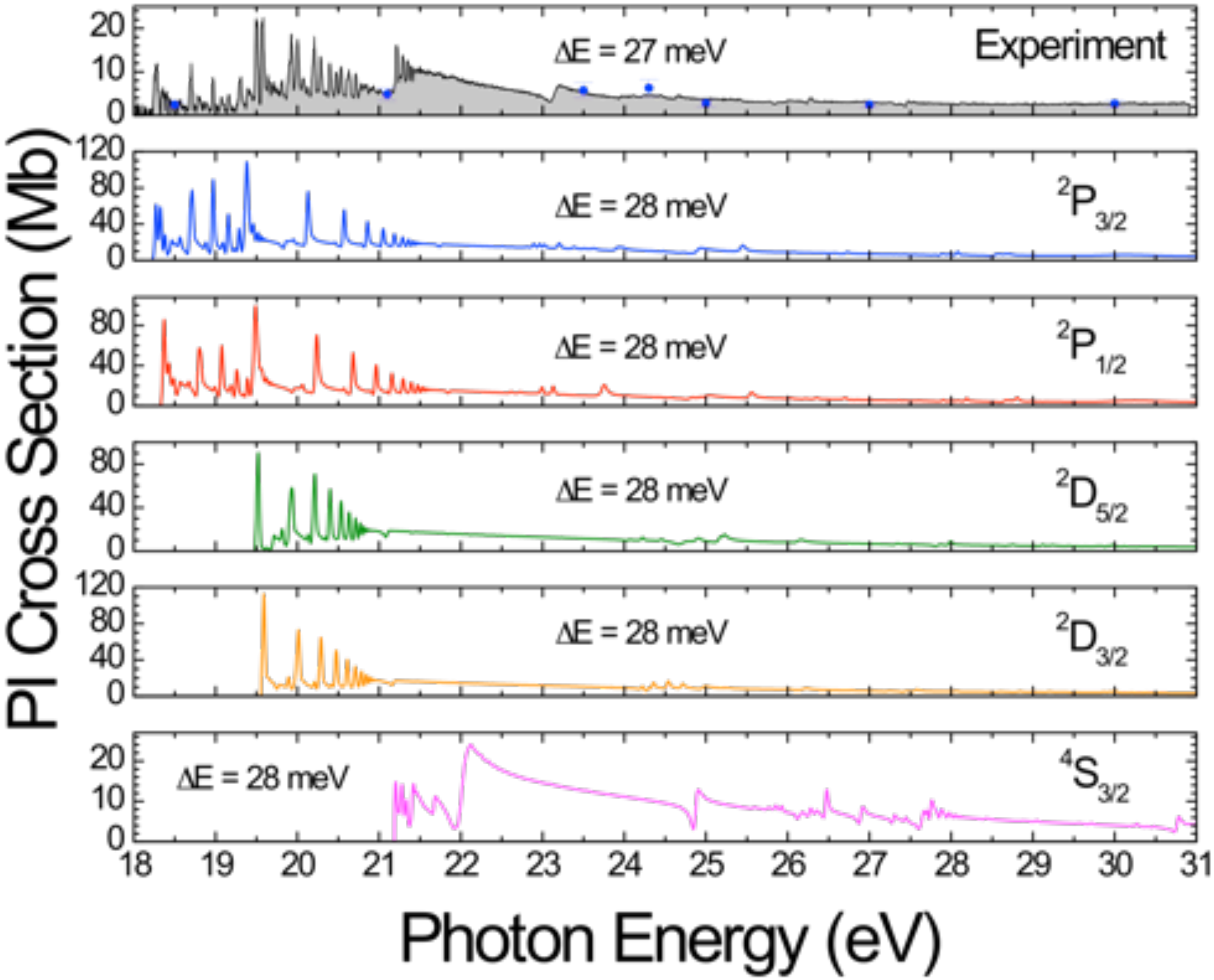

246-state DARC calculations

*see McLaugh

Theoretical Analysis, Se^+

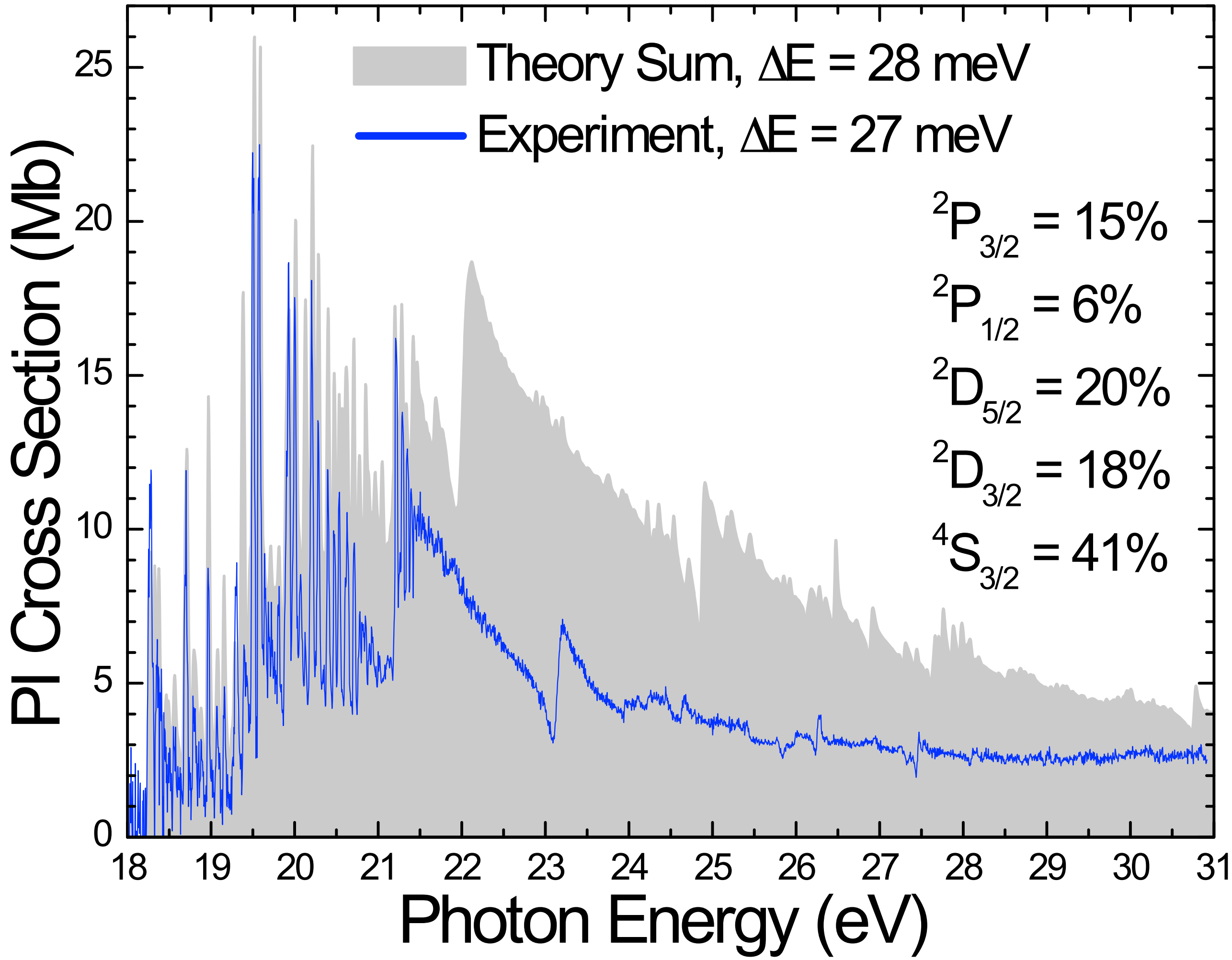

Conclusion

Conclusion

Conclusion

- The photon-ions merged beams method is the “cleanest” method (out of two) that allows highly accurate absolute photoionization cross section meassurements for single and multiply charge positive ions as well as negative ions.

Conclusion

- The photon-ions merged beams method is the "cleanest" method (out of two) that allows highly accurate absolute photoionization cross section meassurements for single and multiply charge positive ions as well as negative ions.

Conclusion

- The photon-ions merged beams method is the "cleanest" method (out of two) that allows highly accurate absolute photoionization cross section meassurements for single and multiply charge positive ions as well as negative ions.

- These cross sections are needed in multiple disciplines and applications. For instance, EUV lithography light source modeling, Tokamak research, Astrophysics, FELs data, etc…

Conclusion

- The photon-ions merged beams method is the “cleanest” method (out of two) that allows highly accurate absolute photoionization cross section meassurements for single and multiply charge positive ions as well as negative ions.

- These cross sections are needed in multiple disciplines and applications. For instance, EUV lithography light source modeling, Tokamak research, Astrophysics, FELs data, etc…

Conclusion

- The photon-ions merged beams method is the “cleanest” method (out of two) that allows highly accurate absolute photoionization cross section meassurements for single and multiply charge positive ions as well as negative ions.

- These cross sections are needed in multiple disciplines and applications. For instance, EUV lithography light source modeling, Tokamak research, Astrophysics, FELs data, etc…

- Contrary to popular believe, in many cases (particularly heavy ions) these cross sections are not and can not be calculated yet, with sufficient accuracy for many of the applications. Therefore, these experiments are providing highly-accurate benchmarks for evolving

Conclusion

- In the case of the absolute photoionization data for Se ions, the data helped on the...
  - 1. Clarification and determination of ionization thresholds
  - 2. Identify resonance features, including Rydberg series resonances
  - 3. Investigate parameters of beamline performance (pushing the beamline capabilities).

*see N.C. Sterling, et al, Pub.Astr. Soc. Australia, **26**, 3, 339-344 (2009)

Conclusion

- In the case of the absolute photoionization data for Se ions, the data helped on the...
  - 1. Clarification and determination of ionization thresholds
  - 2. Identify resonance features, including Rydberg series resonances
  - 3. Investigate parameters of beamline performance (pushing the beamline capabilities).

none of this would have been possible without a third generation light source.

*see N.C. Sterling, et al, Pub.Astr. Soc. Australia, **26**, 3, 339-344 (2009)

Photon-ion merged beams apparatus

• Photoionization of Se ions;
Determination of elemental abundances in PNe

Sterling *et al.*, accepted JPB (2010)

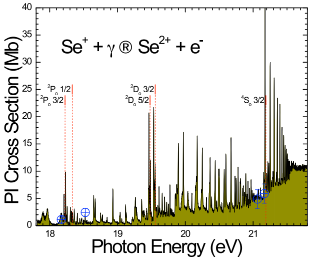

N.C. Sterling, D. Esteves, A.L. Kilcoyne, E. Red, R.A. Phaneu R.C. Bilodeau,and A. Aguilar

• Photoionization of $Ce@C_{82}{}^{+}$ $Xe@C_{60}{}^{+}$;
Confinement resonances,
Quantum computing,
Cancer therapy

Müller *et al.*, PRL 101, 133001 (2008)
Kilcoyne *et al.* PRL 105, 213001 (2010)

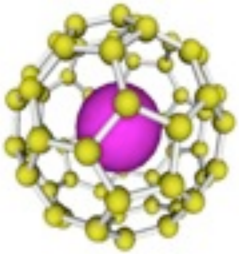

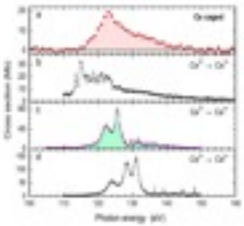

A. Müller, S. Schippers, M.Habibi, D. Esteves, J.C. Wang, R.A. Phaneuf, A.L.D. Kilcoyne, A. Aguilar and L. Dunsch

These experiments were only possible due to the high resolution and high photon flux of this beamline.

Motivations

- From a single atom to a well structured solid sample.
- Attractive to have (manipulate) atoms isolated from their environment.
  - Building blocks for the qubits of quantum computers.
  - Chemical isolated reactive and poisonous atoms for medical imaging and cancer therapy.

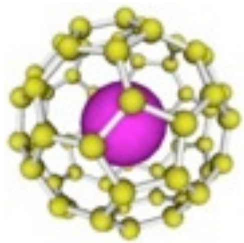

Müller *et al.*, PRL 101, 133001 (2008)

Kilcoyne *et al.* PRL 105, 213001 (2010)

- While there are almost no experimental results available for endohedral molecules in the gas phase, theoretical work flourishes without constraints. Clearly, experiments are needed to test and guide the theoretical developments

Extremely difficult experiment "tour de France"

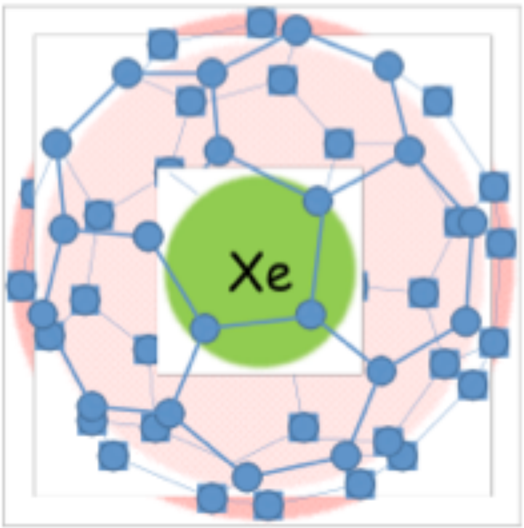

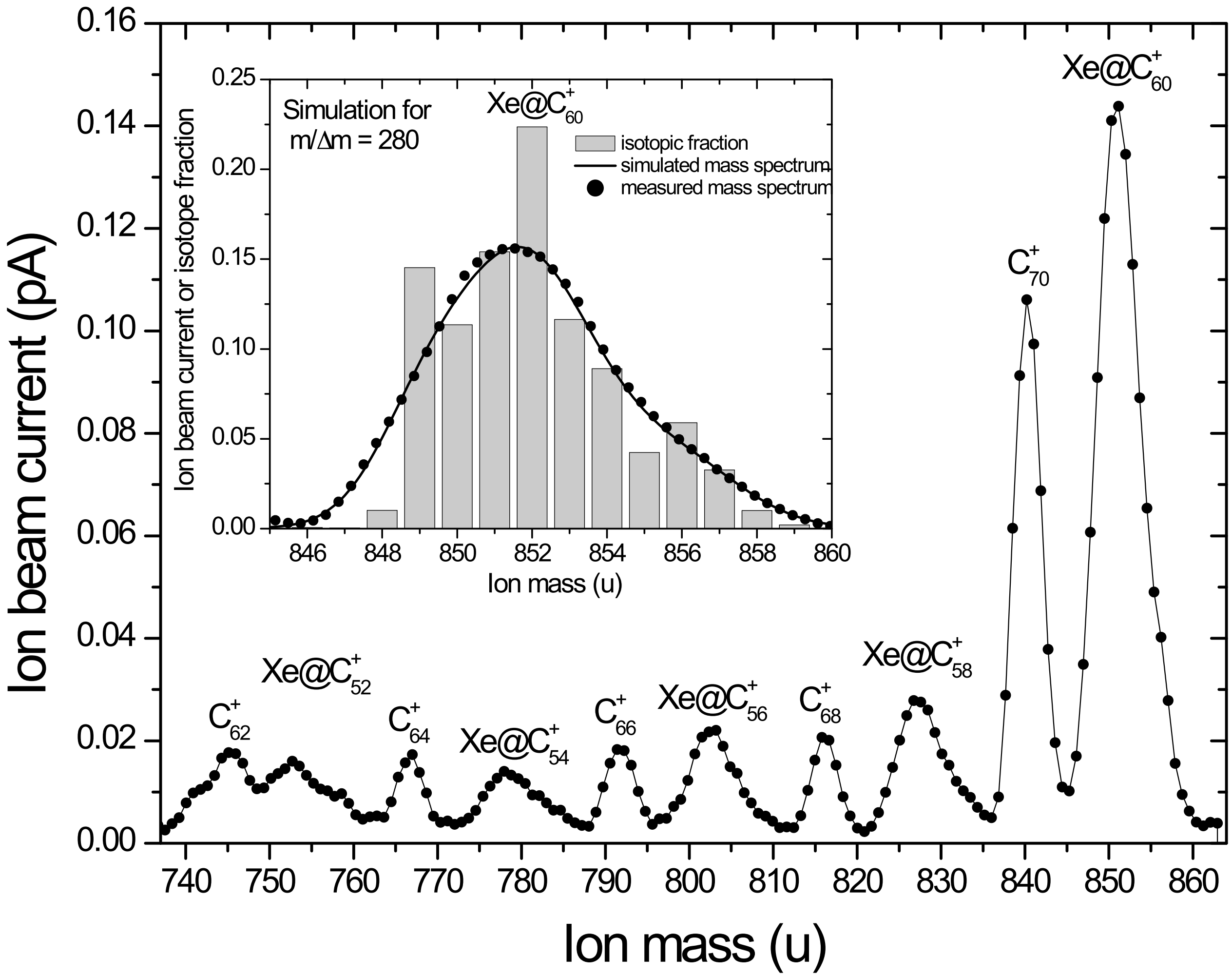

Ion beam current (pA)
Ion mass (u)
0.16
0.14
0.12
0.10
0.08
0.06
0.04
0.02
0.00
740
750
760
770
780
790
800
810
820
830
840
850
860
C_{62}^+
$Xe@C_{52}^+$
C_{64}^+
$Xe@C_{54}^+$
C_{66}^+
$Xe@C_{56}^+$
C_{68}^+
$Xe@C_{58}^+$
C_{70}^+
$Xe@C_{60}^+$
Simulation for
$m/\Delta m = 280$
isotopic fraction
simulated mass spectrum
measured mass spectrum
Ion beam current or isotope fraction
0.25
0.20
0.15
0.10
0.05
0.00
846
848
850
852
854
856
858
860

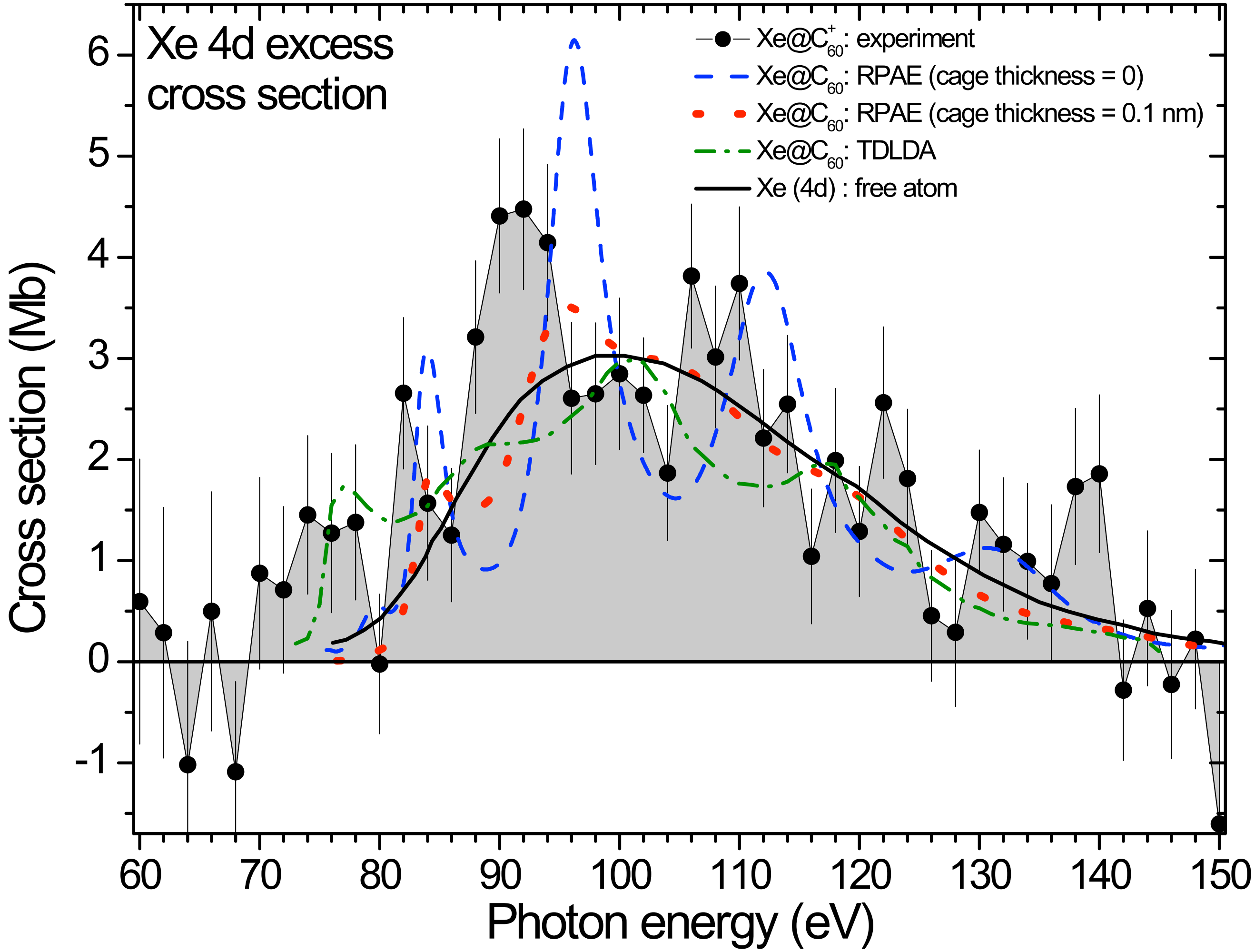
Xe 4d excess
cross section
Xe@C$_{60}^{+}$: experiment
Xe@C$_{60}$: RPAE (cage thickness = 0)
Xe@C$_{60}$: RPAE (cage thickness = 0.1 nm)
Xe@C$_{60}$: TDLDA
Xe (4d) : free atom
Cross section (Mb)
Photon energy (eV)
6
5
4
3
2
1
0
-1
60
70
80
90
100
110
120
130
140
150

Gracias por su atención

Photoionization of endohedral fullerene ions

$Ce@C_{82}^{+}$ in comparison with atomic Ce^{q+} ions (q=2-4)

What is the charge of the atom inside the cage?

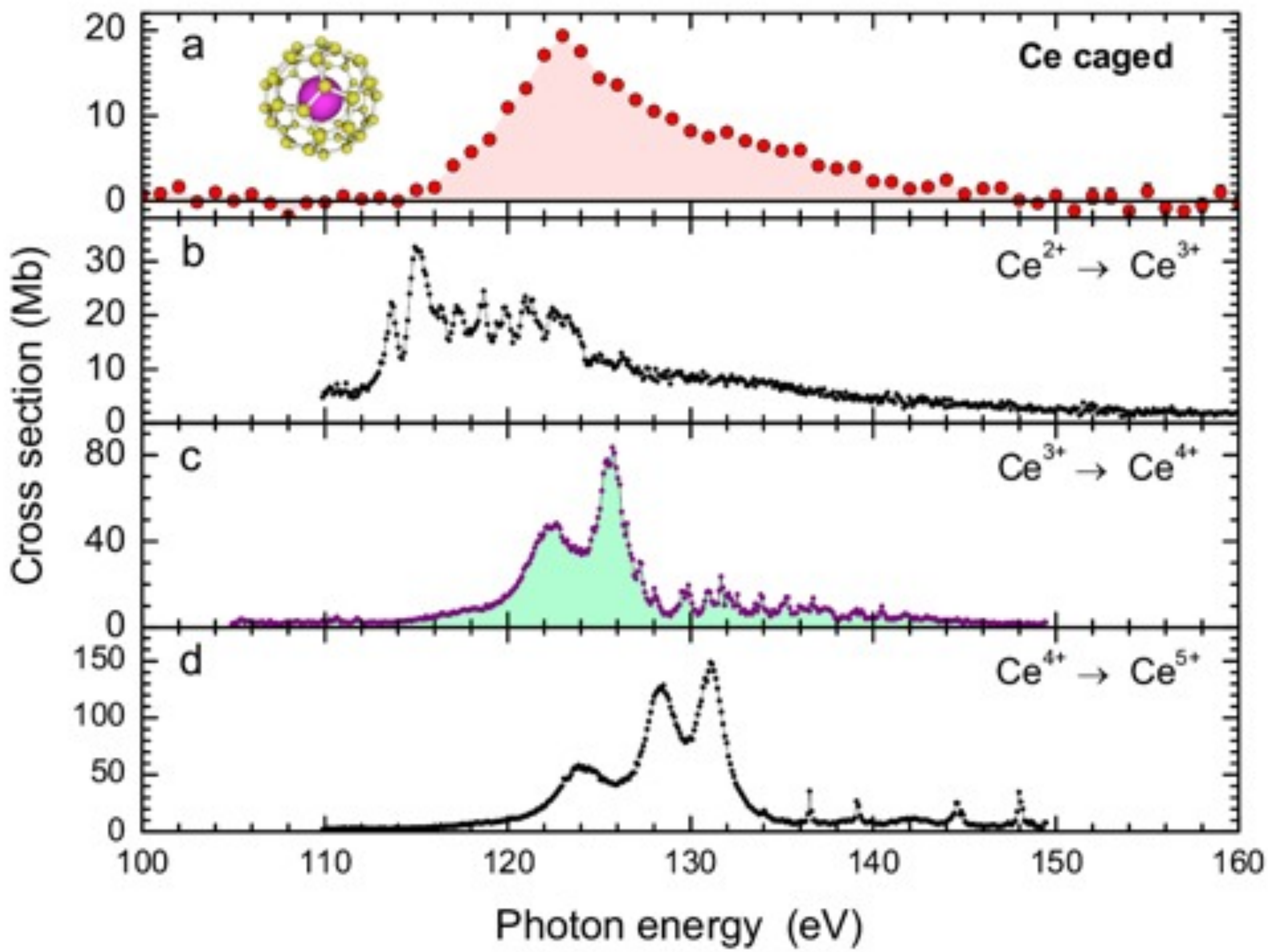

A. Müller et al., PRL 101 (2008) 133001

EUV source candidates (13 -14 nm)

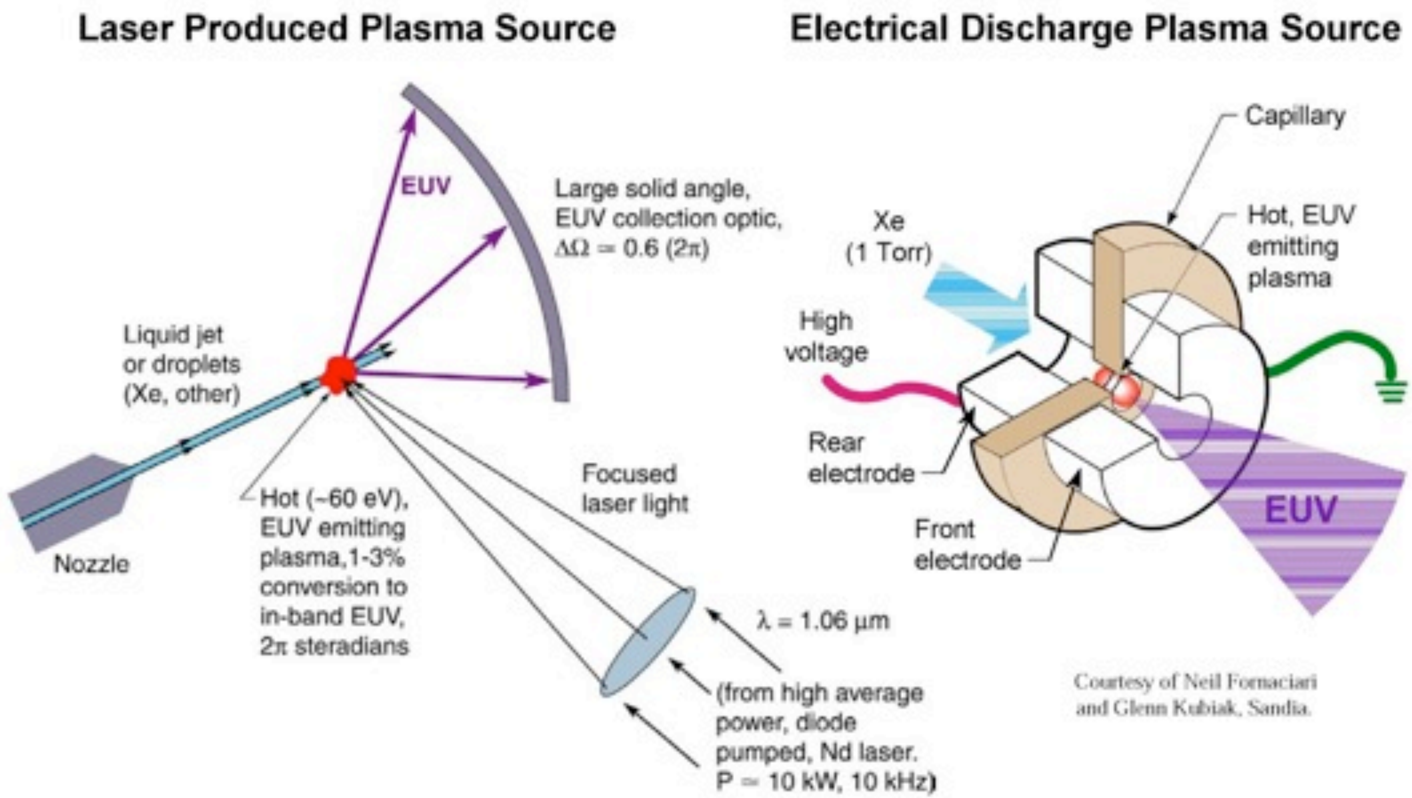

Comparative Xe and Sn Spectra near 13.5 nm

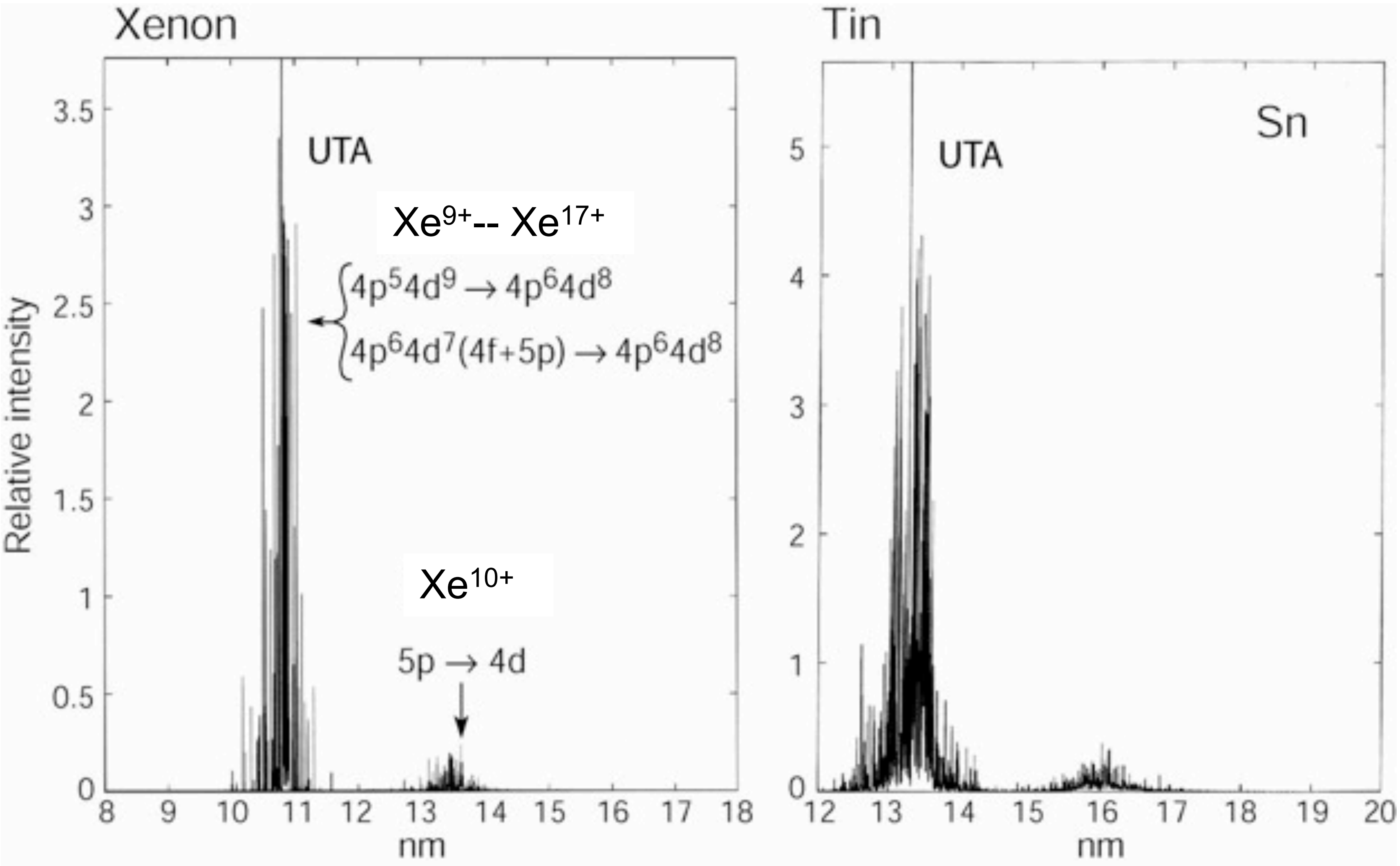

Photoionization of Low Charged Xe Ions

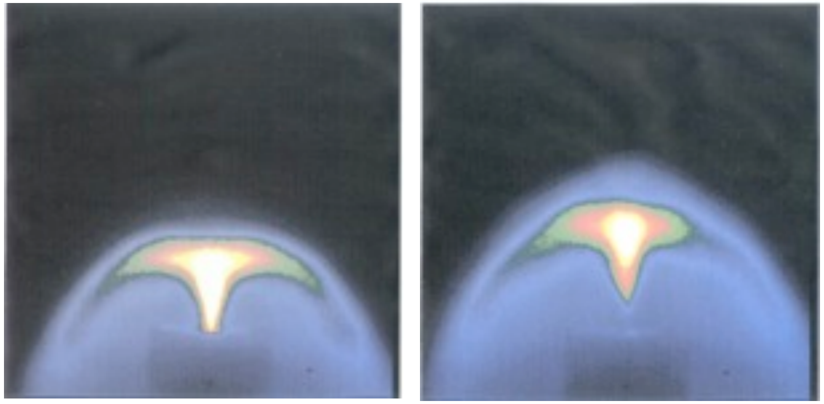

t = 400 nm   t = 600 nm

- Is photoionization of low-charged ions important for DPP and LPP source models?

Photoionization of Low Charged Xe Ions

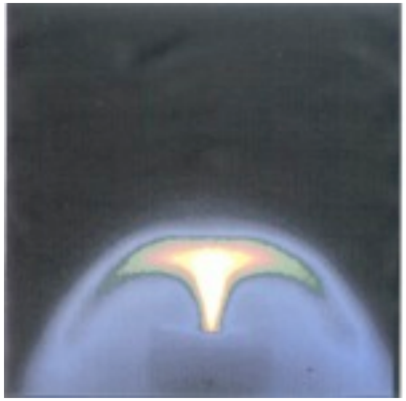

t = 400 nm

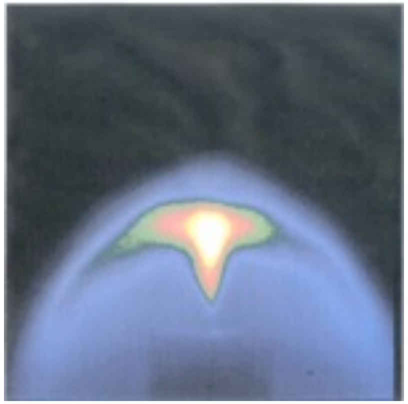

t = 600 nm

- Is photoionization of low-charged ions important for DPP and LPP source models?

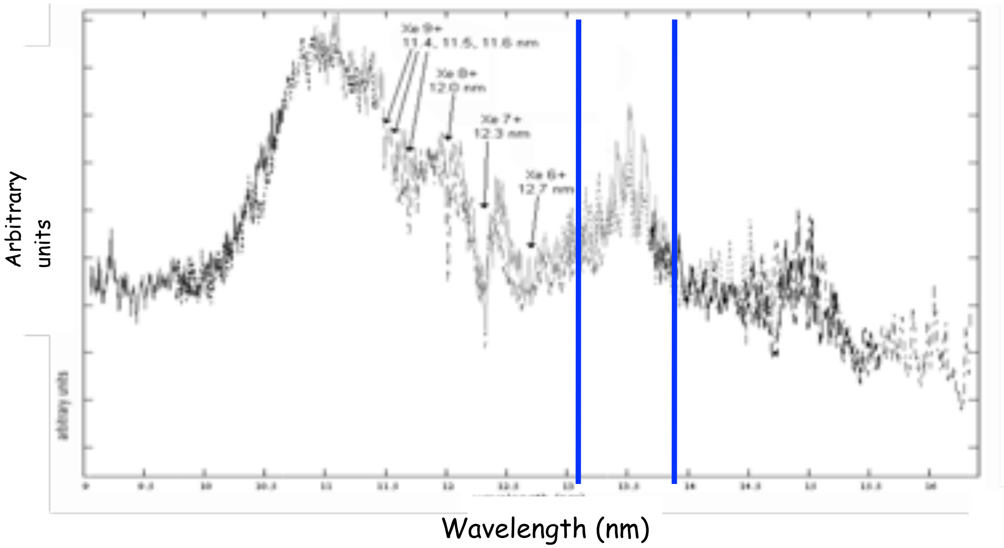

- The blue lines indicate the 13.5 nm ± 2% (90.0 eV to 93.5 eV) region of interest for EUV lithography
- Strong absorption lines due to 4d-nf autoionizing resonances are observed in both LPP and DPP.

Photoionization of Low Charged Xe Ions

13.53 nm   13.12 nm   12.72 nm

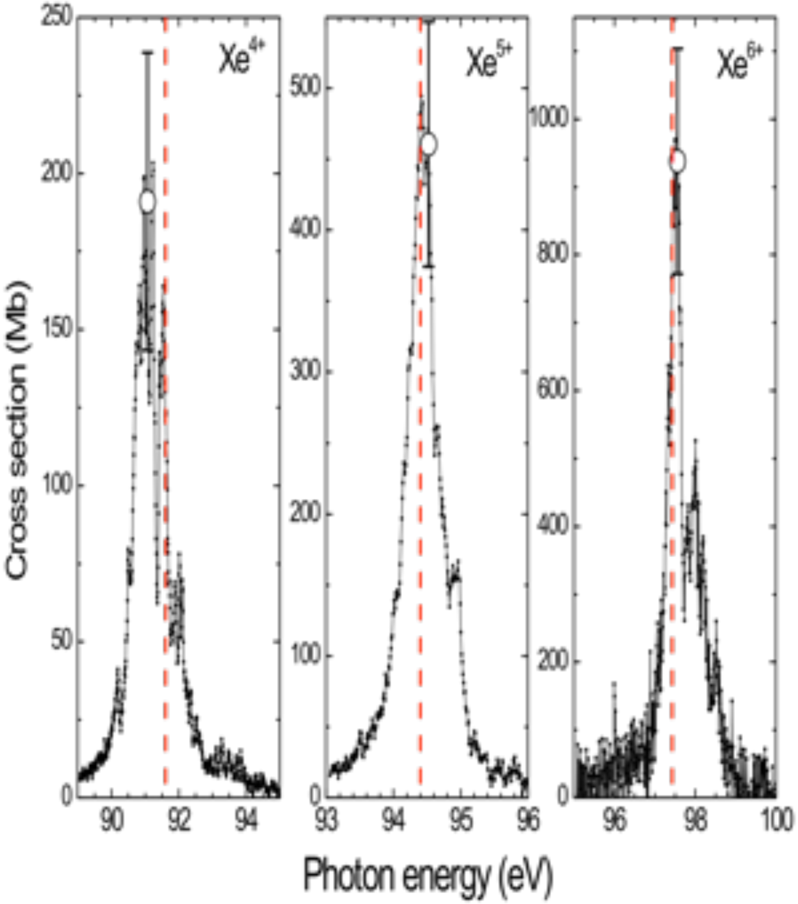

- Absolute photoionization cross sections were measured for Xe^{4+} , Xe^{5+} and Xe^{6+} at the ALS.
- The collapse of the 4f orbital is clear by following the 4d -> 4f oscillator strength increment along the isonuclear sequence.

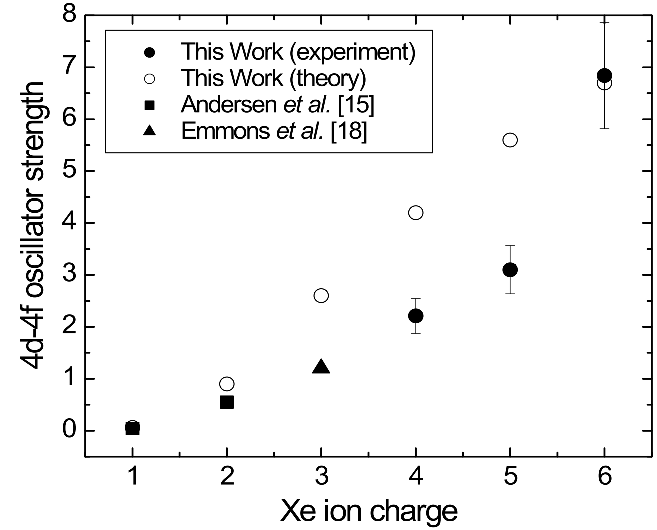

Aguilar *et al.*, "Absolute photoionization cross sections for Xe^{4+} , Xe^{5+} and Xe^{6+} near 13.5 nm: Experiment and Theory", PRA **73** 032717 (2006).